BOEING

Unclassified

Security Classification

DOCUMENT CONTROL DATA - R & D

(Security classification of title, body of abstract and indexing annotation must be entered when the overall report is classified)

1. ORIGINATING ACTIVITY *(Corporate author)*
Vertol Division
The Boeing Company
P. O. Box 16858, Philadelphia PA 19142

2a. REPORT SECURITY CLASSIFICATION
Unclassified

2b. GROUP
N/A

3. REPORT TITLE
Isolated Cyclic Pitch Propeller: Results of Wind Tunnel Test

4. DESCRIPTIVE NOTES *(Type of report and inclusive dates)*
Contractor Test Report (4-7 May 1970)

5. AUTHOR(S) *(First name, middle initial, last name)*
Kolesar, Charles
Kassianides, G.
Andrews, J.and
Armstrong, T.

6. REPORT DATE
June 1970

7a. TOTAL NO. OF PAGES
135

7b. NO. OF REFS
None

8a. CONTRACT OR GRANT NO.
F33615-70-C-1000

b. PROJECT NO.
698BT

c.
Task Area Number: 02
d Work Unit Number: 005

9a. ORIGINATOR'S REPORT NUMBER(S)
Boeing Vertol Document
D170-10037-1

9b. OTHER REPORT NO(S) *(Any other numbers that may be assigned this report)*
AFFDL TR 71-91, Reference 2

10. DISTRIBUTION STATEMENT
Approved for public release; distribution unlimited.

11. SUPPLEMENTARY NOTES

12. SPONSORING MILITARY ACTIVITY
Air Force Flight Dynamics Laboratory
Wright-Patterson AFB, Ohio 45433

13. ABSTRACT

This report presents the results of wind tunnel test BVWT 057 performed in the Boeing Vertol V/STOL wind tunnel on an isolated 3-bladed cyclic pitch propeller with a total Activity Factor of 480. The primary objectives of the test were to determine: (1) the pitching moment capability from the propeller over a wide shaft angle range from 0° up to 120° through the transition flight regime of a tilt wing aircraft and, (2) the effect of cyclic pitch on power.

The effects of cyclic pitch on propeller thrust, normal force, yawing moment, and side force were also measured.

DD FORM 1 NOV 65 1473

Unclassified

Security Classification

14 KEY WORDS	LINK A		LINK B		LINK C	
	ROLE	WT	ROLE	WT	ROLE	WT
Cyclic Pitch Propeller						
Isolated Propeller						

REV LTR

THE BOEING COMPANY

VERTOL DIVISION · PHILADELPHIA, PENNSYLVANIA

CODE IDENT. NO. 77272

NUMBER D170-10037-1

TITLE ISOLATED CYCLIC PITCH PROPELLER:

RESULTS OF WIND TUNNEL TEST

ORIGINAL RELEASE DATE June 1970. FOR THE RELEASE DATE OF SUBSEQUENT REVISIONS, SEE THE REVISION SHEET. FOR LIMITATIONS IMPOSED ON THE DISTRIBUTION AND USE OF INFORMATION CONTAINED IN THIS DOCUMENT, SEE THE LIMITATIONS SHEET.

MODEL _____ CONTRACT F33615-70-C-1000

ISSUE NO. _____ ISSUED TO: _____

PREPARED BY George Kassianides S. Armstrong C. Kolesar Joyce Andrews DATE 6/12/70

APPROVED BY Charles E. Kolesar DATE 6/12/70
C. E. Kolesar

APPROVED BY J. Bevan DATE 6/14/70
D. Bevan, Unit Chief, V/STOL Aerodynamics

APPROVED BY K.B. Gillmore DATE 6/13/70
K.B. Gillmore, Mgr., V/STOL Technology

APPROVED BY P.C. Prager 6/15/70
P.C. Prager, Program Manager

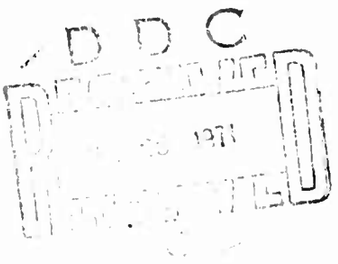

LIMITATIONS

This document is controlled by V/STOL Aerodynamics Org. 7481

All revisions to this document shall be approved by the above noted organization prior to release.

ACTIVE SHEET RECORD

SHEET NUMBER	REV LTR	ADDED SHEETS				SHEET NUMBER	REV LTR	ADDED SHEETS			
		SHEET NUMBER	REV LTR	SHEET NUMBER	REV LTR			SHEET NUMBER	REV LTR	SHEET NUMBER	REV LTR
i						36					
ii						37					
iii						38					
iv						39					
v						40					
1						41					
2						42					
3						43					
4						44					
5						45					
6						46					
7						47					
8						48					
9						49					
10						50					
11						51					
12						52					
13						53					
14						54					
15						55					
16						56					
17						57					
18						58					
19						59					
20						60					
21						61					
22						62					
23						63					
24						64					
25						65					
26						66					
27						67					
28						68					
29						69					
30						70					
31						71					
32						72					
33						73					
34						74					
35						75					

FORM 46283 (7/67)

ACTIVE SHEET RECORD

SHEET NUMBER	REV LTR	ADDED SHEETS				SHEET NUMBER	REV LTR	ADDED SHEETS			
		SHEET NUMBER	REV LTR	SHEET NUMBER	REV LTR			SHEET NUMBER	REV LTR	SHEET NUMBER	REV LTR
76						116					
77						117					
78						118					
79						119					
80						120					
81						121					
82						122					
83						123					
84						124					
85						125					
86						126					
87						127					
88						128					
89						129					
90						130					
91											
92											
93											
94											
95											
96											
97											
98											
99											
100											
101											
102											
103											
104											
105											
106											
107											
108											
109											
110											
111											
112											
113											
114											
115											

FORM 46283 (7/67)

REVISIONS			
LTR	DESCRIPTION	DATE	APPROVAL

ABSTRACT

This report presents the results of wind tunnel test BVWT 057 performed in the Boeing Vertol V/STOL wind tunnel on an isolated 3-bladed cyclic pitch propeller with a total Activity Factor of 480. The primary objectives of the test were to determine: (1) the pitching moment capability from the propeller over a wide shaft angle range from 0° up to 120° through the transition flight regime of a tilt wing aircraft and, (2) the effect of cyclic pitch on power.

The effects of cyclic pitch on propeller thrust, normal force, yawing moment, and side force were also measured.

KEY WORDS

Cyclic Pitch Propeller

Isolated Propeller

NOMENCLATURE

The following nomenclature was used for the isolated cyclic pitch propeller Model VRO73Q in test BVWT 057.

Symbol		
A_p	Propeller disc area	ft^2
b	Propeller blade chord	ft
C_{M_p}	Hub pitching moment coefficient, $\frac{\text{Pitching moment}}{\rho n^2 D^5}$	
C_{M_s}	Pitching moment coefficient (slipstream notation), $\frac{M}{q_s S c}$	
C_{NF_p}	Prop normal force coefficient, $\frac{\text{Normal force}}{\rho n^2 D^4}$	
C_{NF_s}	Prop normal force coefficient (slipstream notation), $\frac{\text{Normal force}}{q_s S}$	
C_p	Shaft power coefficient, $\frac{\text{Shaft power}}{\rho n^3 D^5}$	
C_{SF_p}	Prop side force coefficient, $\frac{\text{Side force}}{\rho n^2 D^4}$	
C_T	Thrust coefficient, $\frac{T}{\rho n^2 D^4}$	
C_{T_s}	Thrust coefficient (slipstream notation), $\frac{T}{q_s A_p}$	
C_{YM_p}	Hub yawing moment coefficient, $\frac{\text{Yawing moment}}{\rho n^2 D^5}$	
c	Reference wing chord	ft
D	Propeller diameter	ft

Symbol		
h	Propeller blade thickness	ft.
J	Propeller advance ratio, $\frac{V}{nD}$	
M	Pitching moment (positive~nose up)	ft.lbs.
n	Propeller rotational speed	rps
q	Freestream dynamic pressure	lbs/ft^2
q_s	Slipstream dynamic pressure, $q+T/A_p$	lbs/ft^2
q_T	Tunnel dynamic pressure	lbs/ft^2
R	Propeller blade radius	ft.
r	Radial station along blade	ft.
S	Reference wing area	ft^2
T	Propeller thrust	lbs.
V	Velocity	ft/sec
α_p	Shaft angle	degrees
γ	Cyclic angle (positive~ nose down pitching moment)	degrees
$\theta_{.75}$	Propeller blade pitch angle at .75R	degrees
ρ	Density	$slugs/ft^3$

TABLE OF CONTENTS

TABLE OF CONTENTS

1.0 INTRODUCTION

During the period of May 4th to May 7th, 1970 inclusive, wind tunnel test BV057 was carried out on an isolated 3-bladed, 2.143ft diameter, cyclic pitch propeller in the 20ft x 20 ft test section of the Boeing Vertol V/STOL wind tunnel. This pedestal mounted model (VRO73Q) featured an internal six component strain gage balance mounted between the propeller/cyclic hub assembly and the air motor power service. Both model propeller and associated dynamic system were developed for a 1/12th scale full span model of a four prop tilt wing aircraft.

The major objectives of this test were to establish: (1) the pitching moment capability from cyclic pitch of this high Activity Factor (480 AF total) propeller over a wide shaft angle range from 0° up to 120° throughout the transition flight regime of a tilt wing aircraft and, (2) the effect of cyclic pitch on power. Additional objectives were to determine the effect of cyclic pitch on thrust, propeller normal force, hub yawing moment, and propeller side force.

Of special interest were the propeller pitching moment characteristics at high shaft angles (greater than 90 degrees) in the low speed portions of the transition flight regime (high thrust coefficient or low advance ratio).

Results from the subject test will be used in conjunction with the results from the subsequent test of the 1/12 scale four prop tilt wing model to ascertain any influence of the wing forces and moments on the propeller generated forces and moments, and also to better understand the effects of power on transition stability and control.

2.0 MODEL DESCRIPTION AND INSTALLATION

The general arrangement and geometry of the isolated propeller Model VRO73Q and wind tunnel installation details are presented in this section. Figure 1 is a photograph of the model as installed in the Boeing-Vertol V/STOL wind tunnel for this test.

2.1 PROPELLER, HUB, GEOMETRY

Geometric characteristics of the three bladed propeller (left hand rotation~ pilot's seat) used in this test are shown in Figure 2. The variation with radial station, of blade chord, design lift coefficient, thickness ratio and blade twist are presented in this figure. Principal dimensional information and airfoil designations are listed below:

Diameter	2.143 ft
Disc area	3.61 ft^2
Root chord (at .2r/R)	3.20 in.
Tip chord	2.32. in.
Root section	NACA 64A030
Tip section	NACA 64A306
Activity Factor	160 per blade
Overall Blade Twist	33.5°

Figure 3 depicts the blade planform. Note that the blade pivots for manual collective settings about the 35% chord line.

Figure 4 is a photograph of the 4.80 in. diameter cyclic hub. This hub employed a swashplate mounted on a cyclic stack fixed to the front of the six component nacelle balance. The outer annulus of the swashplate was driven by scissors mounted on the rear face of the hub. Cyclic pitch was applied to the blades through a set of pitch links. Elastomeric (Lamiflex) bearings were used in the hub to support the blade retention housing and thus enable blade angle motion. Cyclic pitch angle was manually set.

2.2 NACELLE DESCRIPTION AND MODEL INSTALLATION

Figure 5 details the arrangement of the propeller hub, swashplate, slip ring, strain gage internal balance, and air motor in the nacelle package. The six component balance, located between the swashplate and the pneumatic motor, was mounted to the front face of the motor. A flexible bellows joint in the drive shaft isolated propeller forces and moments.

The motor, which utilizes a four stage turbine, is designed to deliver 90 shaft horsepower at 9000 RPM. At the design point, approximately 2 lb/sec of air flow is required. Compressed air, metered by the main tunnel air control valve, was introduced into the motor plenum in front of the first stage turbine. The available power at the desired propeller RPM precluded the use of reduction gears.

A diverging nozzle with eight straightening vanes for eliminating exhaust swirl was attached to the rear end of the motor. An opening at the rear end of the nacelle permitted the jet efflux to emerge in the freestream.

The 3.75 inch diameter mounting tube, 25 inches in length, supporting the propeller/hub/motor package in the horizontal nacelle assembly, was welded to a vertical 3.50 inch diameter tube located 1.2 propeller diameters behind the hub ℄ . This vertical tube was fixed to the standard Boeing Vertol pedestal mount which was in turn attached to the yaw table. The resultant distance of the propeller centerline above the tunnel floor was approximately 6.7 ft. See Figure 6 for a schematic drawing of the installation in the wind tunnel.

2.3 TEST FACILITY

As mentioned previously, the test was conducted in the 20ft x 20ft test section of the Boeing Vertol V/STOL wind tunnel. See Figure 7 for a schematic drawing of the tunnel.

Two test section configurations are currently available, namely: closed throat and slotted throat. Walls, floor and ceiling used for the closed throat configuration are also used for the slotted throat configuration by simply removing covers from slots which are built into the walls. The slotted throat was used during BVWT 057.

The auxiliary air for powering the nacelle pneumatic motor was supplied by a 20 pound per second, 1000 psi compressor system.

Figure 1

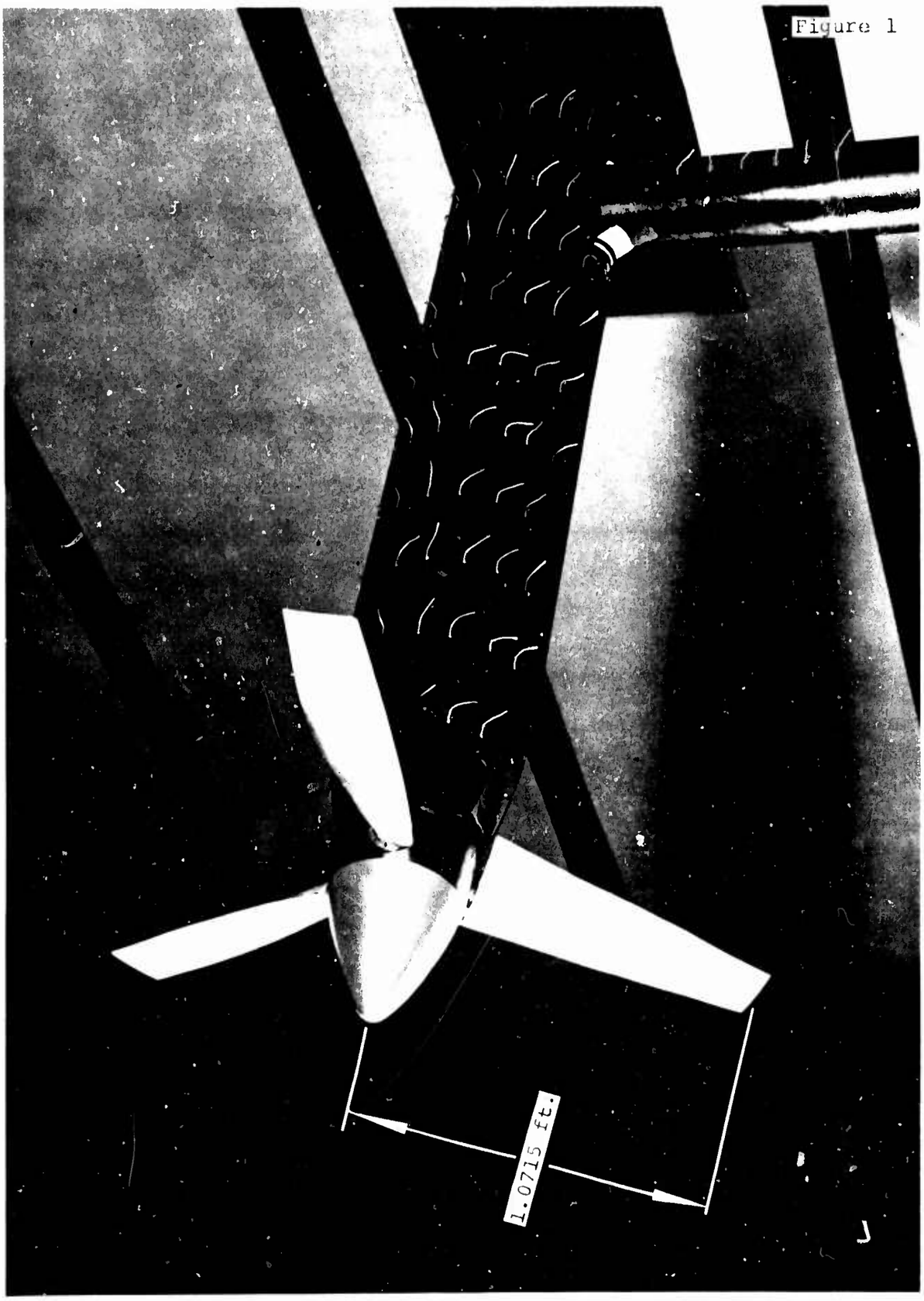

Isolated Propeller Model VRO73Q Installation
in Boeing-Vertol V/STOL Wind Tunnel

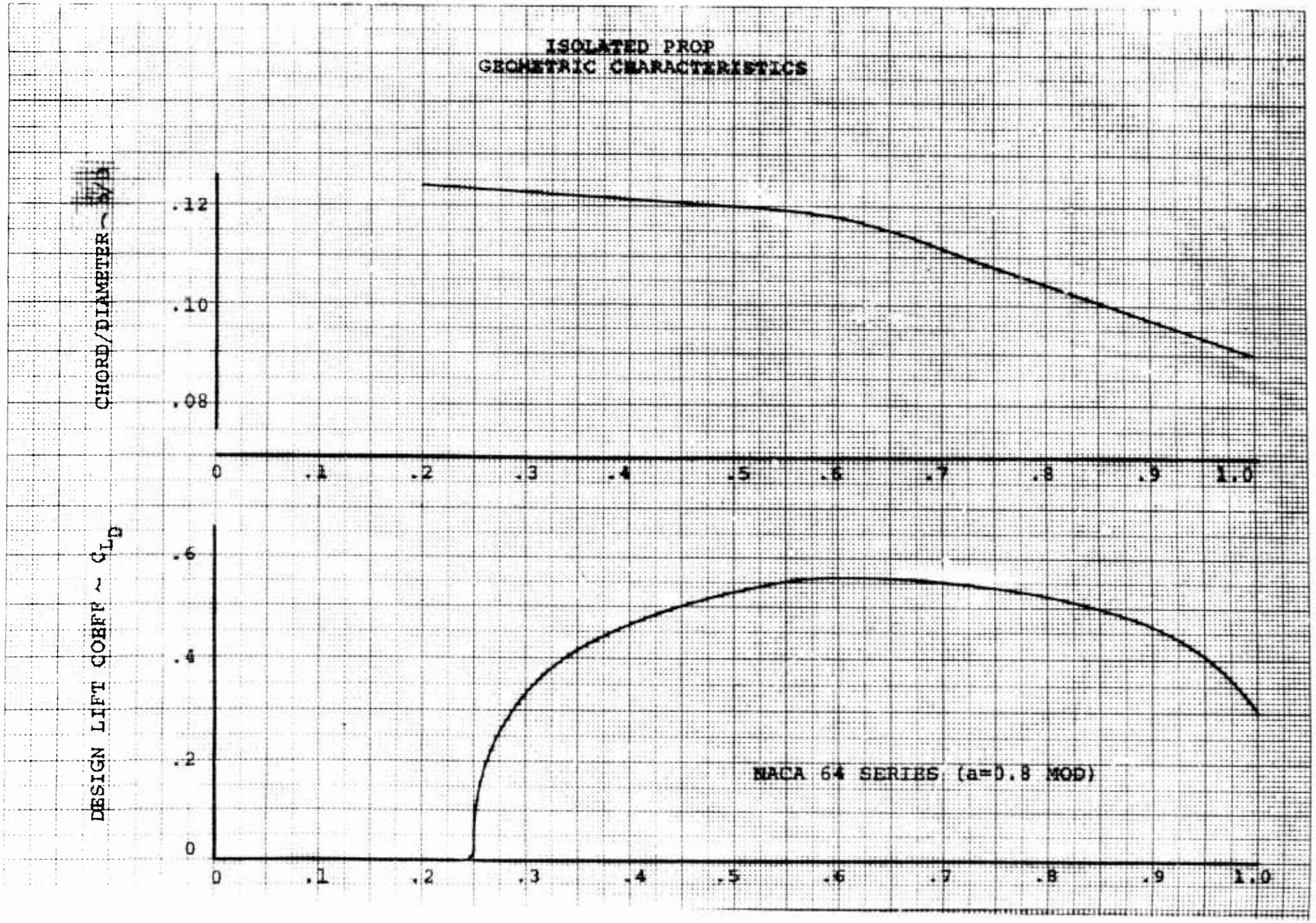

Figure 2

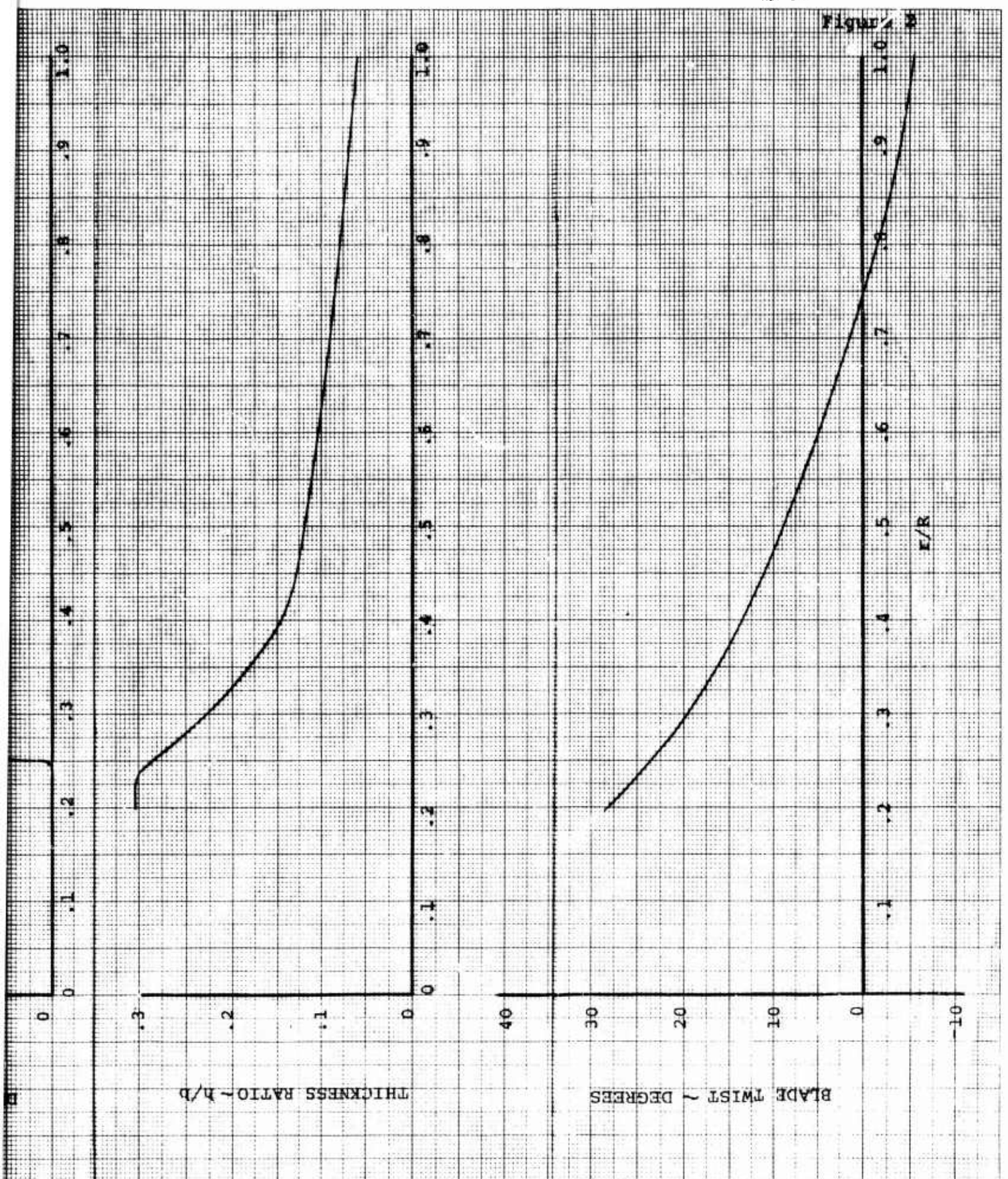
E/R
0
.1
.2
.3
.4
.5
.6
.7
.8
.9
1.0
BLADE TWIST ~ DEGREES
40
30
20
10
0
-10
THICKNESS RATIO ~ h/b
.3
.2
.1
0

A

MODEL VR

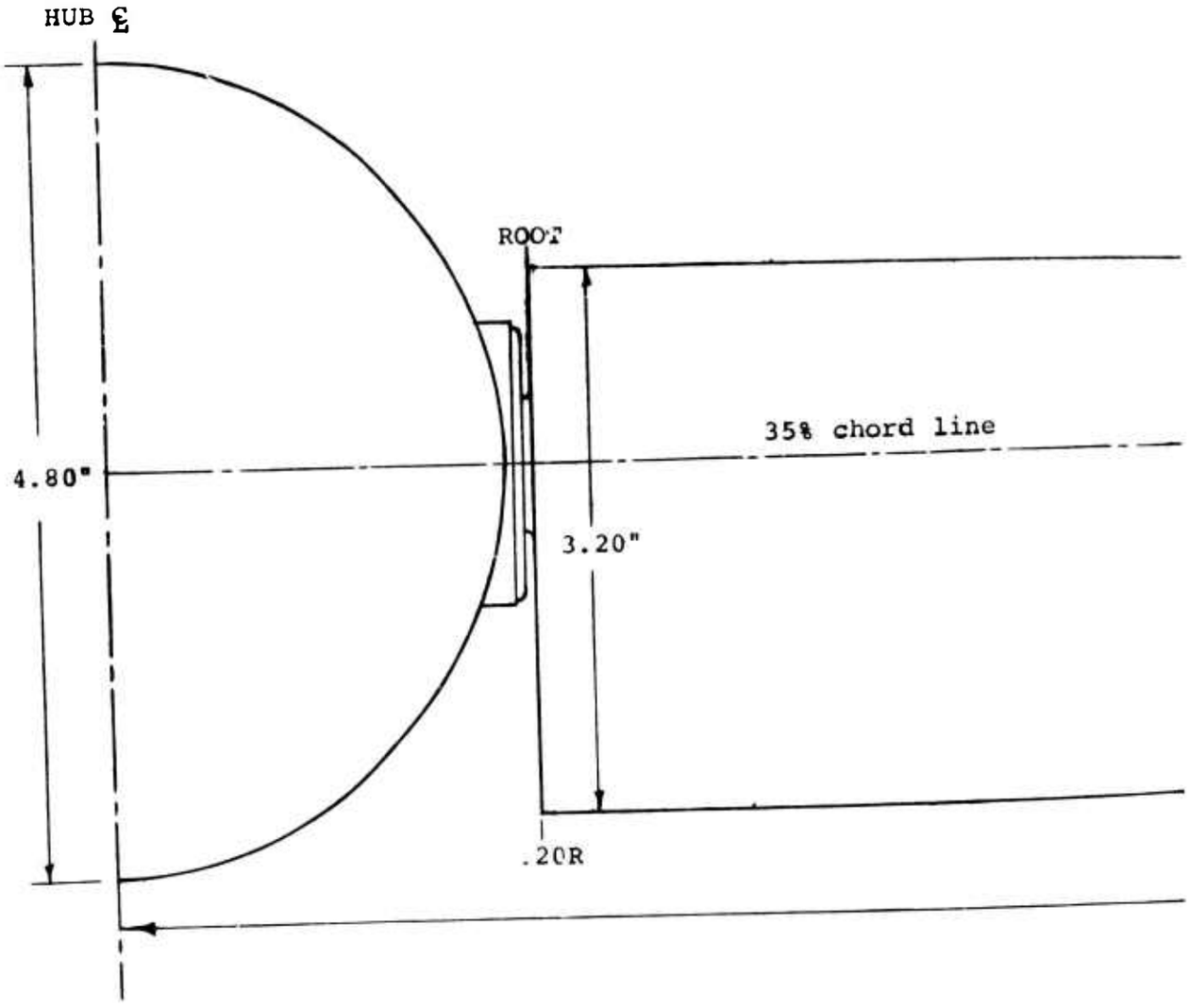

SCALE: FULL

NOTE: Actual Dimensions (Untwisted)

FORM 19510 (5/68)

Figure 3

MODEL VRO73Q - ISOLATED PROPELLER

BLADE PLANFORM

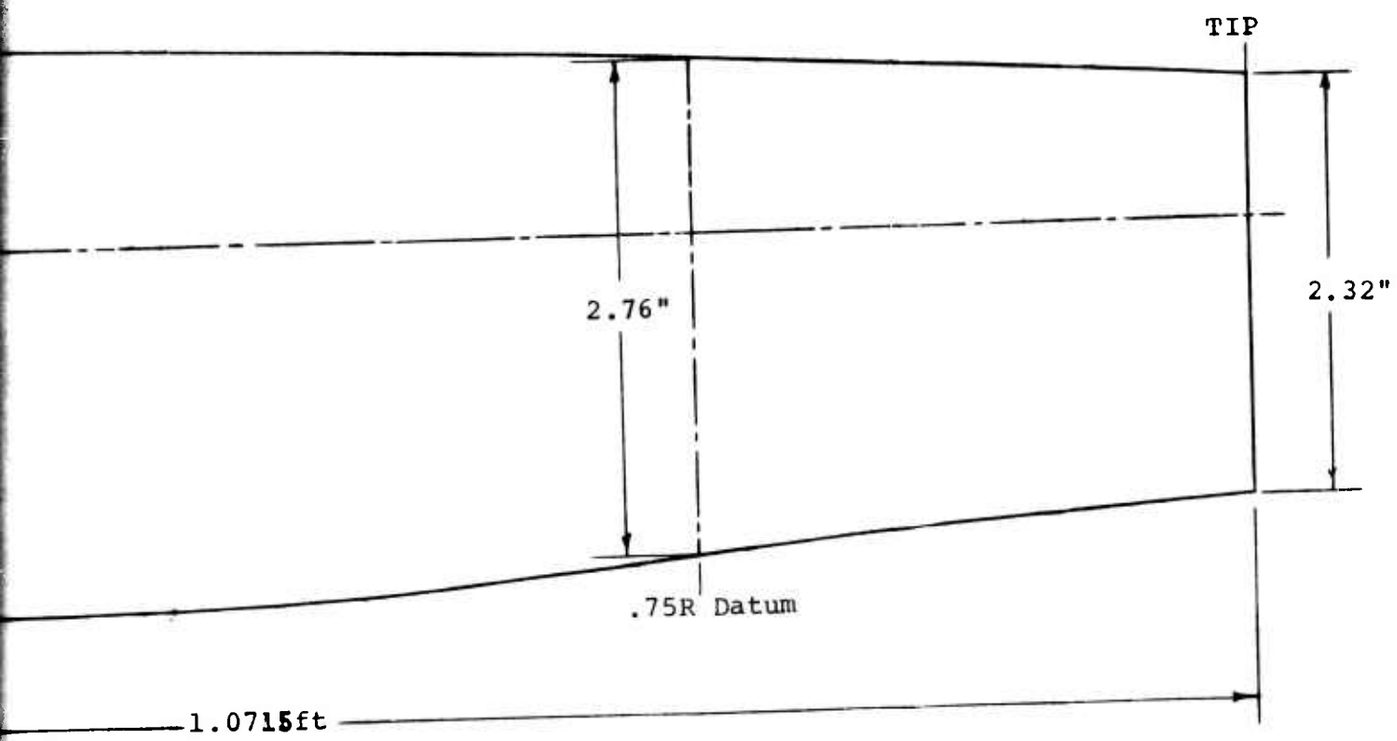

Figure 4

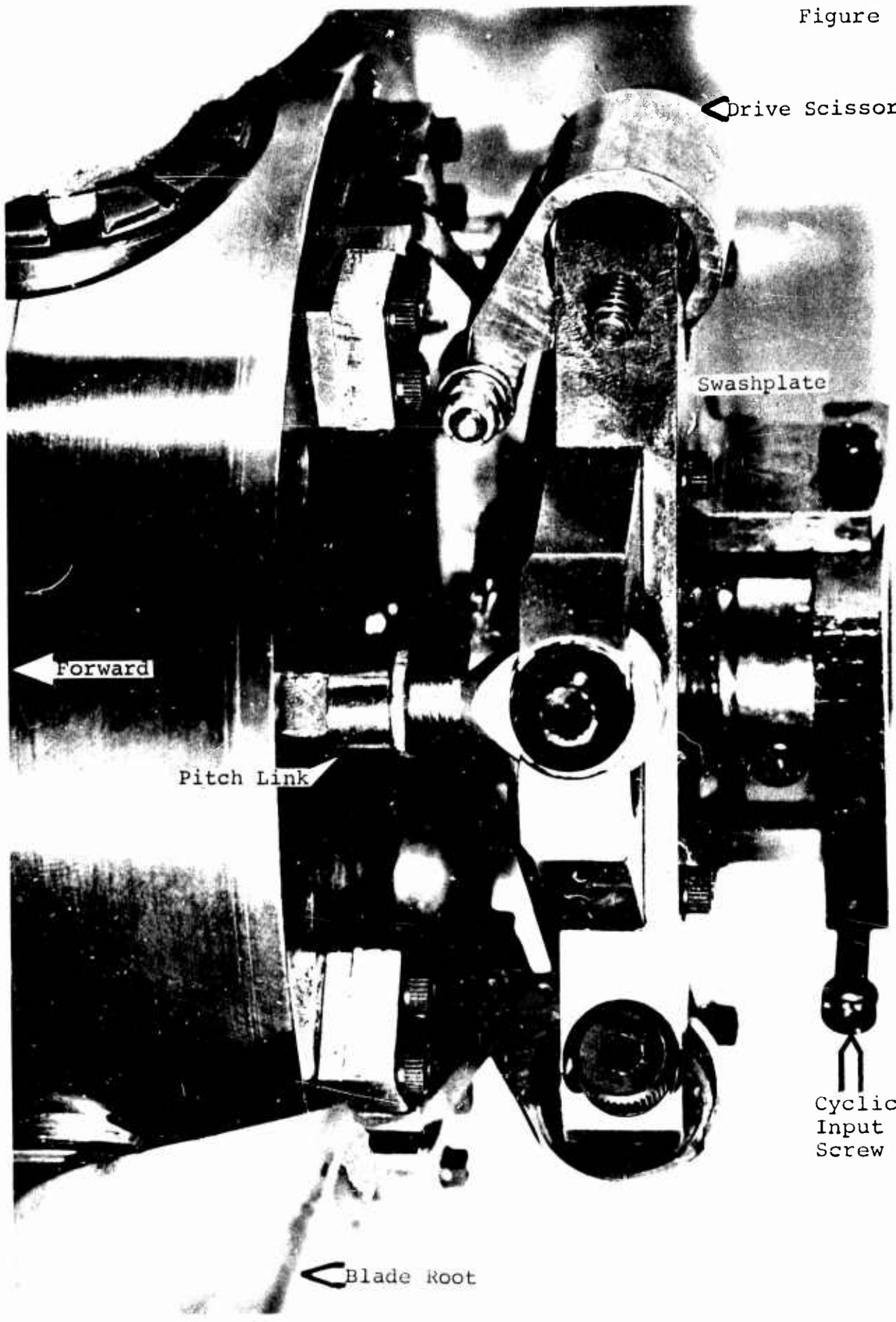

Details of Cyclic Hub Mechanism

Figure 5

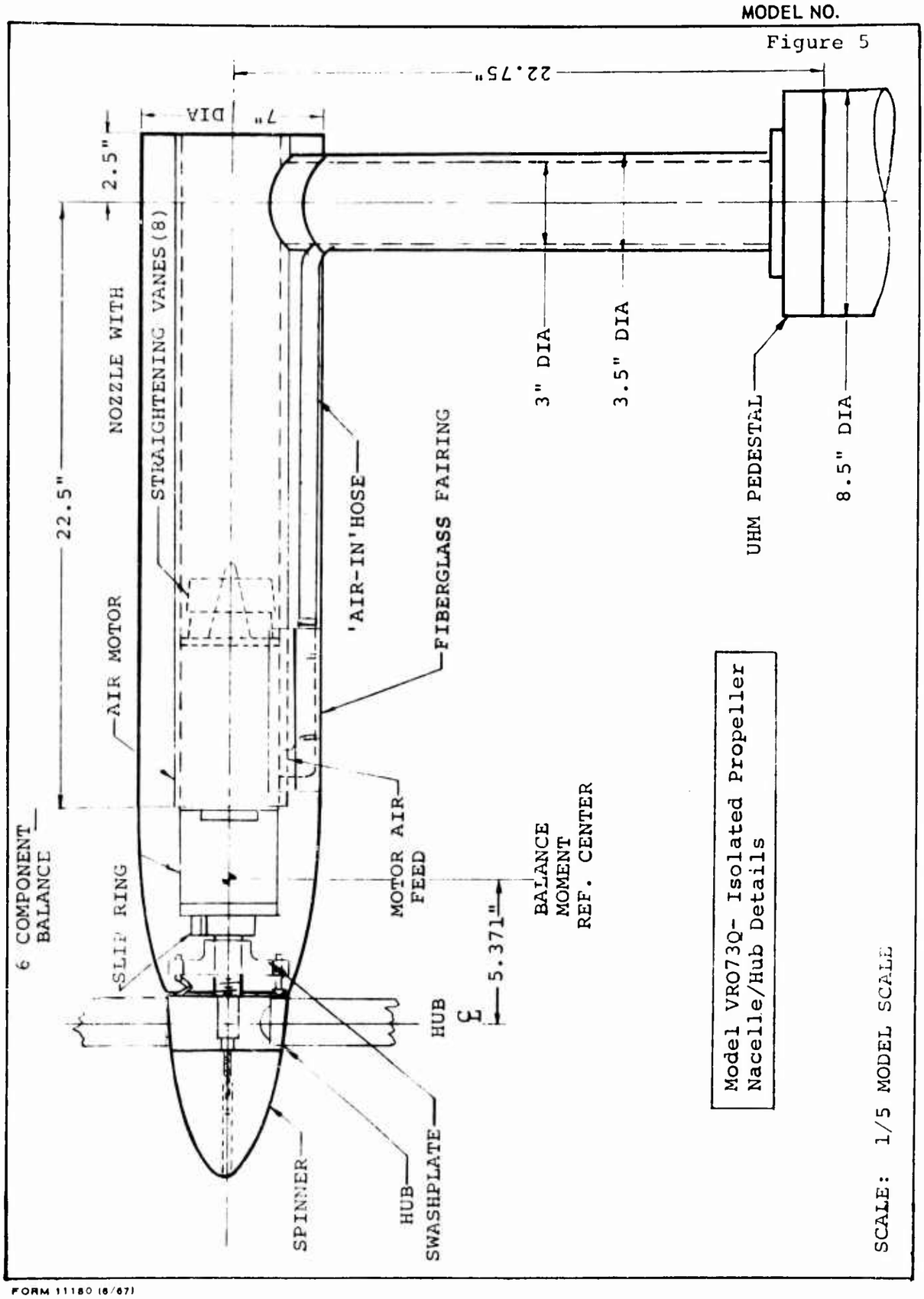

FORM 11180 (8/67)

Figure 6

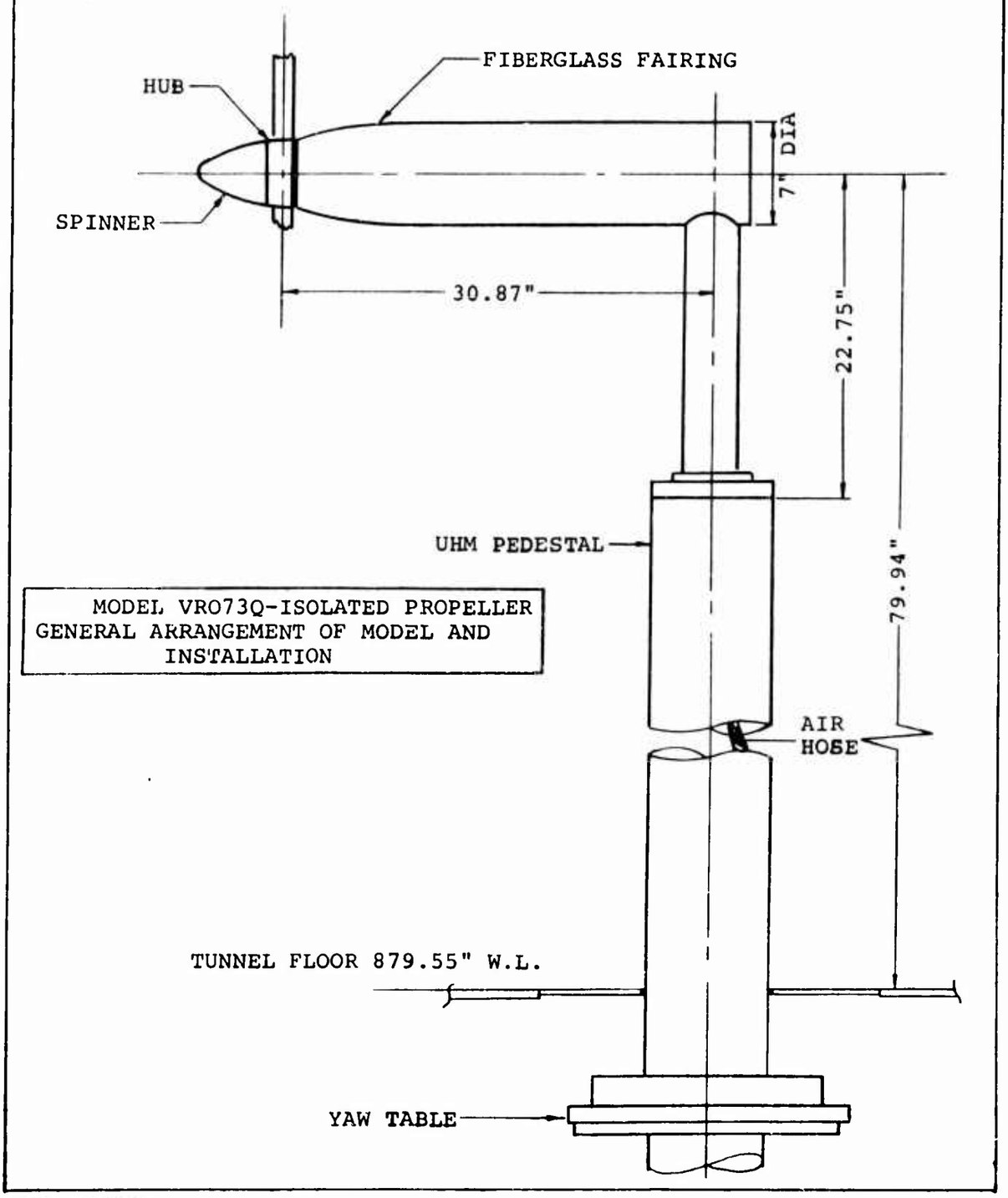

MODEL VRO73Q-ISOLATED PROPELLER
GENERAL ARRANGEMENT OF MODEL AND INSTALLATION

Figure 7

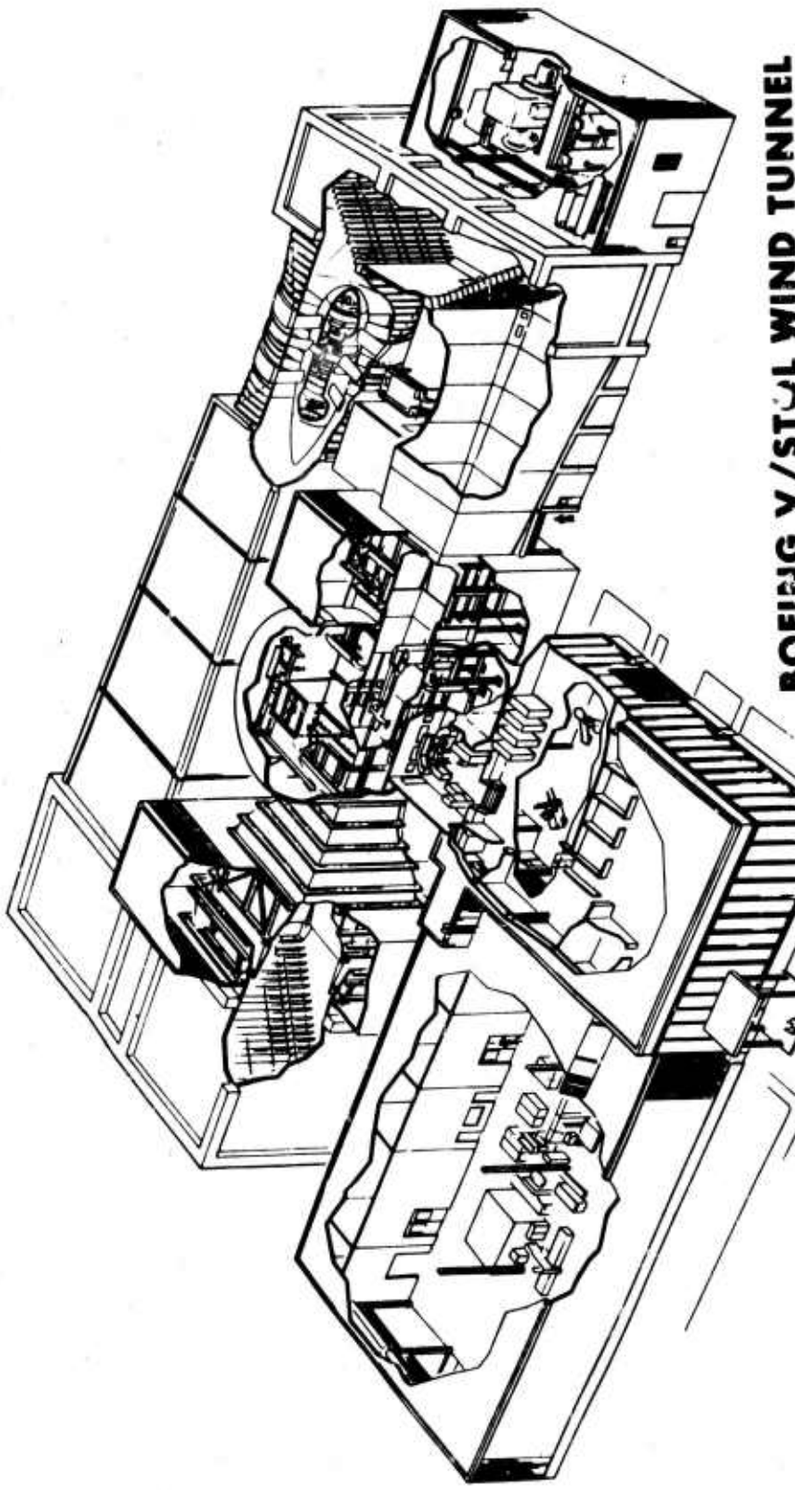

3.0 INSTRUMENTATION AND EQUIPMENT

3.1 MODEL INSTRUMENTATION

Model instrumentation consisted of the following items:

a) Six component Strain Gauge Balance

The balance, attached to the front of the motor as shown in Figure 5, measured thrust, pitching moment, normal force, yawing moment, side force and rolling moment. In addition to measuring steady values, normal force, side force, pitching moment and yawing moment were displayed on oscilloscopes so that dynamic loads in the flexures could be monitored.

b) Strain Gauged Drive Shaft

A high speed slip ring assembly was utilized to transmit the electrical signals from this shaft. The torque measured was used to calculate power coefficient.

c) Tachometer

Propeller RPM was measured by a tachometer, installed internally behind the front bearing of the motor, that worked on the pulse generator principle(thirty pulses per cycle).

d) Shaft Angle Potentiometer

Shaft angle (same as yaw table angle) was calibrated and measured using a potentiometer.

3.2 DATA ACQUISITION SYSTEM

The flow diagram of the wind tunnel data system used in this test is shown in Figure 8. This data system can accept up to 120 channels from a model and the tunnel itself. These signals are routed as illustrated to an IBM 1800 computer for processing and data reduction. The computed results are tabulated by a line printer and selected quantities are plotted by the X-Y plotters. Final data is stored on magnetic tape.

A digital display of any nine channels is also available during testing for monitoring purposes. Dynamic data of six quantities can be continuously displayed on oscilloscopes. This provides assistance in preventing balance or structural limits from being exceeded.

A choice of sampling rates of 2,4,10,20,40, 100 and 200 samples per channel/sec. is available. The sampling process is accomplished with channel switching devices called multiplexers (MPX).

Figure 8

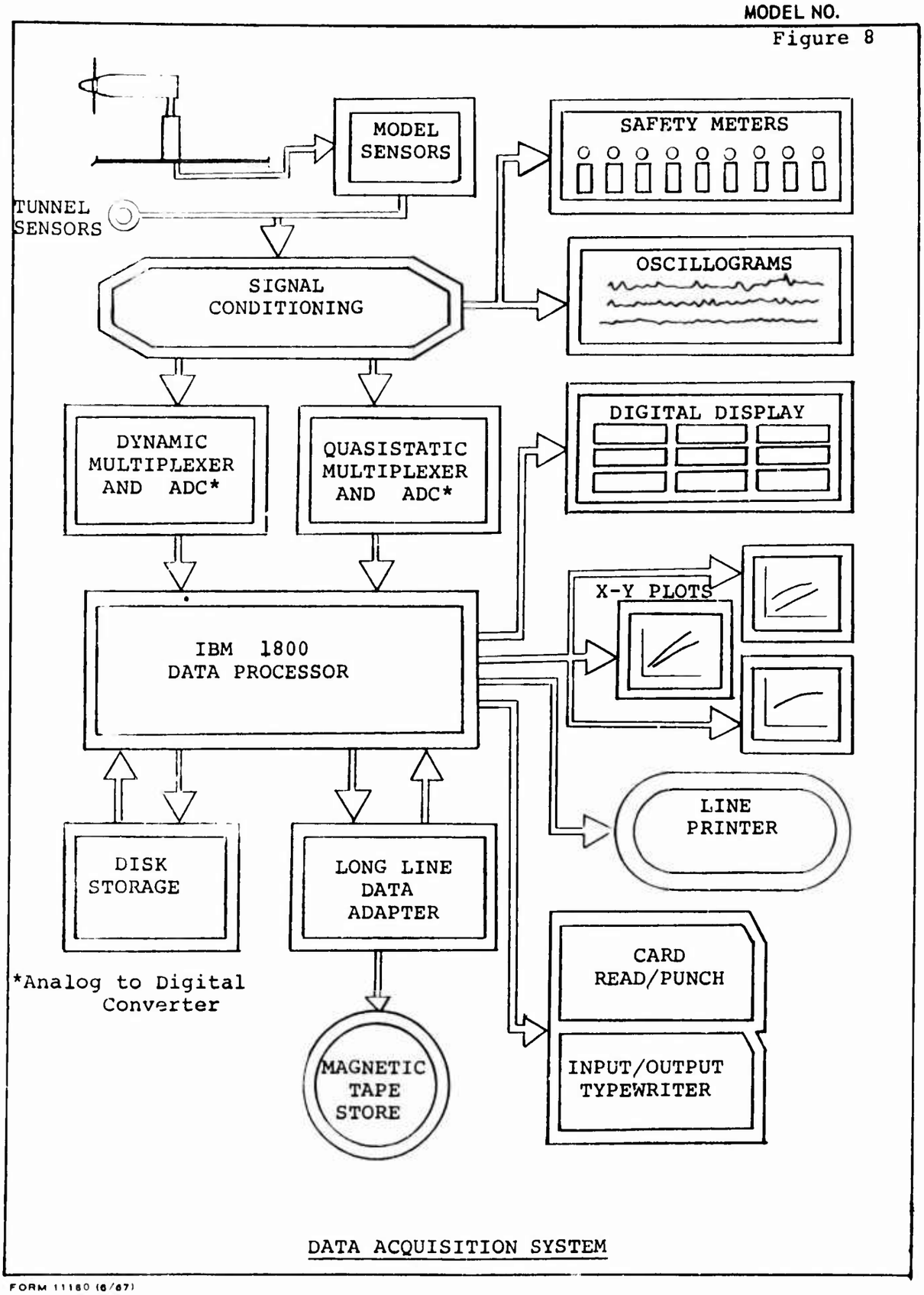

DATA ACQUISITION SYSTEM

FORM 11160 (6/67)

4.0 DATA REDUCTION

At each test point, measurements were taken for computing and printing out on-line the listed quantities.

Density, ρ	slugs/ft^3
Dynamic pressure, q	lb/ft^2
Propeller RPM	
Shaft angle (same as yaw table angle) α_p	degrees
Shaft torque (includes friction on cyclic pitch hub)	ft.lbs.
Thrust, T	lbs.
Normal force	lbs.
Side force	lbs.
Pitching moment (about balance center)	ft.lbs.
Yawing moment (about balance center)	ft.lbs.
Rolling moment (same as friction torque)	ft.lbs.

Both the measured pitching moment and yawing moment were transferred to the hub $\mathbb{C}$ so that hub moment coefficients could be calculated at the plane of the propeller.

Propeller forces and moments measured from the internal balance were reduced to coefficient form in propeller terminology. The propeller-type coefficients computed and printed out on-line were as follows.

Advance ratio, $J = \frac{V}{nD}$

Thrust coefficient, $C_T = \frac{T}{\rho n^2 D^4}$

Prop pitching moment coefficient, $C_{M_p} = \frac{\text{Pitching moment}}{\rho n^2 D^5}$

Shaft power coeficient, $C_p = \frac{\text{Shaft power}}{\rho n^3 D^5}$

Prop normal force coefficient, $C_{NF_p} = \frac{\text{Normal force}}{\rho n^2 D^4}$

Prop side force coefficient, $C_{SF_p} = \frac{\text{Side force}}{\rho n^2 D^4}$

Prop yawing moment coefficient, $C_{YM_p} = \frac{\text{Yawing moment}}{\rho n^2 D^5}$

Friction power coefficient, $C_{P_F} = \frac{\text{Rolling moment}}{\rho n^2 D^5}$

Coefficients for thrust, prop pitching moment, and prop normal force in slipstream notation were also calculated and printed out on-line, per the following listing.

Thrust coefficient, $C_{T_s} = \frac{T}{q_s A_p}$

Prop pitching moment coefficient, $C_{M_s} = \frac{\text{Pitching moment}}{q_s S c}$

Prop normal force coefficient, $C_{NF_s} = \frac{\text{Normal force}}{q_s S}$

where $q_s = q + T/A_p$

The reference wing area (9.14 ft^2) and wing chord (.997 ft) used in calculating these coefficients, are the geometric values for the wing of the 1/12 scale four prop tilt wing model to be tested at a subsequent date. Where isolated prop data (one propeller) is shown in slipstream notation only 1/4 of the reference wing area was used.

No tunnel wall corrections were applied.

5.0 TEST PROCEDURE AND TEST CONDITIONS

5.1 TEST PROCEDURE

The nacelle balance was calibrated statically by applying known forces and moments. Resultant calibration data including balance interactions was incorporated into the computer program for on-line data reduction.

The test was initiated by determining the tunnel dynamic pressures (q_T) corresponding to a spread of C_{T_S} values from .90 to zero, i.e., 90, .75, .60, .35, and 0, for a collective pitch setting ($\theta_{.75}$) of 12° and 5000 RPM. This was achieved by increasing tunnel q until the required C_{T_S} was reached at the preselected shaft angle corresponding to a typical wing incidence angle of a tilt wing aircraft at that particular C_{T_S}. The tunnel q's established were 1.50, 3.73, 5.73, 9.18 and 14.15 lbs/ft^2.

All data runs or shaft angle sweeps (except the zero C_{T_S} run) were performed with a constant propeller speed, blade pitch, and tunnel q. The selected propeller speed of 5000 RPM was based on previous test experience with essentially the same cyclic hub including cyclic pitch mechanism and elastomeric bearing system. The selection of the basic collective pitch setting of 12° was also based on previous test experience with a 2.143 ft. diameter model propeller. Of concern, was the possibility of partial blade stall at the low propeller blade Reynolds number prevalent during the testing of a 2ft. diameter propeller.

The shaft angle range encompassed during this test varied from -10° or 0° up to 80° at a tunnel q of 9.18 lbs/ft^2 and up to 120° at the lowest test tunnel q. Shaft angles beyond 100° were of particular interest in the low speed portion of the transition flight regime where high angles can be encountered during operations near the hover condition.

5.2 TEST CONDITIONS

Test variables were: collective pitch angle, cyclic pitch angle (both manually adjusted), tunnel q, and shaft angle.

As stated previously, the primary collective pitch setting used during this test was 12°. Collective angles of 10° and 15° were also investigated. Testing of the 10° setting at the two lowest tunnel q's and the 15° setting at the lowest tunnel q, was conducted to ascertain the influence of propeller pitch angle on cyclic pitch effectiveness, power due to cyclic, and normal force.

Cyclic pitch angles from +8 to -8° were tested. The test program was phased so that the full range of cyclic pitch was evaluated at the lowest tunnel q condition, where the maximum pitch control due to cyclic is required, with progressively lower cyclic angles being investigated at higher tunnel q's.

Data points were obtained at negative shaft angles during several test runs to check the symmetry of the thrust and power characteristics.

The propeller speed of 5000 RPM utilized in this test, corresponded to a tip speed of 561 ft/sec and a tangential blade Reynolds number at 0.75 radius of 620,000. Figure 9 shows a comparison between the blade Reynolds number of the model propeller and that for a representative full scale propeller.

Included in the test were two data runs with the propeller blades removed to evaluate spinner/hub alone force and moment characteristics.

Upon completion of the originally scheduled 27 runs, time permitted conducting some optional runs. Four hover runs were performed with 0, 4, 6 and 8 degrees of cyclic applied to the basic 12° collective setting. Additional cyclic pitch runs with 12° and 10° of collective were made in the transition regime before the test was concluded.

A tabulation on the following page summarizes the data runs performed during the subject test in terms of key test variables.

BVWT 057
RUN SUMMARY

RUNS	$\theta_{.75}$	CYCLIC ANGLE	C_{T_s}
3-7	12°	0°	.9, .75, .60, .35
8	↓	0°	Zero
9-12	↓	+4°	.9, .75, .60, .35
13-14	↓	+6°	.9, .75
16-19	↓	-4°	.9, .75, .60, .35
20-21	↓	-6°	.9, .75
23-24	10°	0°	↓
25-26	↓	+4°	↓
27	15°	0°	.9
28	↓	+4°	↓
29	12°	+8°	↓
30-31	--	--	Hub Tares
32	12°	0°	Hover
33	↓	+4°	↓
34	↓	+6°	↓
35	↓	+8°	↓
36-37	10°	-4°	.9, .75
38-39	↓	+6°	↓
40	12°	-8°	.9

NOTE:

Constant propeller speed (5000 RPM) except Run 8.

FORM 46284 (2/86)

Figure 9

COMPARISON OF BLADE REYNOLDS NUMBER
MODEL AND FULL SCALE PROP

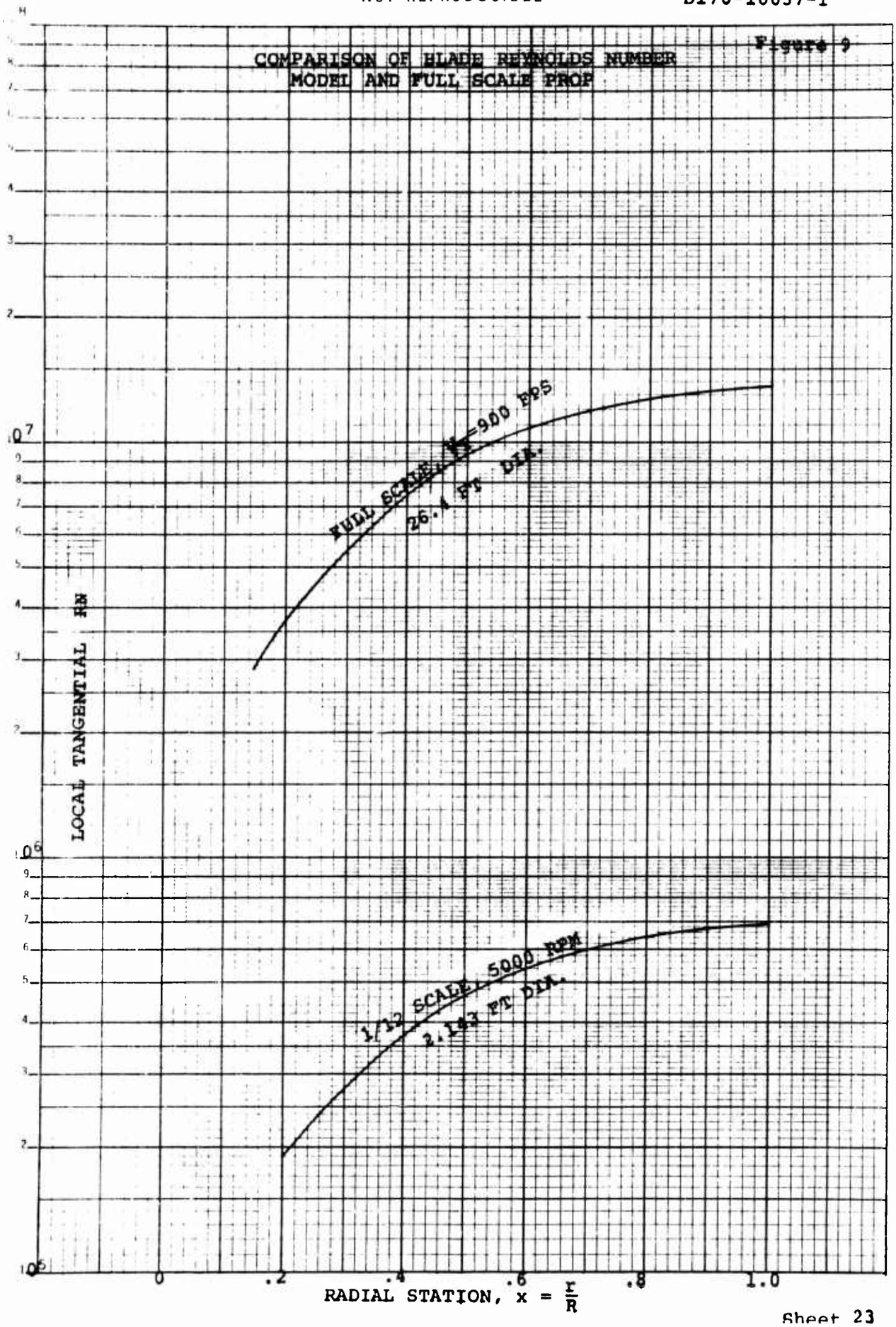

SEMI-LOGARITHMIC 46 5493

6.0 TEST RESULTS AND DISCUSSION

The data obtained in BVWT 057 has been transferred to the hub center and reduced in propeller coefficient form. Thrust, hub pitching moment and prop normal force have also been reduced per the slipstream notation. The discussion of test results that follows, is primarily directed towards the data in propeller terminology.

6.1 BASIC PROPELLER THRUST CHARACTERISTICS

Figures 10 through 18 depict the variations of propeller thrust, slipstream thrust coefficient and slipstream dynamic pressure obtained during the shaft angle sweeps with no cyclic. Data is presented for the three collective pitch angles used: 12°(basic), 10° and 15°. Corresponding values in hover with the 12° collective setting are also shown.

The level of thrust obtained with 12 degrees of collective varied from 51 lbs. in hover to 15 lbs. at zero shaft angle and 9.18 tunnel q. Thrust exhibited the normal increase with shaft angle plus normal intersection of the constant tunnel q/constant RPM curves in the vicinity of 70° shaft angle. See Figures 10 and 13. Note that the thrust continued to increase up to the maximum shaft angle evaluated (120°).

As discussed earlier in the report, the desired values of C_{T_s} were determined prior to the test and the tunnel q was adjusted to produce these values at representative tilt wing shaft angles. The target C_{T_s} values were: .35 at 20°α_p, .60 at 30°, .75 at 40°, and .90 at 45°. See Figure 11.

At these same conditions, slipstream q (q_s) varied from 14.3 to 14.7 lbs/ft^2, respectively, as can be determined from Figure 12. In hover, slipstream q is equivalent to the disc loading (T/A_p) which at 12 degrees collective was measured to be 14.2 lbs/ft^2.

Thrust data acquired at 15° of collective and 1.50 tunnel q is presented in Figures 16 through 18. When compared to the corresponding 12° collective data at 45° shaft angle, the 15° pitch setting increased the slipstream q from 14.7 to 18.1 lbs/ft^2 and the resultant C_{T_s} from .90 to .92.

Figure 19 illustrates the variation of thrust with collective for zero, 30, 60, and 90 degrees of shaft angle and 1.50 tunnel q. The data indicates that the increase in thrust with collective departs from the normal linear variation at pitch angles above approximately 13.5°. This could have resulted from the inboard section of the blade commencing to stall as a result of the high twist in this region.

The variation of thrust with advance ratio at zero and 60° shaft angles is shown in Figure 20 to further illustrate the model propeller thrust characteristics.

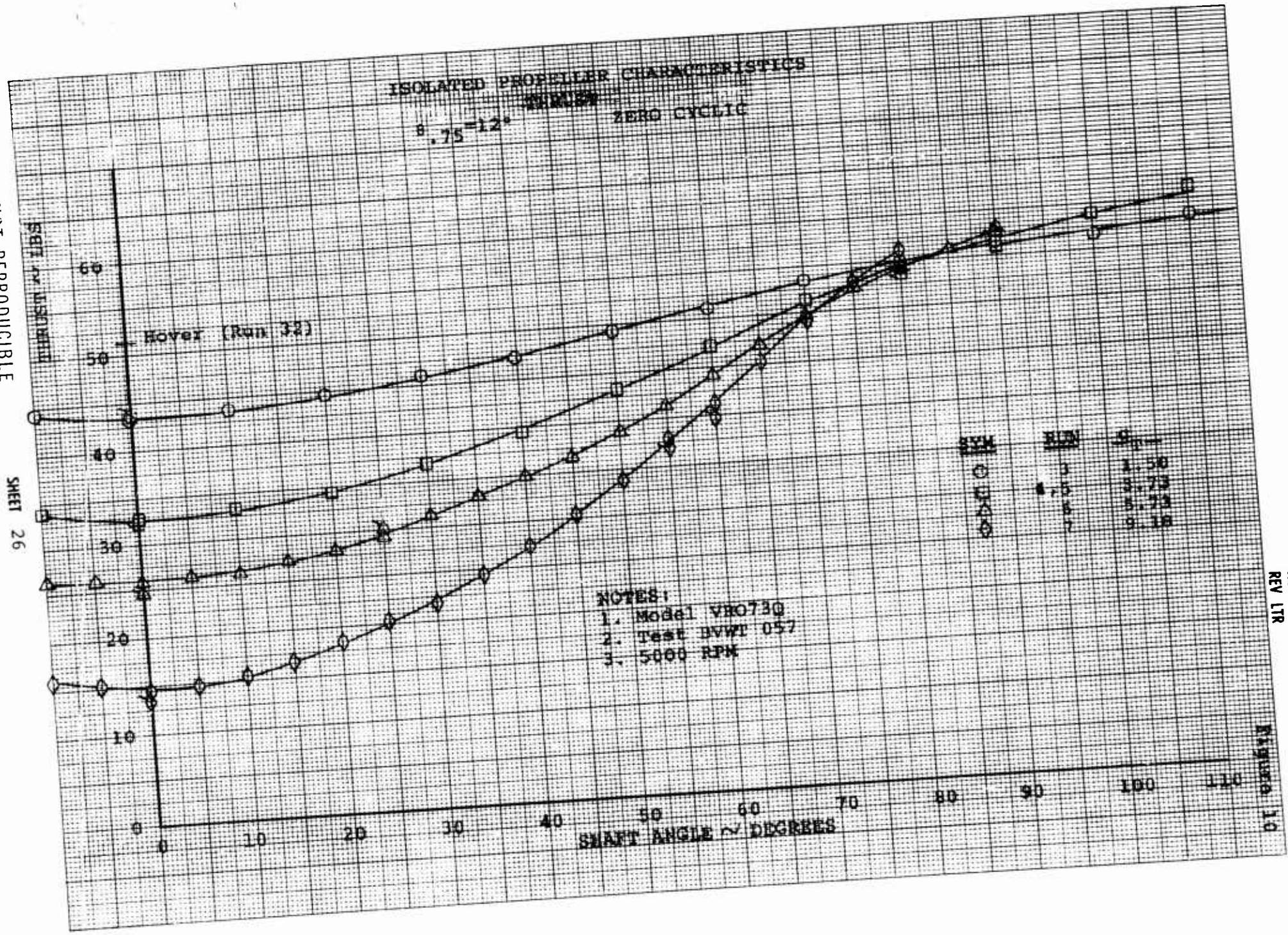

NOT REPRODUCIBLE

SHEET 26

NUMBER D170-10037-1
REV LTR

Printed in U.S.A.

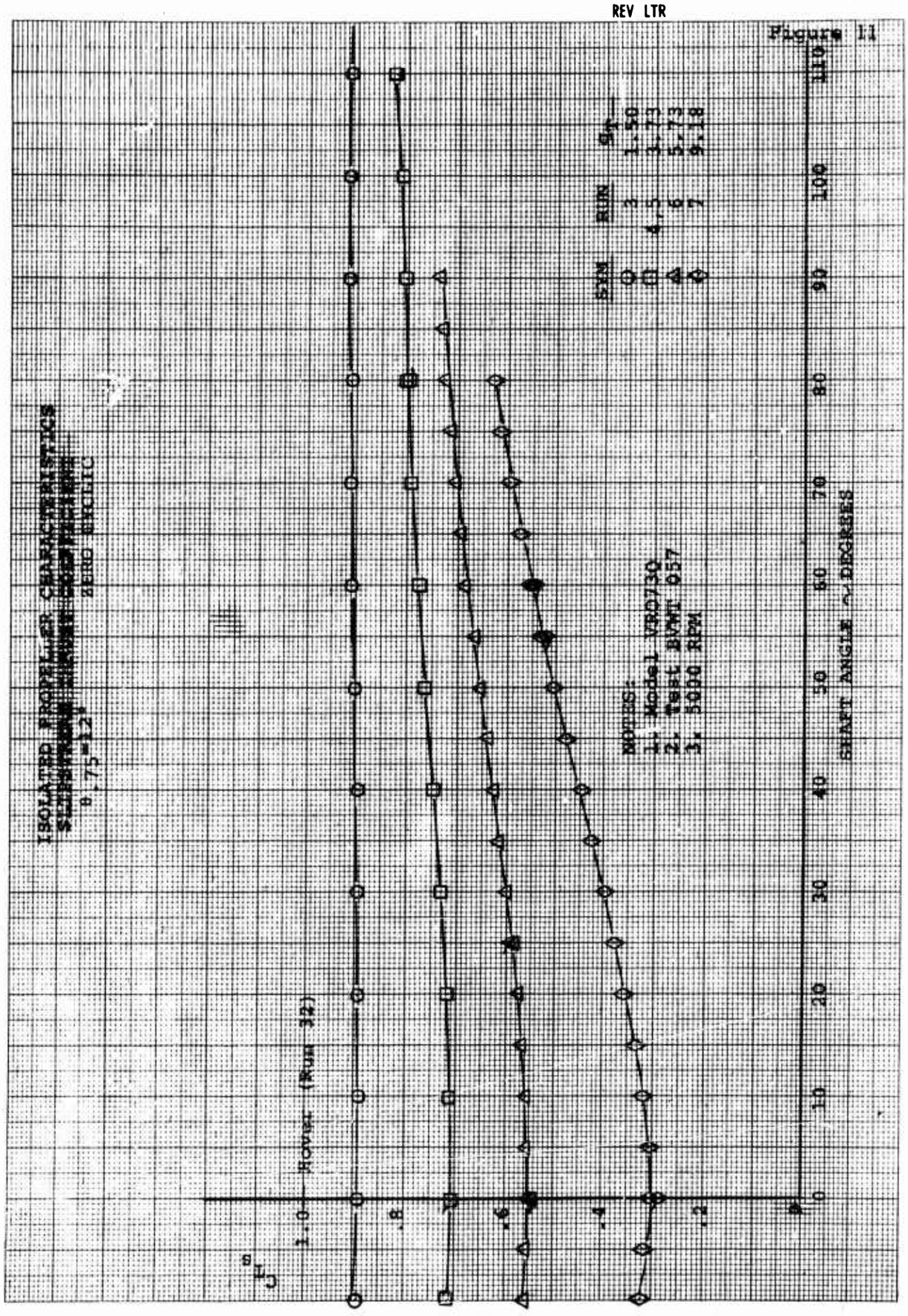

Figure 11

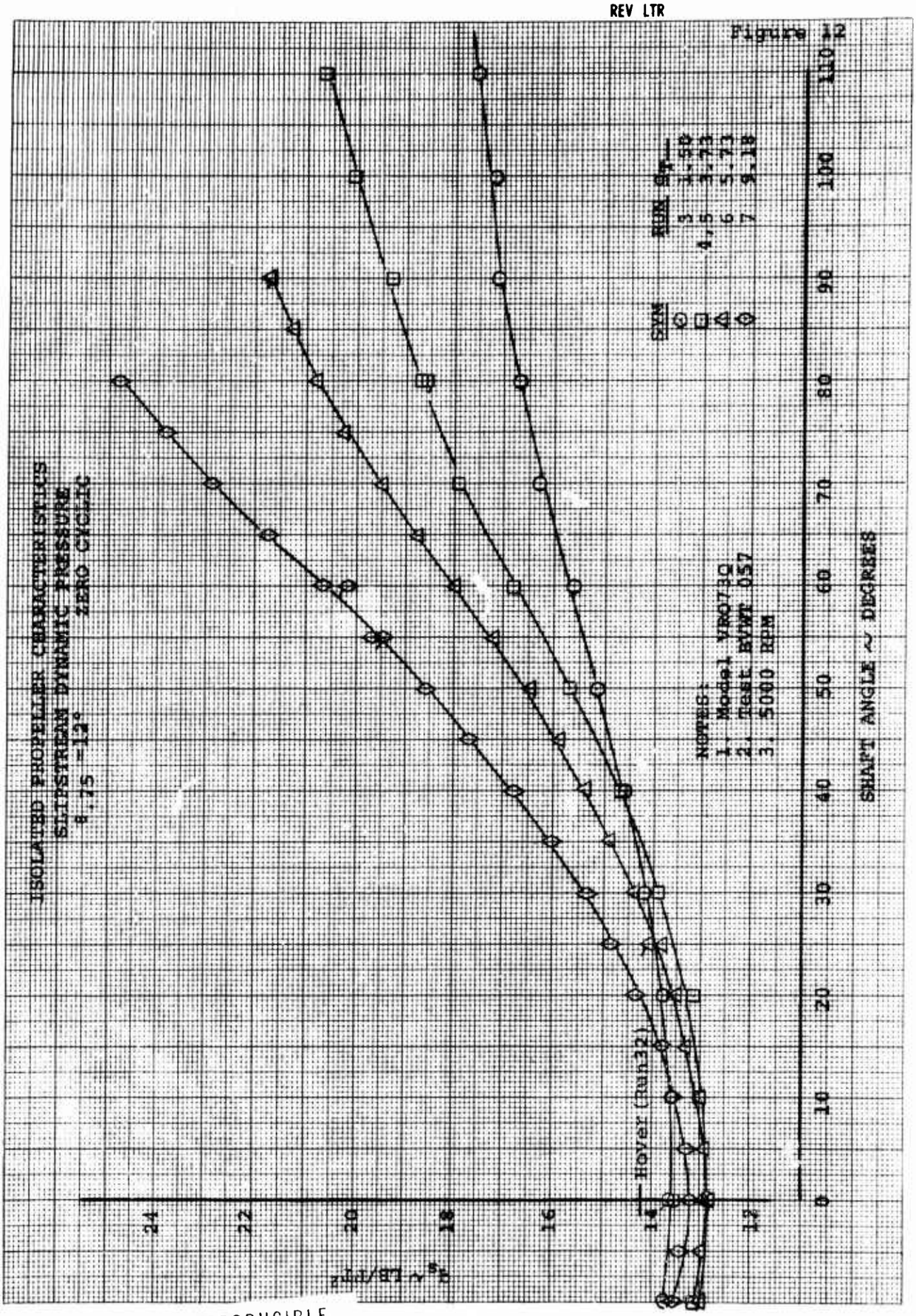

Figure 12

NUMBER
REV LTR

Figure 13

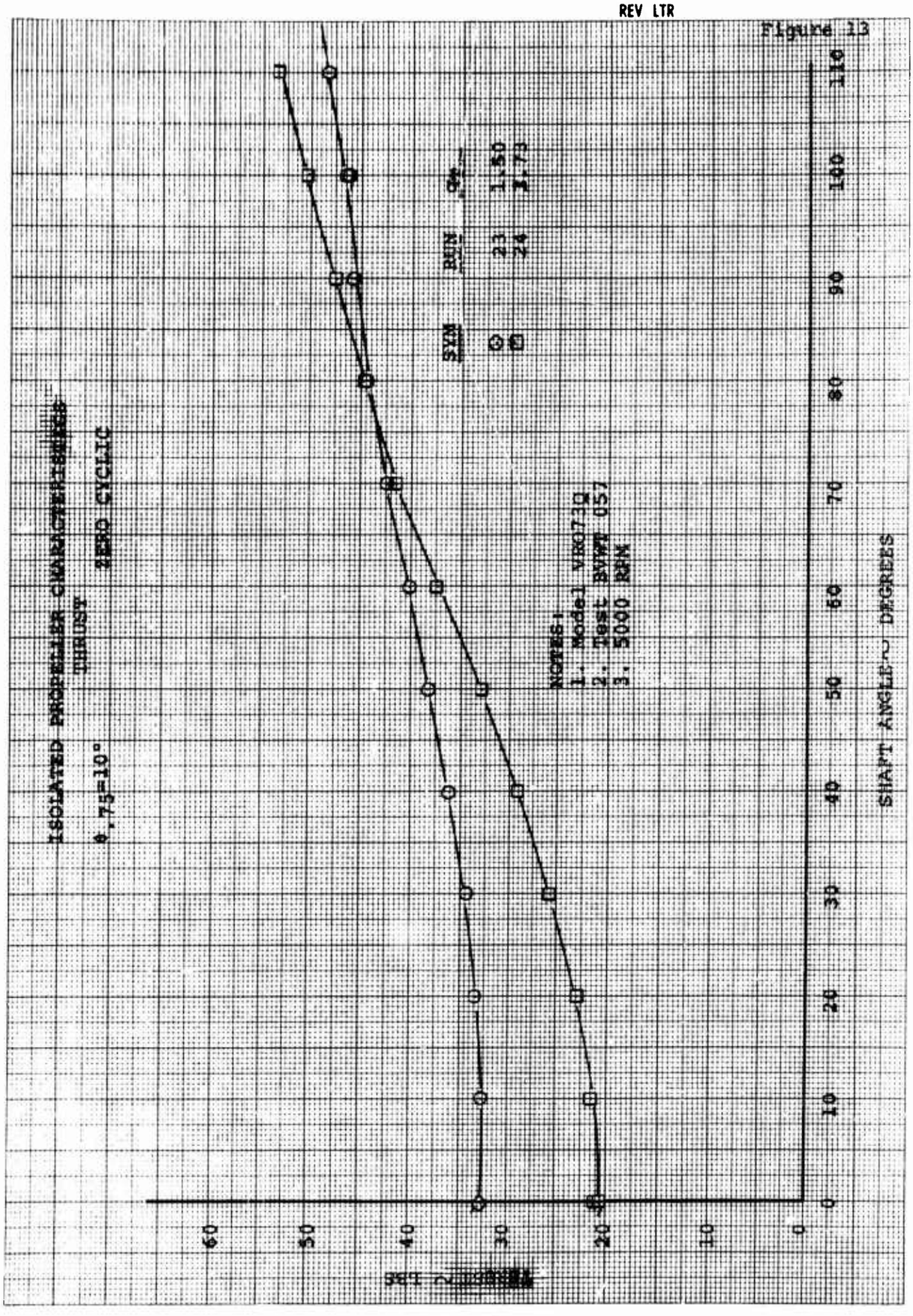

EUGENE DIETZGEN CO.
MADE IN U. S. A.

NO. 340R-MP DIETZGEN GRAPH PAPER
MILLIMETER

Figure 14

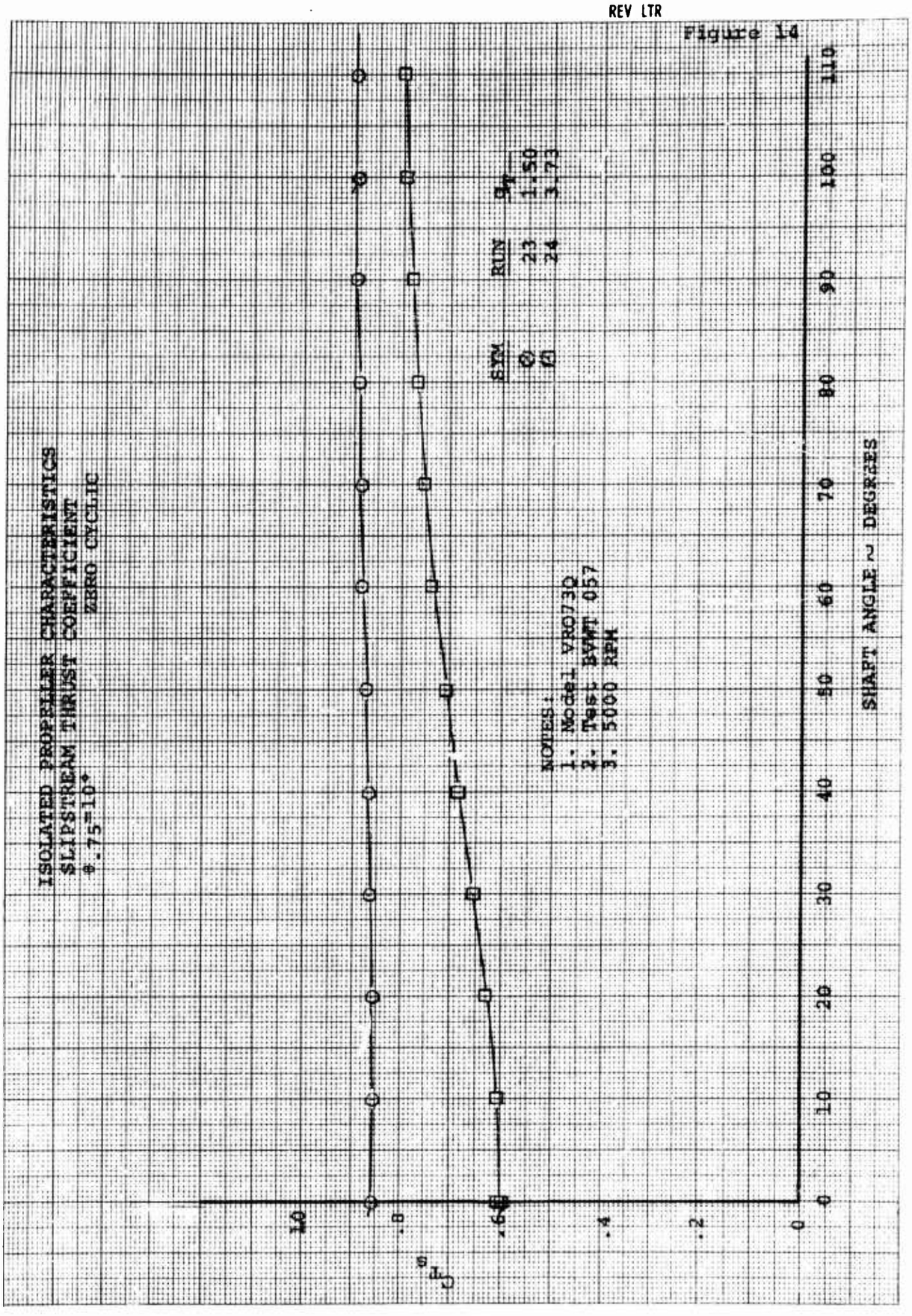

Figure 15

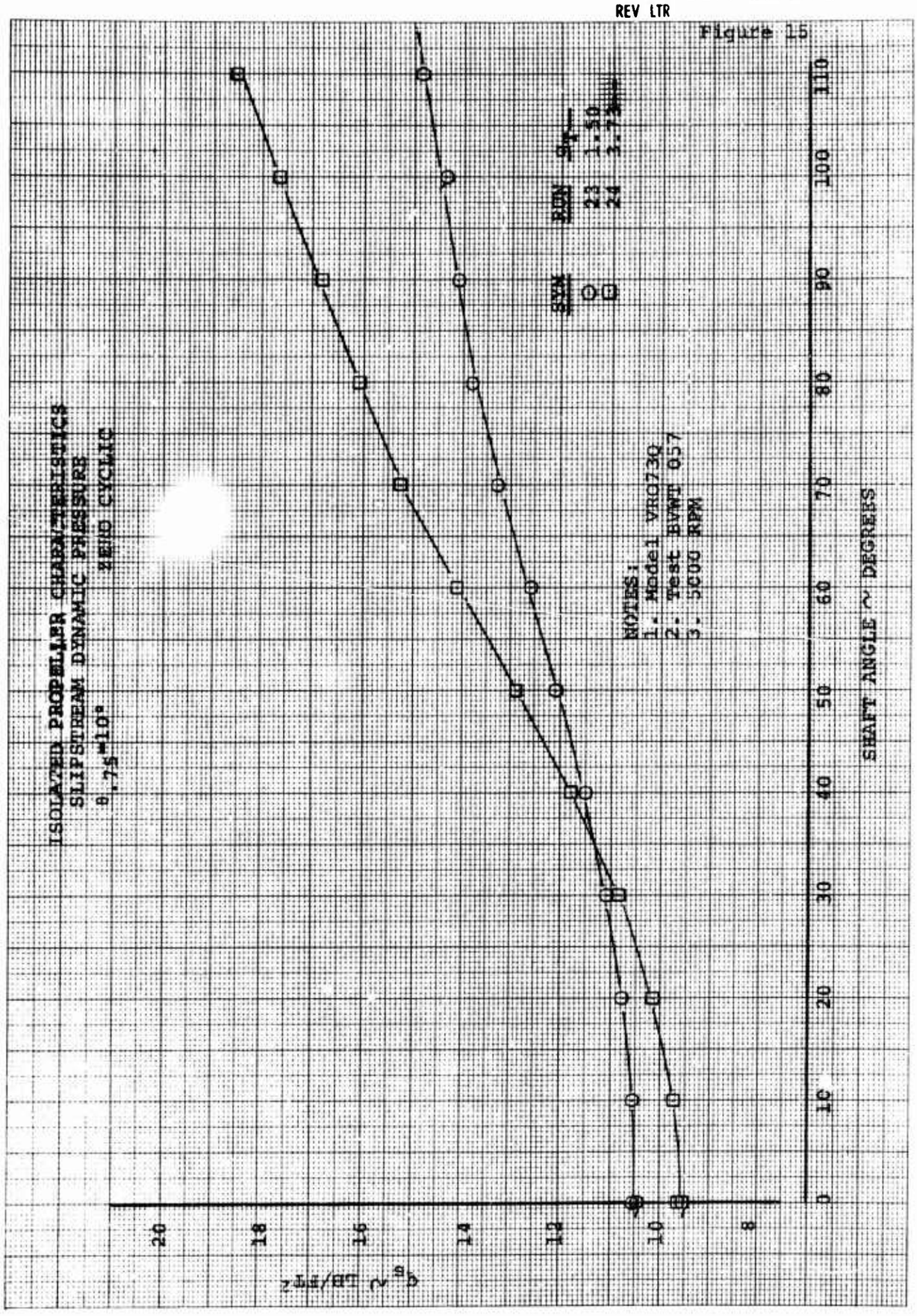

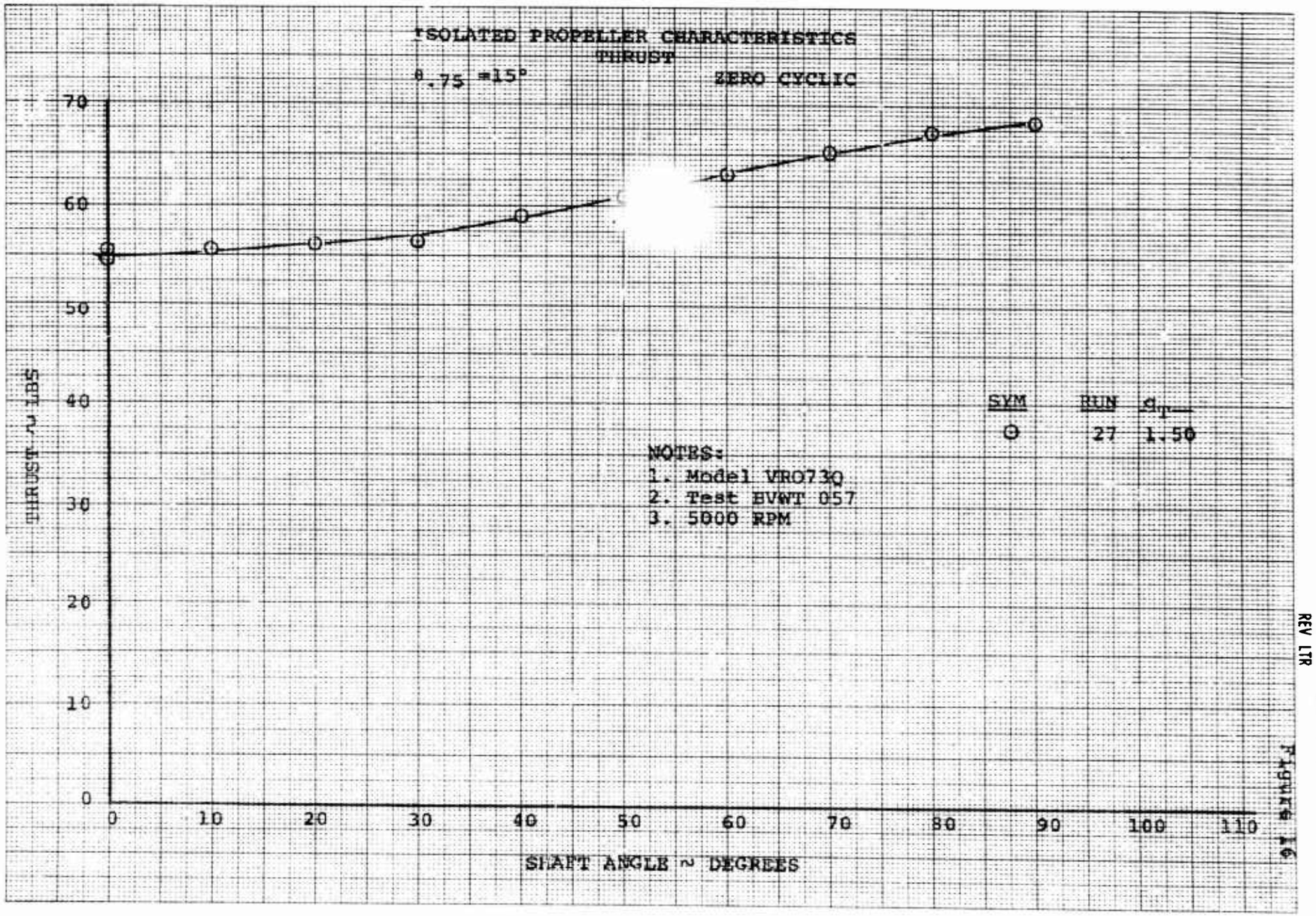

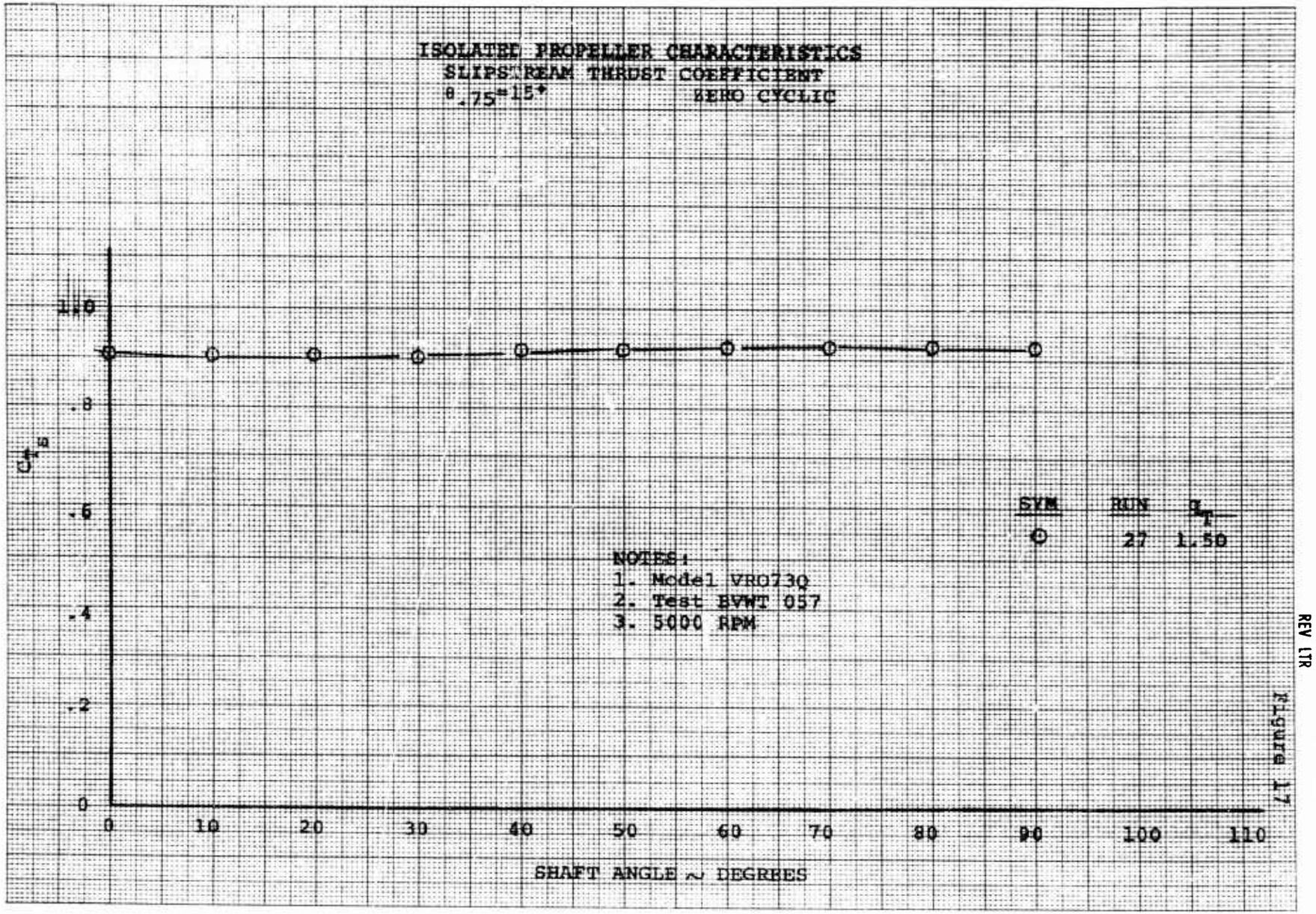
ISOLATED PROPELLER CHARACTERISTICS
SLIPSTREAM THRUST COEFFICIENT
θ.75=15°
ZERO CYCLIC
1.0
.8
.6
.4
.2
0
C_{T_s}
0
10
20
30
40
50
60
70
80
90
100
110
SHAFT ANGLE ~ DEGREES
SYM
RUN
q_T
27
1.50
NOTES:
1. Model VRO730
2. Test BVWT 057
3. 5000 RPM

Figure 17

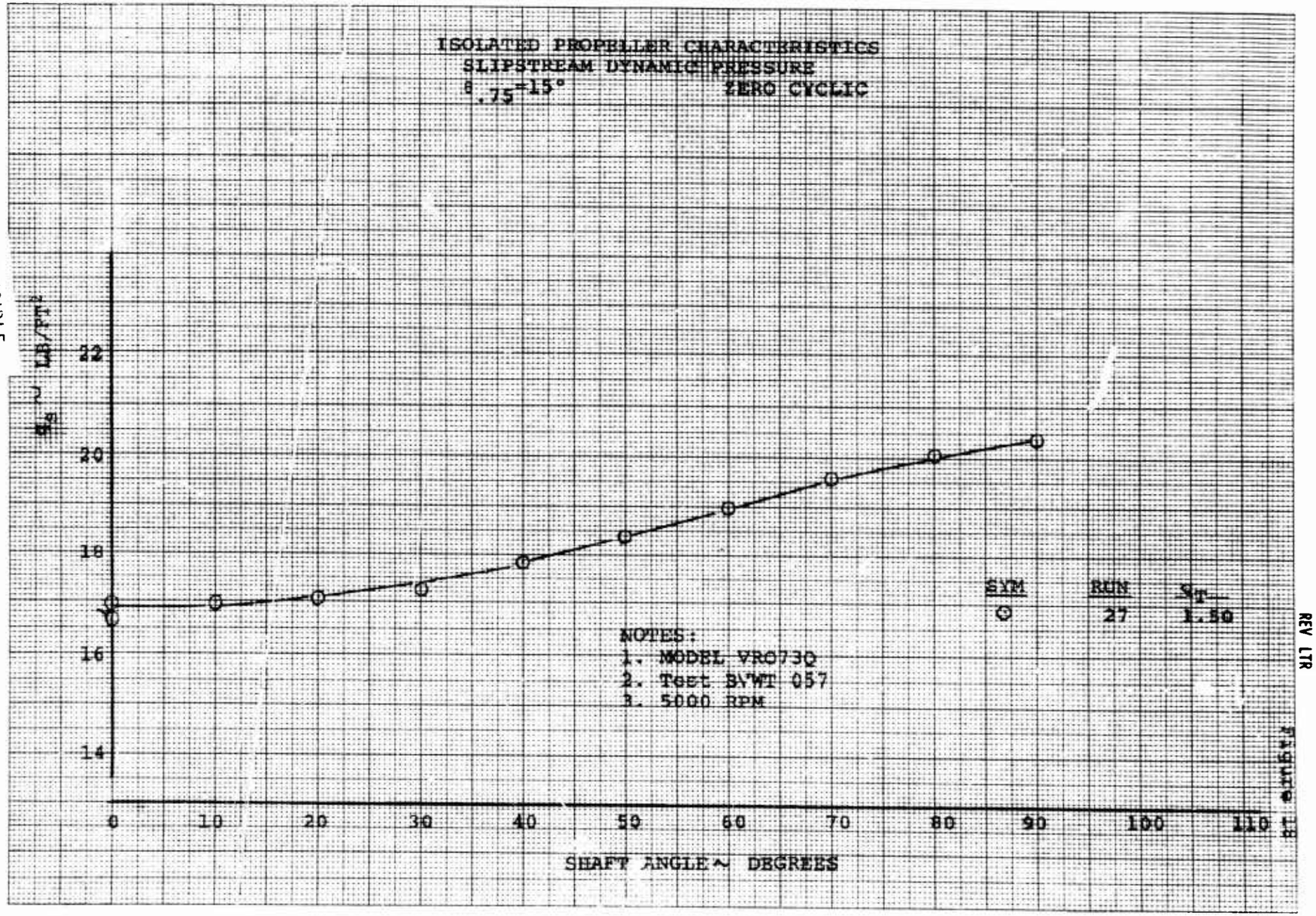

Figure 19

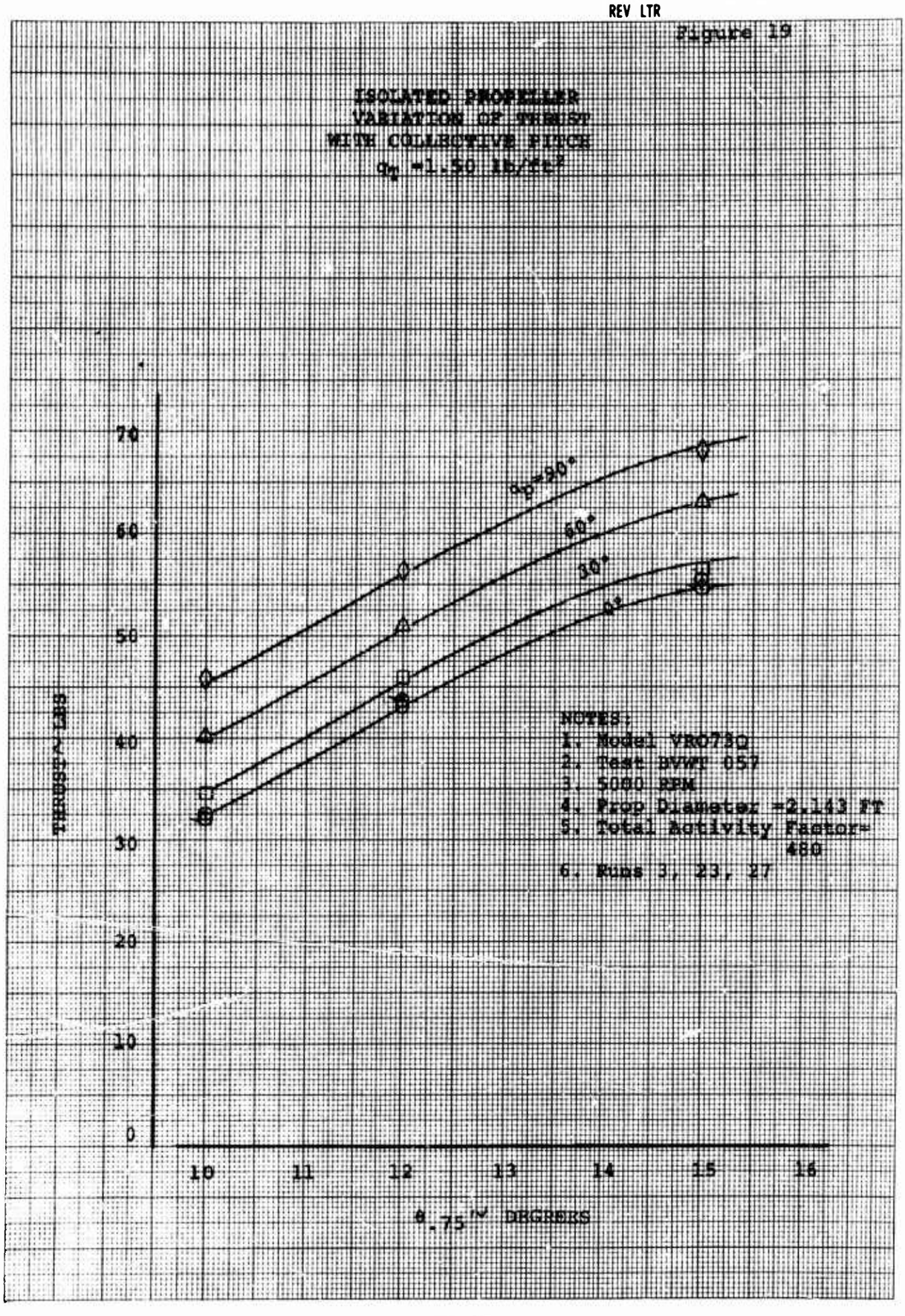

Figure 29

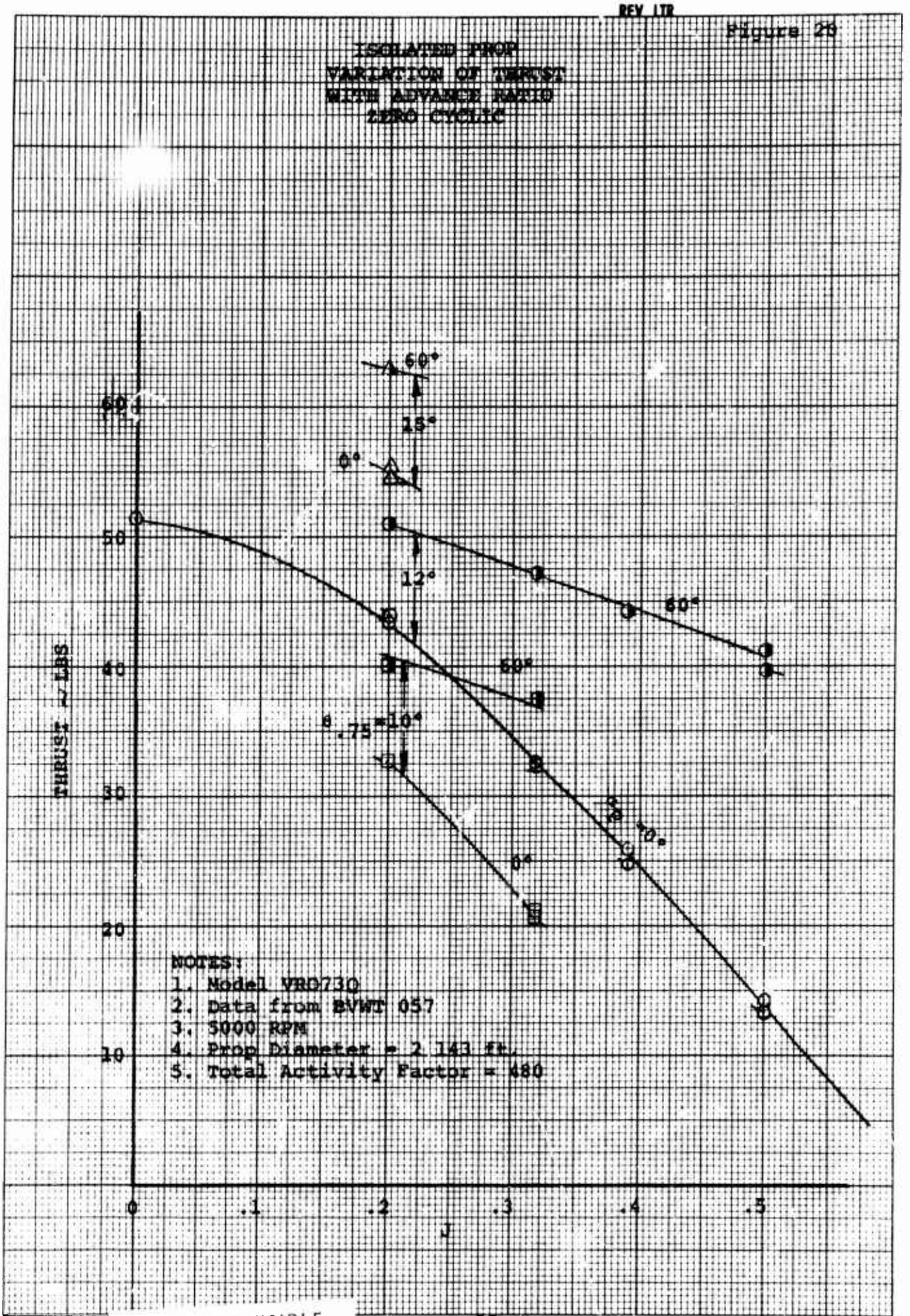

6.2 CYCLIC PITCH EFFECTIVENESS

The data showing the effectiveness of the cyclic pitch propeller in producing pitching moment over the shaft angle range and advance ratios tested is presented in this section.

Figure 21 shows that the hub pitching moment produced per degree of cyclic (-.0021) is essentially constant from hover up to an advance ratio of 0.4 at a shaft angle of 60°. An increase (approximately 12%) at a higher advance ratio is indicated. Cyclic pitch effectiveness varied only slightly with collective setting over the range evaluated.

The linearity of incremental hub pitching moment due to cyclic pitch over the cyclic pitch angle range tested (-8° to +8°) is illustrated in Figure 22 (hover case) and Figure 23 (1.50 tunnel q or 0.2J). Further indications of the linearity are presented in Figures 24 through Figure 28 (which include data from all 12° and 10° collective runs.)

Figures 24 through 28 and Figure 29 (15° collective case) also show that the incremental hub pitching moment due to cyclic pitch is virtually independent of shaft angle up to 90° (ΔC_{m_p} increases an average of 4%, from zero shaft angle to 60° over the speed range and collective settings tested). The exception is the 120° shaft angle case with positive cyclic which was evaluated for both 12° and 10° of collective at the lowest advance ratio. See Figures 23 and 29. As can be noted, the slope of the $\Delta C_{m_p} \sim \gamma$ line is significantly less than the slope shown for lower shaft angles. An explanation is given in a later paragraph.

The incremental hub pitching moment plots (Figures 23 through Figure 29) were developed from the hub pitching moment vs shaft angle plots presented in Figures 30 through 36. Each plot presents the cyclic pitch data acquired from the series of runs performed at a particular collective pitch setting and tunnel q.

Considering the 12° collective/0.2J case (Figure 30), it is seen that the hub pitching moment increases continuously from zero shaft angle to approximately 90° for all cyclic pitch settings. Above 90° of shaft angle, the pitching moment curves for +8°, +6° and +4° of cyclic continue to increase up to the maximum shaft angle tested (120°). At zero cyclic a pitching moment "break" can be observed at 120° of shaft angle. This "break" in the zero cyclic curve produced the decrease in incremental hub pitching moment with positive cyclic for 120° of shaft angle, noted earlier. See Figure 23.

The pitching moment "break" recorded with zero cyclic at 120° of shaft angle, occurs at successively lower shaft angles as the negative cyclic angle is increased. Indications of the pitching moment reaching a maximum value by the "rounding" of the curves at 110° of shaft angle are also apparent in Figure 31 which presents similar 12° collective data except at a higher advance ratio or tunnel q.

Figure 21

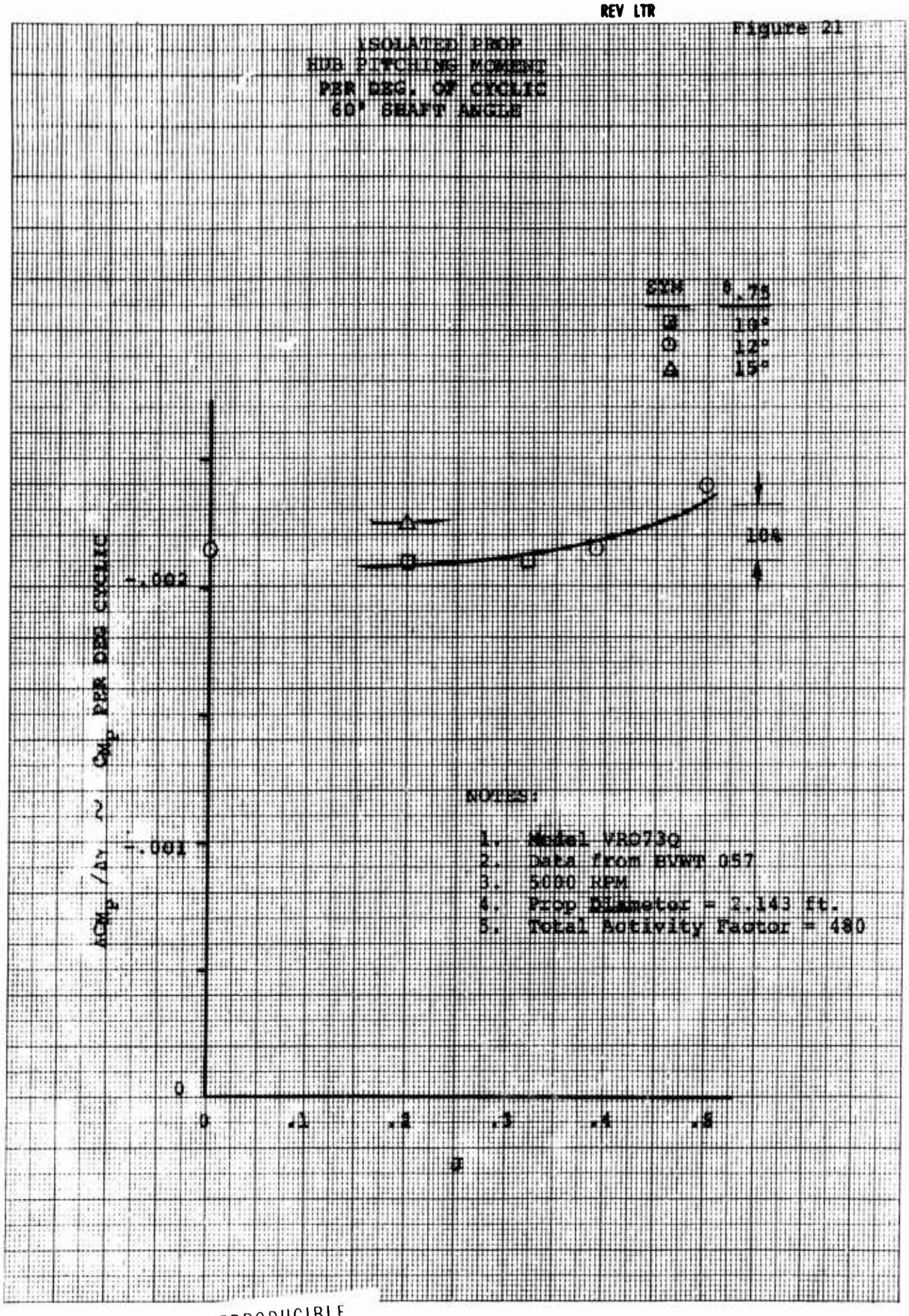

Figure 22

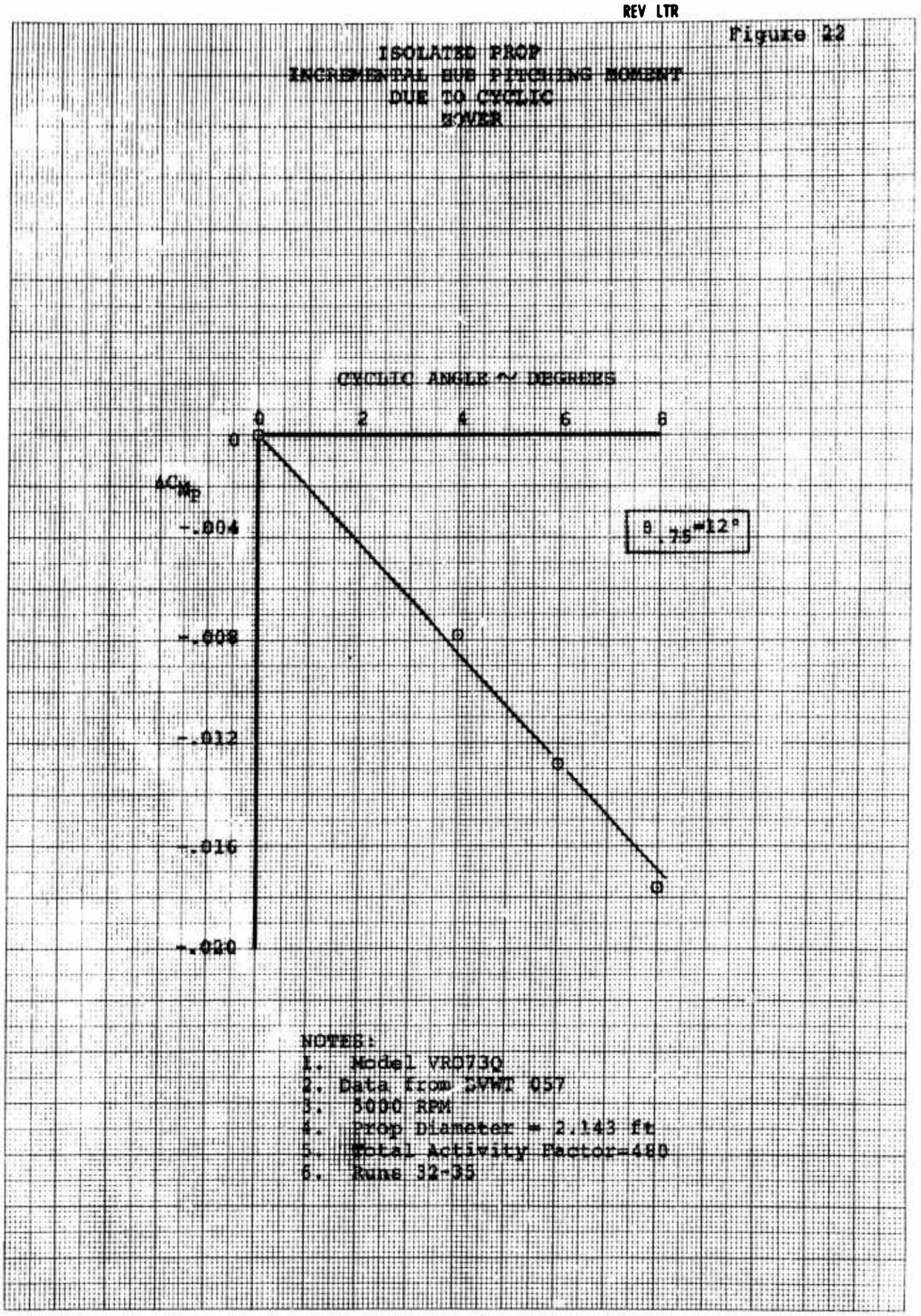

NUMBER
REV LTR

Figure 23

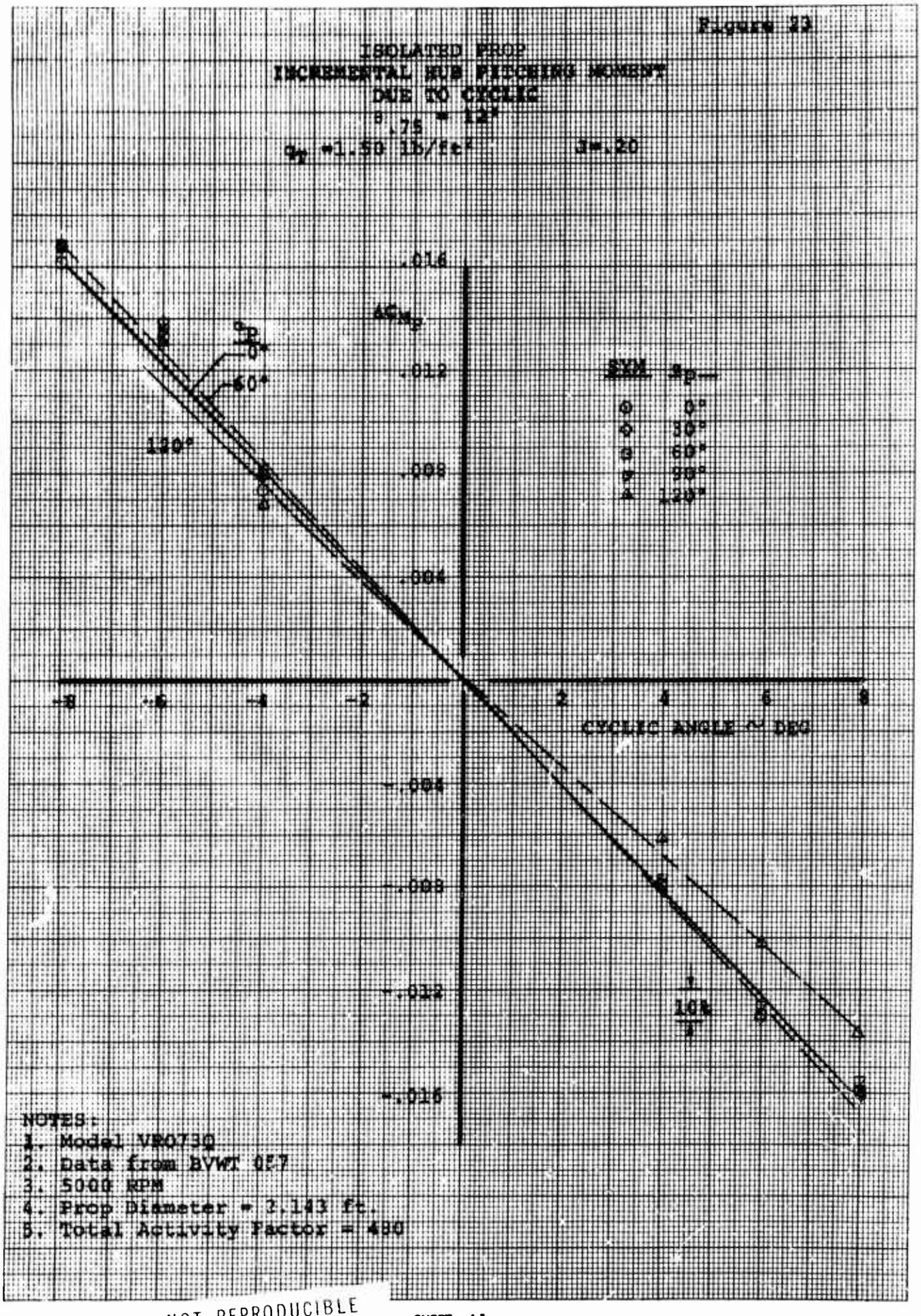

NOTES:
1. Model VR0730
2. Data from BVWT 057
3. 5000 RPM
4. Prop Diameter = 3.143 ft.
5. Total Activity Factor = 480

EUGENE DIETZGEN CO.
MADE IN U.S.A.

NO. 340R-MP DIETZGEN GRAPH PAPER
MILLIMETER

Figure 24

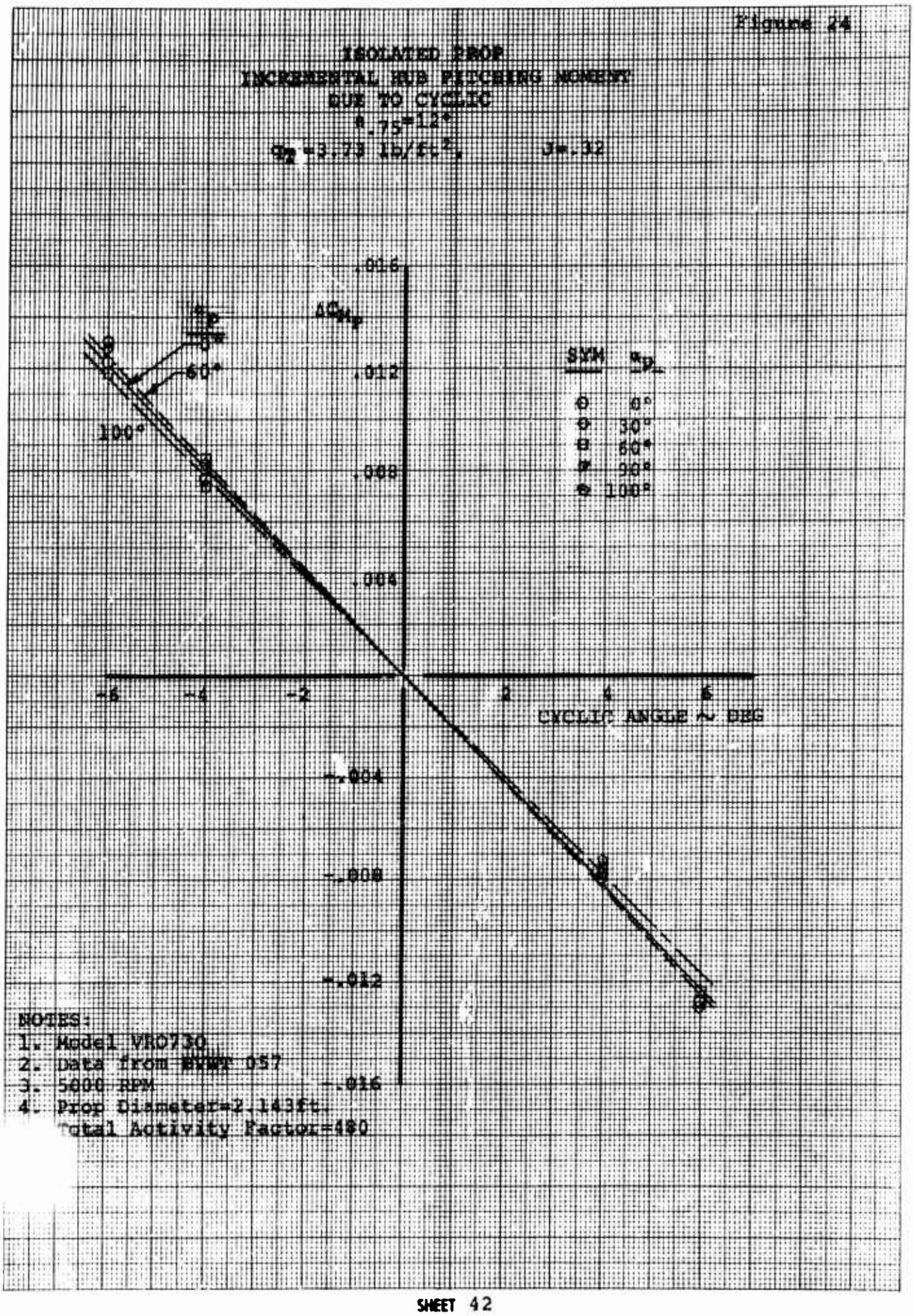

Figure 25

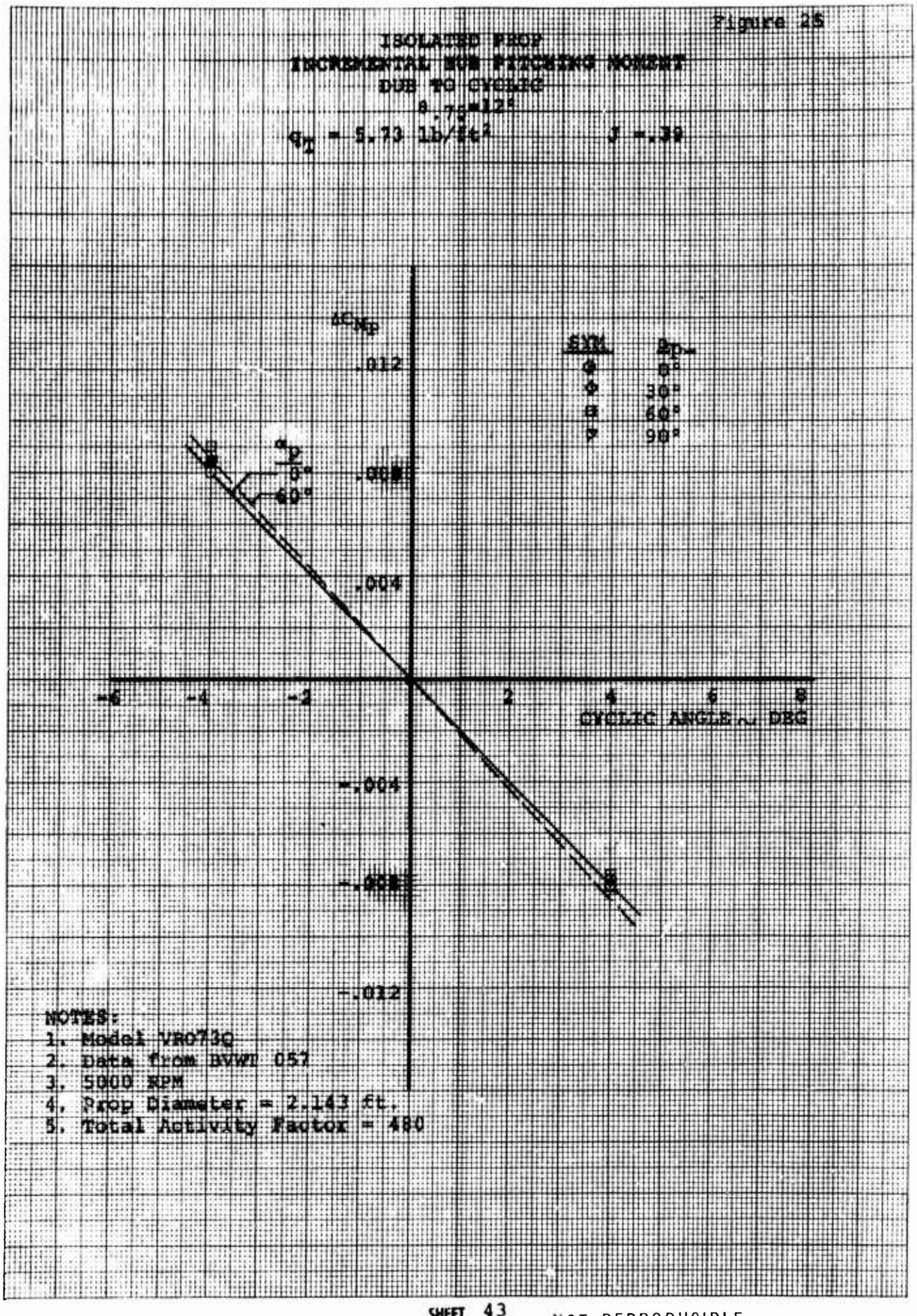

Figure# 26

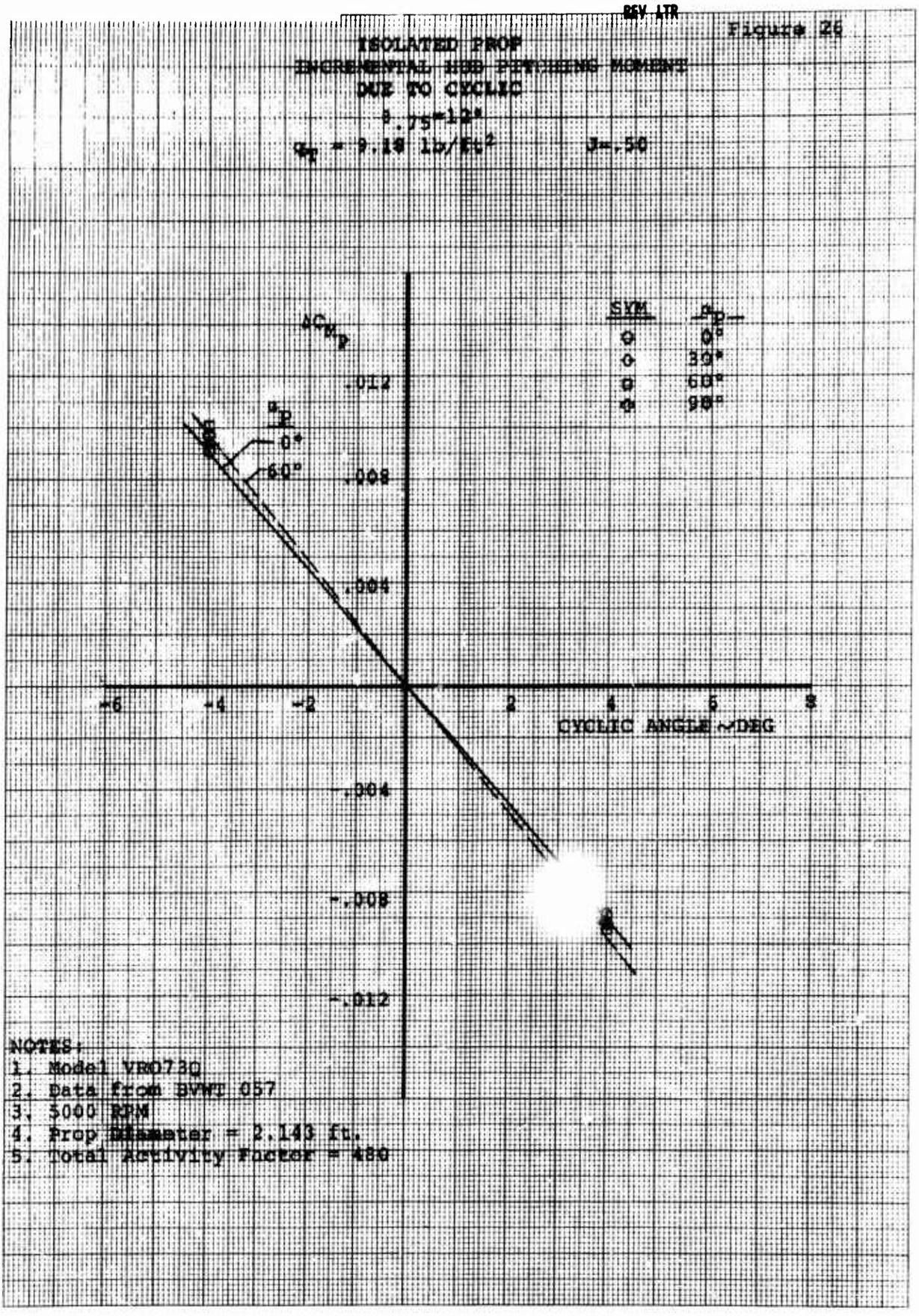

NOTES:
1. Model VRO730
2. Data from BVWT 057
3. 5000 RPM
4. Prop Diameter = 2.143 ft.
5. Total Activity Factor = 480

Figure 27

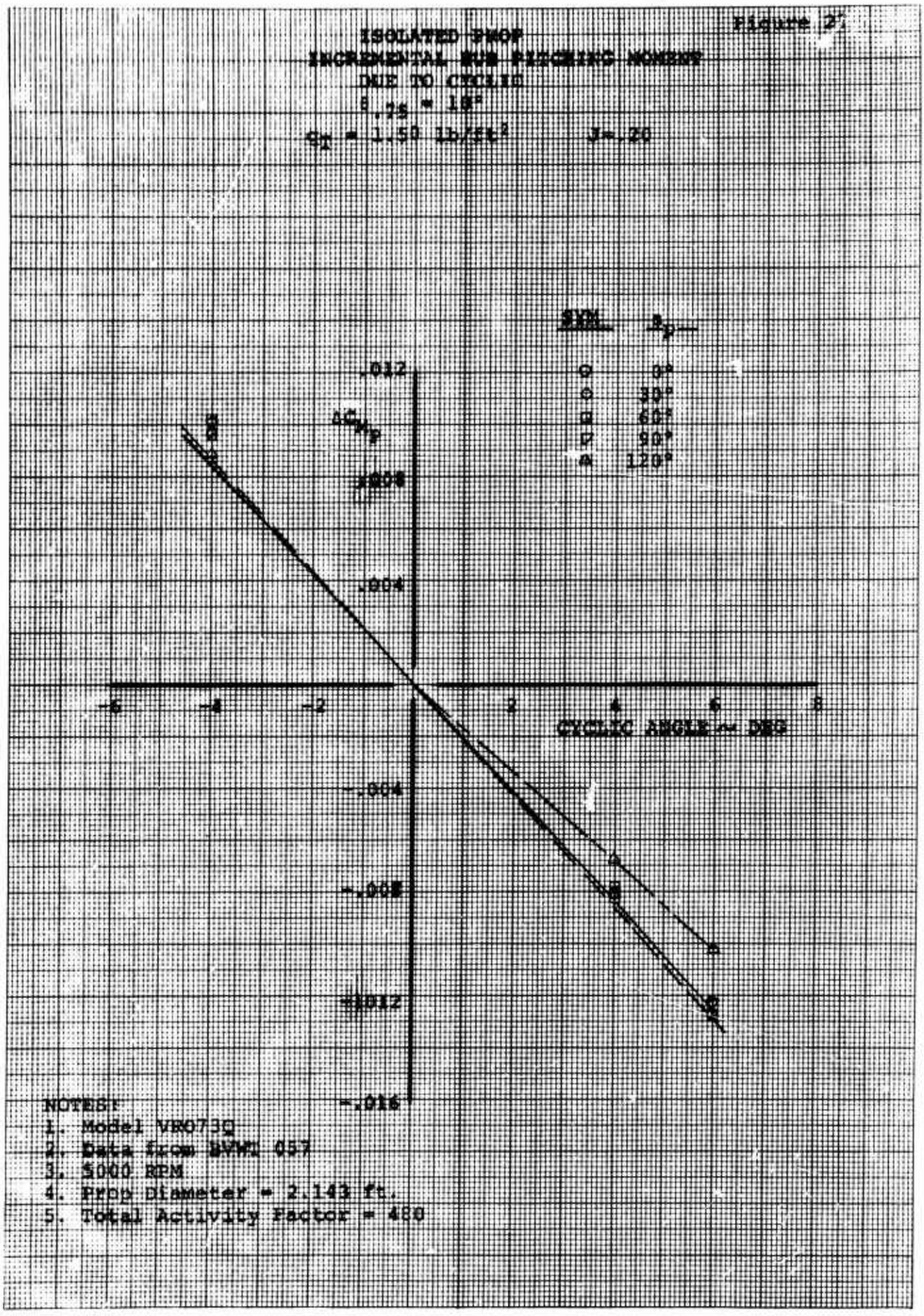

NOTES:
1. Model VR0730
2. Data from BVWT 057
3. 5000 RPM
4. Prop Diameter = 2.143 ft.
5. Total Activity Factor = 480

Figure 28

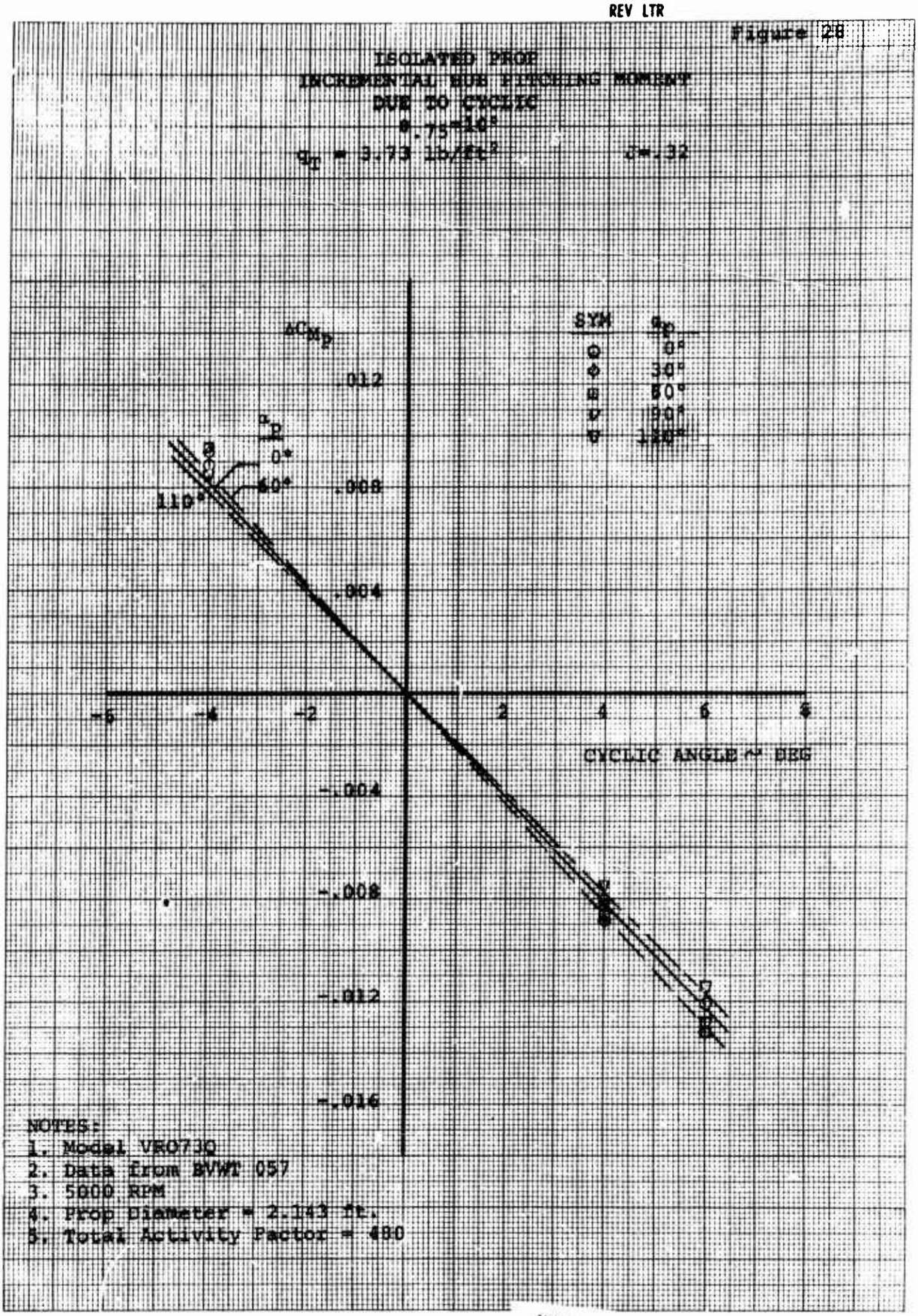

NOTES:
1. Model VR0730
2. Data from BVWT 057
3. 5000 RPM
4. Prop Diameter = 2.143 ft.
5. Total Activity Factor = 480

Figure 22

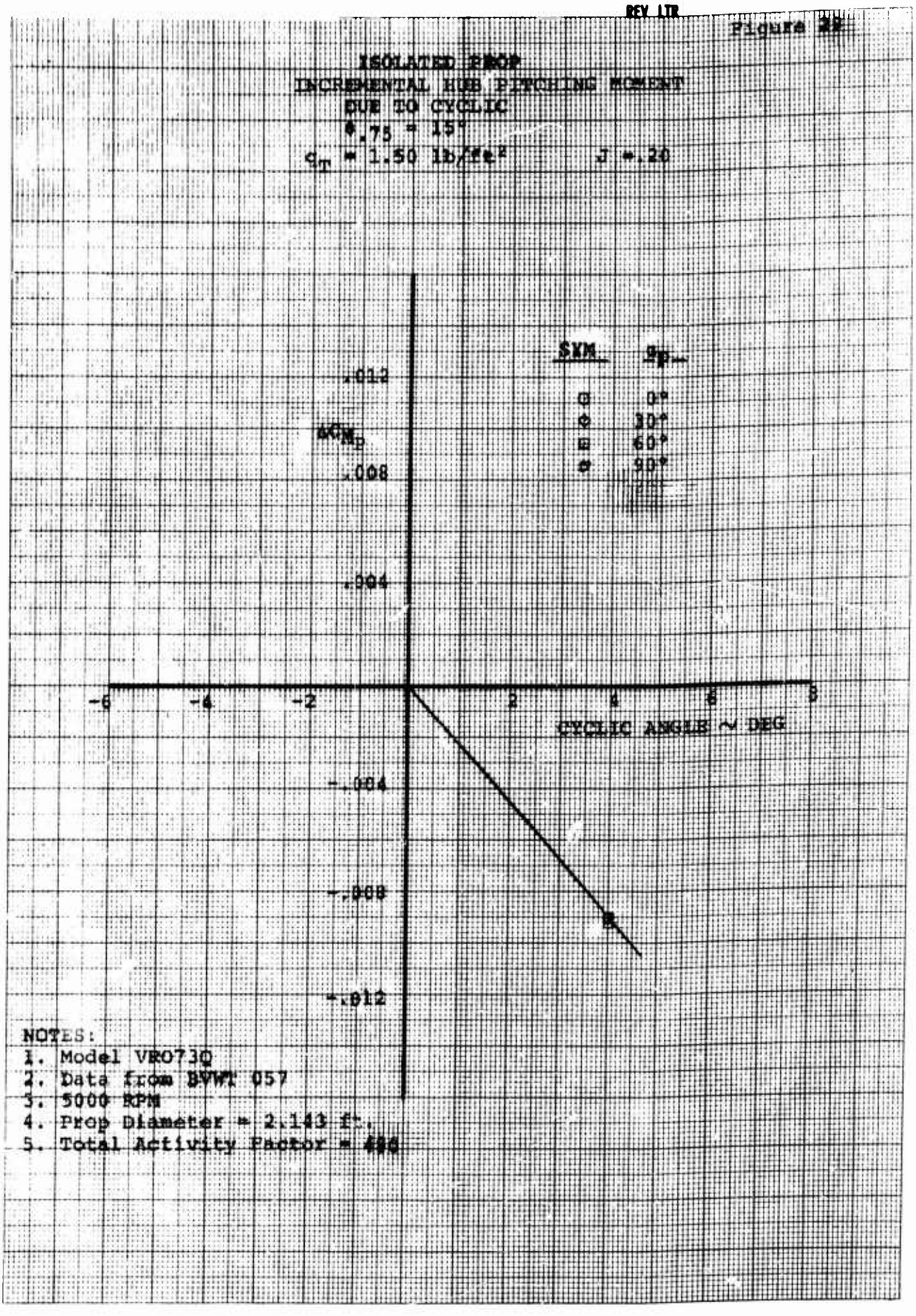

NOTES:
1. Model VRO73Q
2. Data from BVWT 057
3. 5000 RPM
4. Prop Diameter = 2.143 ft.
5. Total Activity Factor = 486

Figure 30

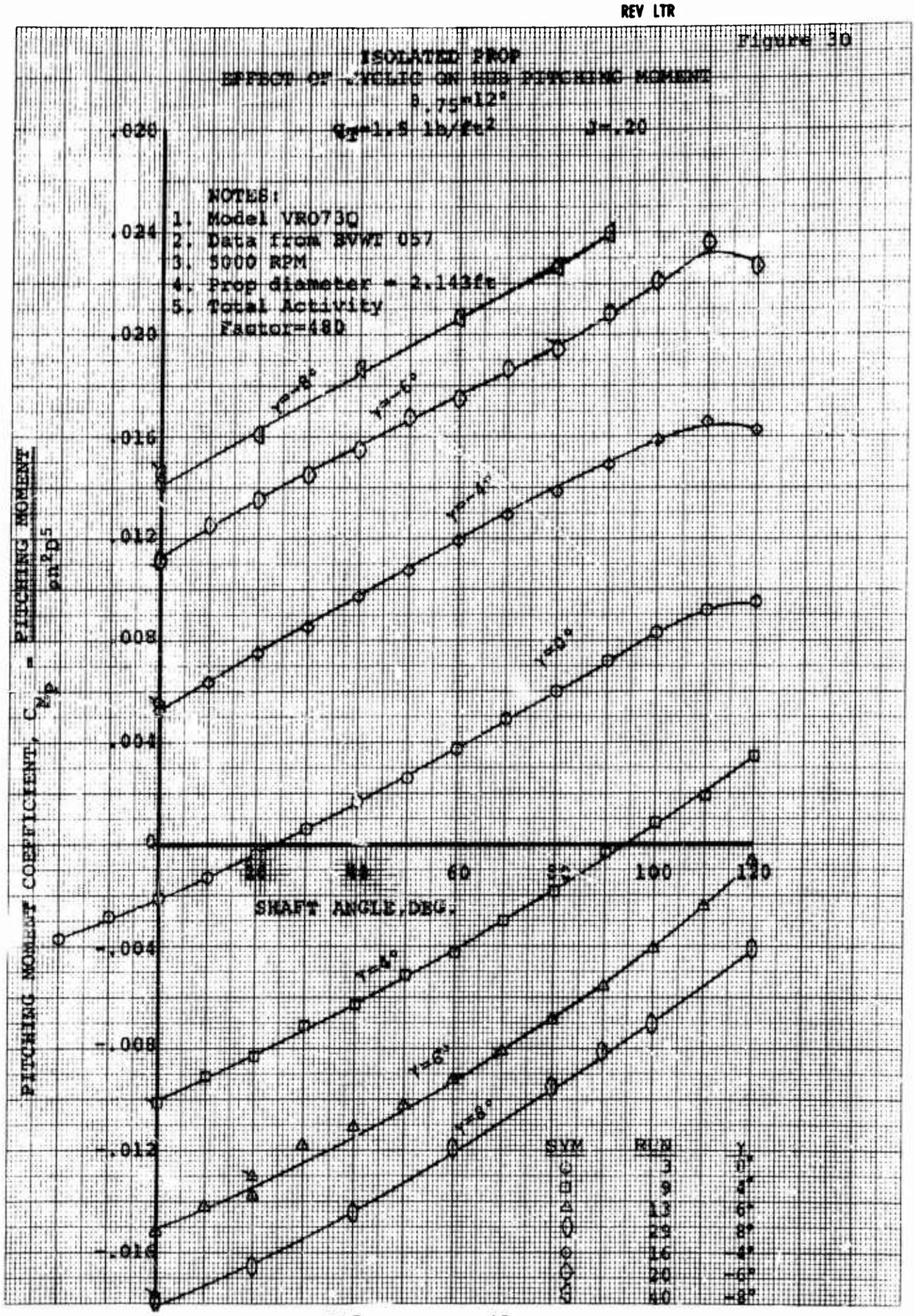

NUMBER
REV LTR

Figure 31

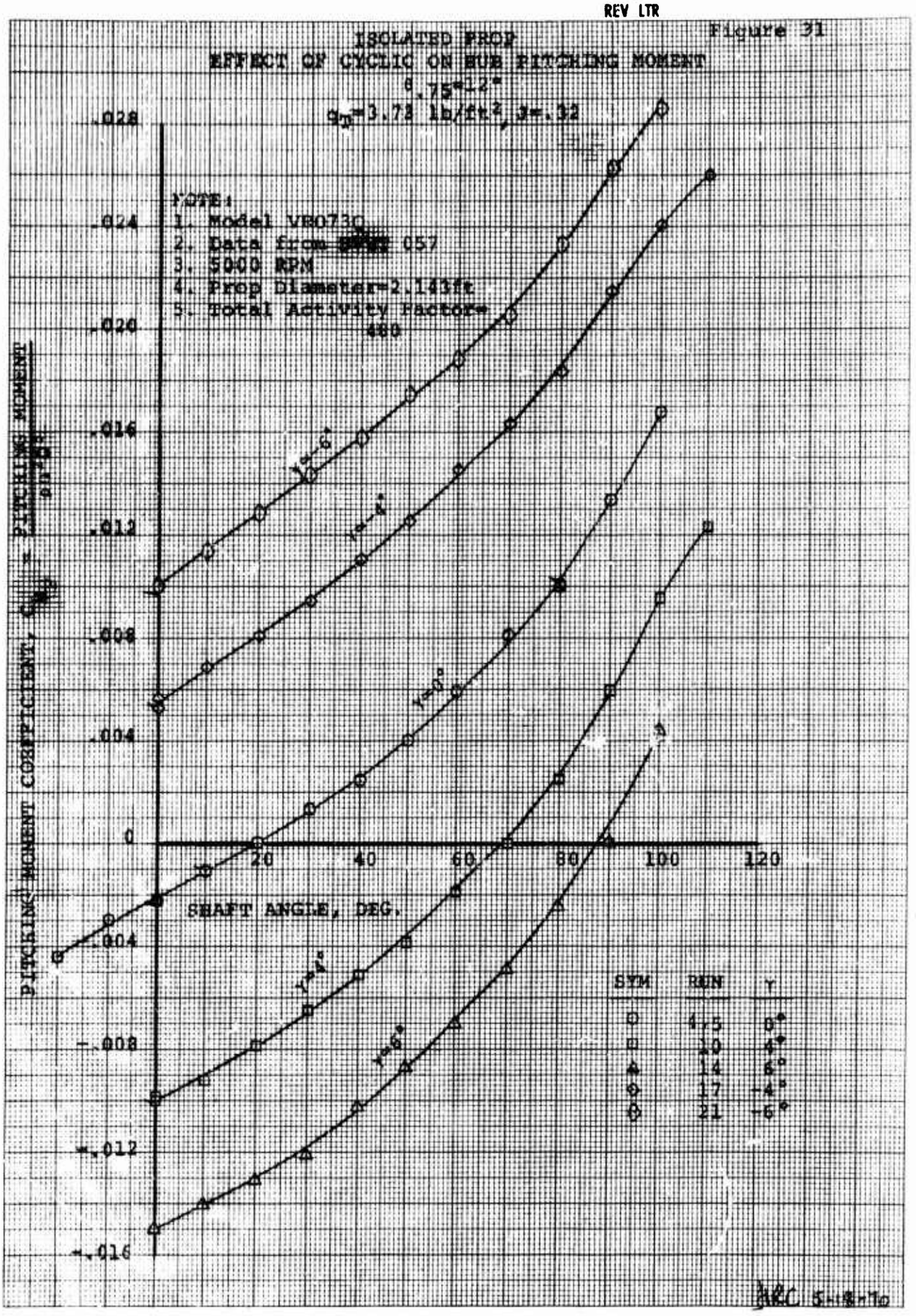

Figure 32

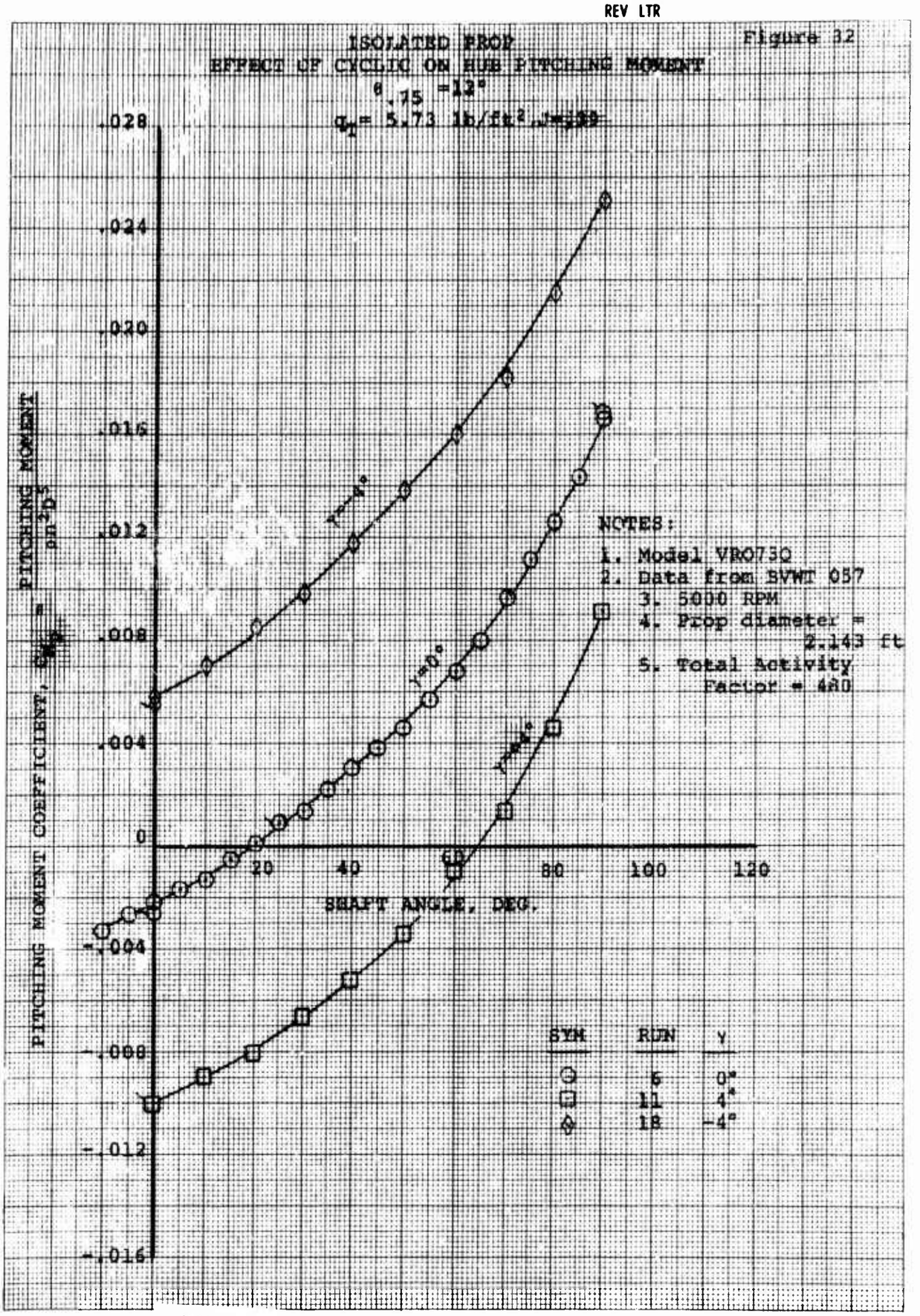

NUMBER
REV LTR

Figure 24

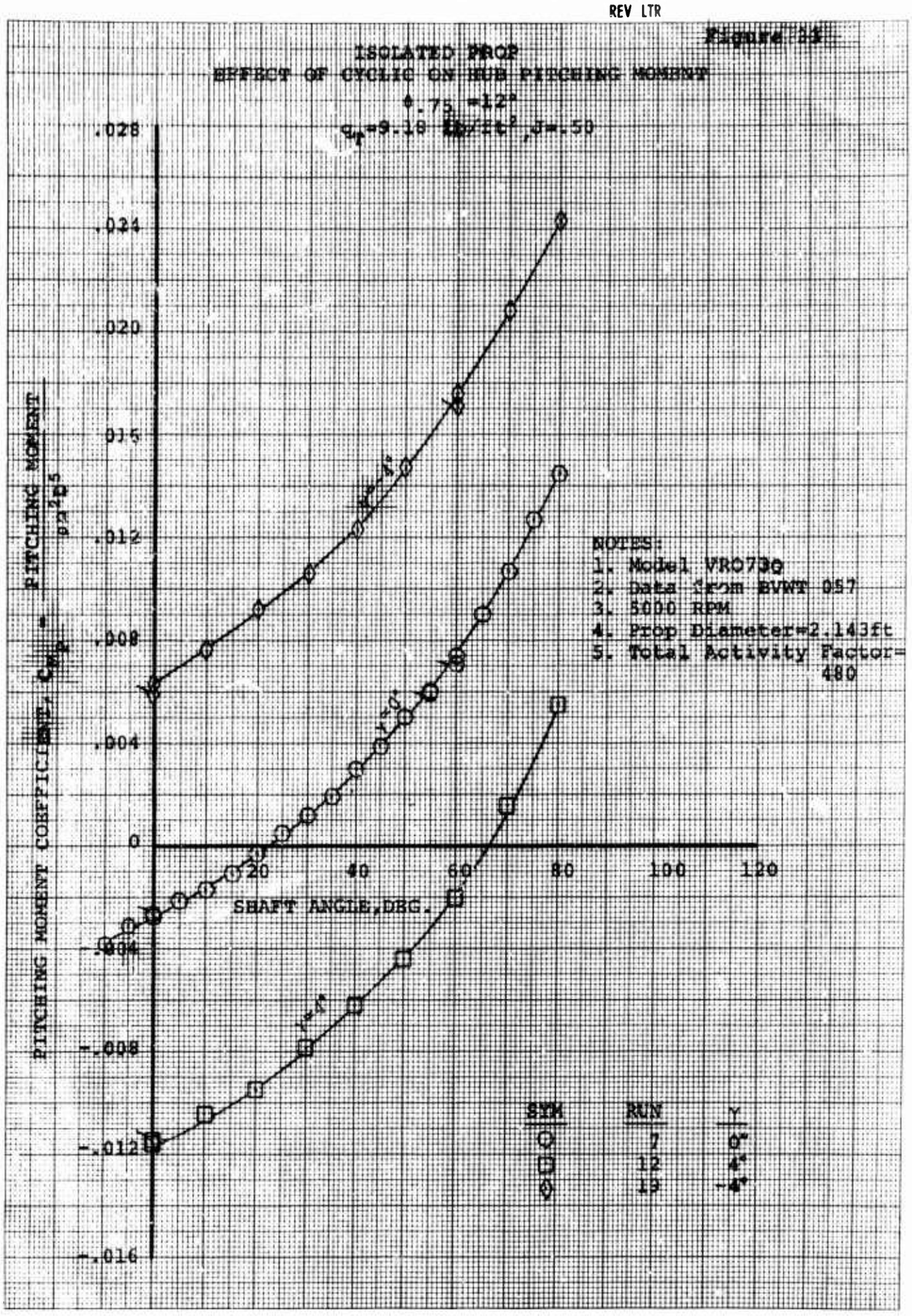

Figure 34

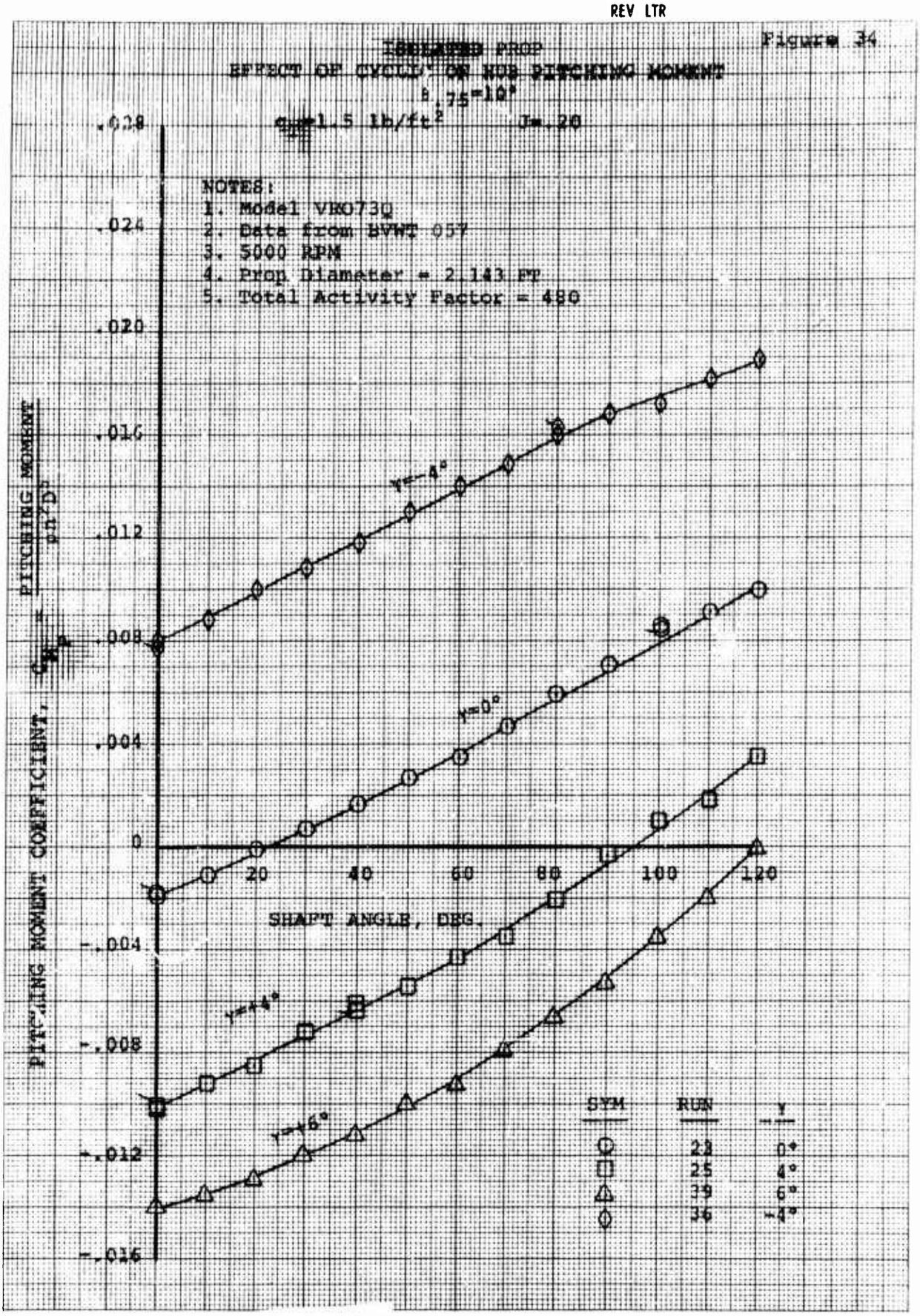

NOT REPRODUCIBLE

Figure 35

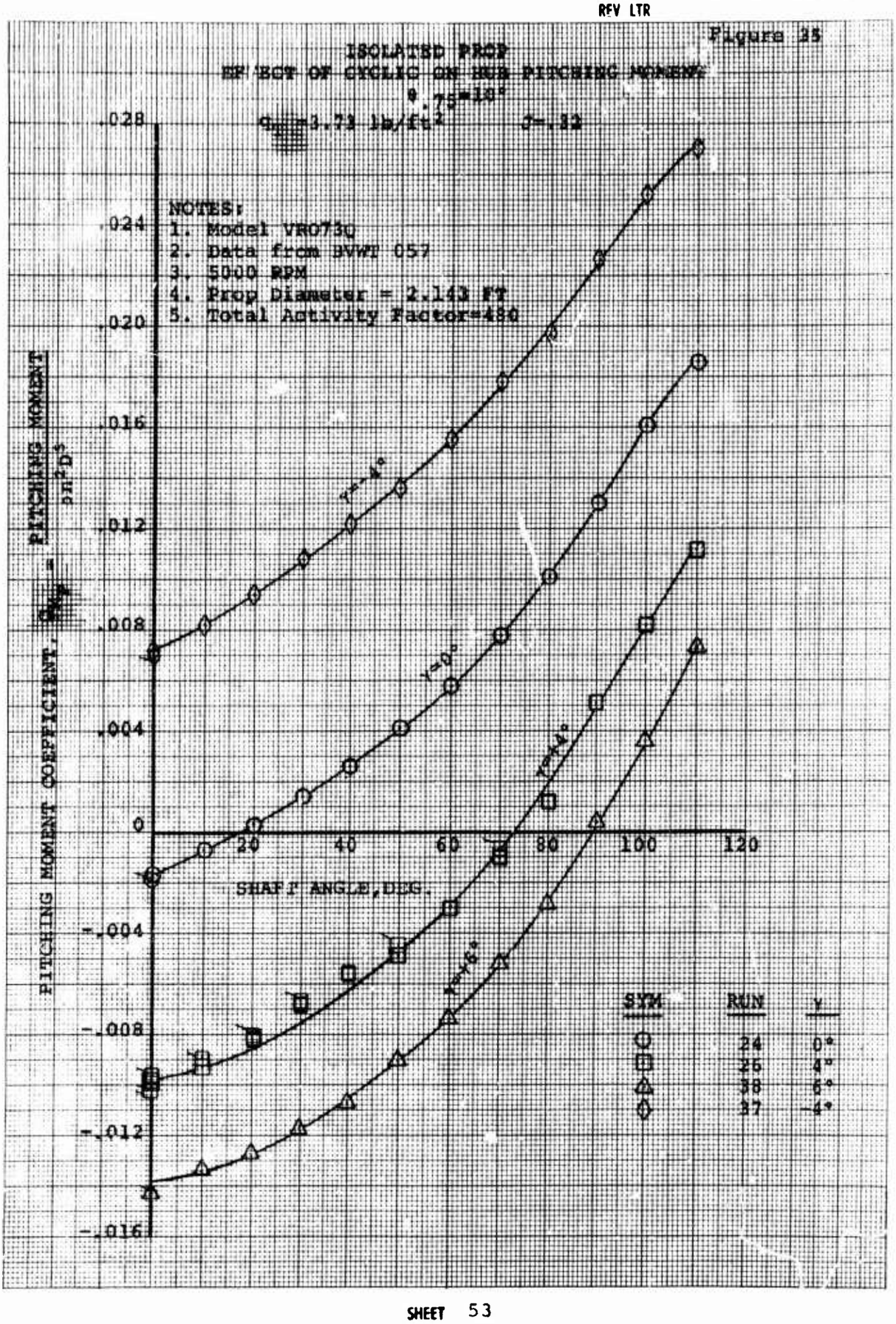

Figure 36

ISOLATED PROP
EFFECT OF CYCLIC ON HUB PITCHING MOMENT
$\theta_{.75}=25°$
$\rho_{SL}=1.5$ lb/ft^2, J=.20

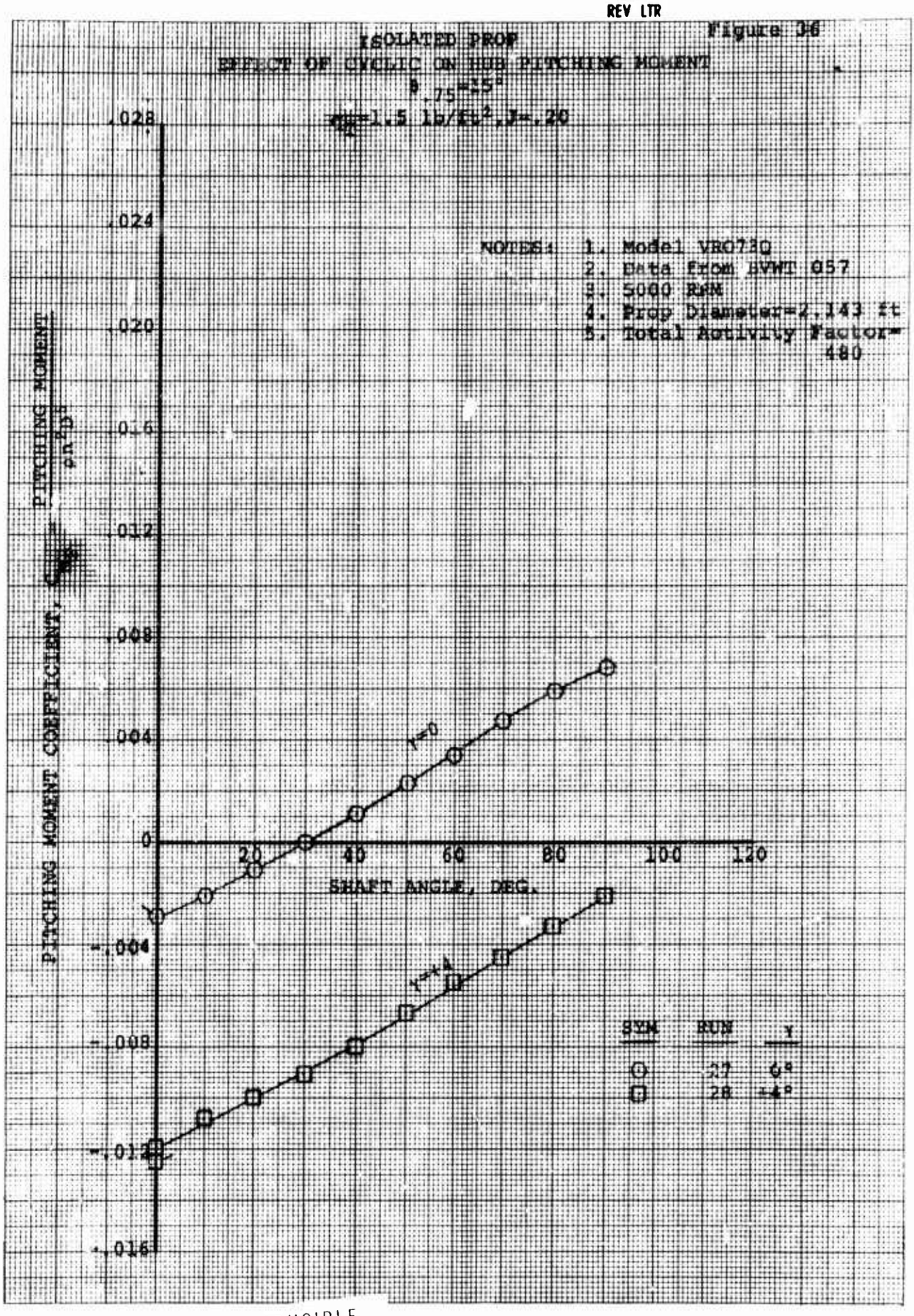

6.3 EFFECT OF CYCLIC ON POWER

The power coefficient (C_P) data presented in this section was calculated from shaft torque measurements obtained via the strain - gauged drive shaft. Since this drive shaft was a direct link between the power source (air motor) and the propeller, torque data acquired from the shaft includes the friction losses in the cyclic hub assembly.

Also presented in this section are friction power coefficients calculated from rolling moment or friction torque measurements of the six component strain gage balance attached to the front of the air motor. The friction torque measurements include losses from the following items: drive shaft bearings, hub support bearings, swashplate bearing, drive scissor bearings, pitch link rod ends, and blade retention bearings (elastomeric bearing hysteresis). It is recognized that the friction losses in the model cyclic hub are high compared to those in a full scale cyclic hub due to the large difference in propeller rotational speeds between the model and a full scale article (5000 RPM vs 650 RPM for a 26.4 ft. diameter full scale propeller operating at 900 fps tip speed).

The increase in power due to cyclic is presented in Figure 37 (hover), Figure 38 (0.2J and 0.32J with zero shaft angle), and Figure 39 (0.2J and 0.32J with 60° shaft angle as curves of power ratio, i.e., ratio of shaft power measured with a finite cyclic angle to shaft power measured with zero cyclic, $(C_P/C_{P_{\gamma=0}})$. This ratio was calculated from the power coefficient (C_P) curves depicted in Figures 40 through 44. Note that increasing the collective from 12° to 15° had no significant change on the power ratio when 4° of cyclic pitch was utilized.

Included in Figures 37 through 39, is the friction power increment that was measured during the hover case and the 0.2 advance ratio case with 12° of collective. The data from which the increment was derived, is presented in Figure 45. This figure indicates that the friction power required by the model cyclic hub assembly is only a function of the cyclic angle input at 5000 RPM.

The increase in aerodynamic power due to cyclic is obtained by subtracting the friction power from the shaft power. Figure 37 (hover) and Figure 38 (0.2J and zero shaft angle) show that with 8° of cyclic, aerodynamic power required is increased by approximately 14%. Figure 37 (hover) and Figure 38 (0.2J and zero shaft angle) show that advance ratio has only a small effect on the power ratio, and that the increase in aerodynamic power required by 8° of cyclic is approximately 14%.

The effect of shaft angle on the power ratio ($C_p/C_{p_{\gamma=0}}$) for a condition other than hover, is illustrated in Figure 46 for the 0.2J case wherein the power ratio curves from Figures 38 and 39 for zero shaft angle and 60° shaft angle are compared. Increasing the shaft angle from zero to 60° results in decreasing power requirements for positive cyclic and increasing power requirements for negative cyclic.

The difference in power demands between negative and positive cyclic at high shaft angles is also apparent from an examination of the shaft power data shown in Figures 47 through 53. Each of these plots present the shaft power data obtained in the series of shaft angle sweeps performed for a range of cyclic pitch settings with a constant collective setting and at a constant tunnel q or advance ratio.

Referring to Figure 47 and the corresponding hub pitching moment plot (Figure 30), it is evident that when the hub pitching moment is large (high shaft angle and negative cyclic) the power requirements are highest and that when the hub pitching moment is small (high shaft angle and positive cyclic) the power requirements are low.

Figure 37

ISOLATED PROP
INCREASE IN POWER DUE TO CYCLIC
HOVER

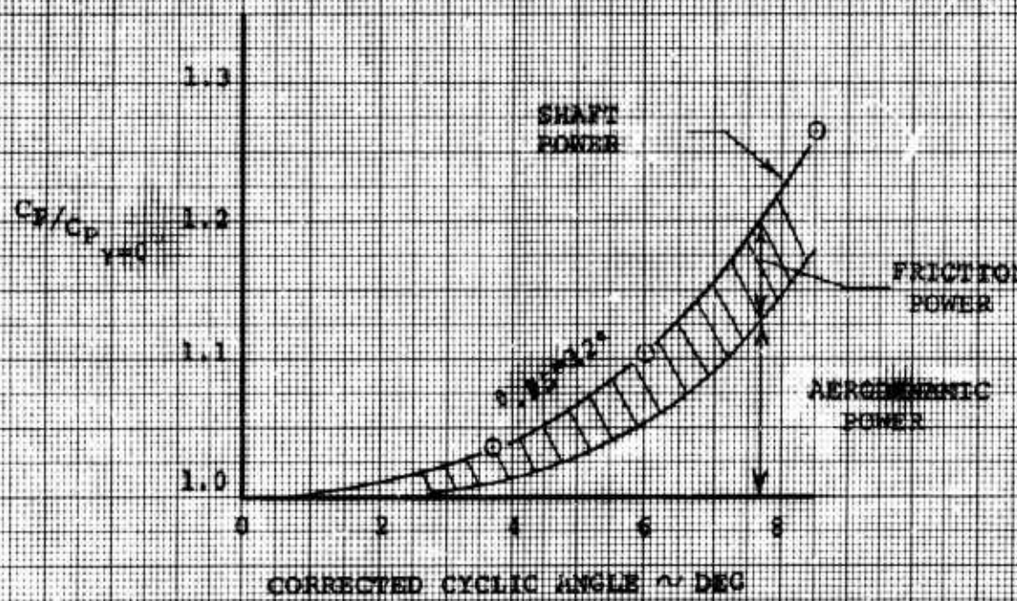

NOTES:
1. Model VRC73Q
2. Data from Test BVWT 057
3. 5000 RPM
4. Prop Diameter = 2.143 ft.
5. Total Activity Factor = 480

Figure 38

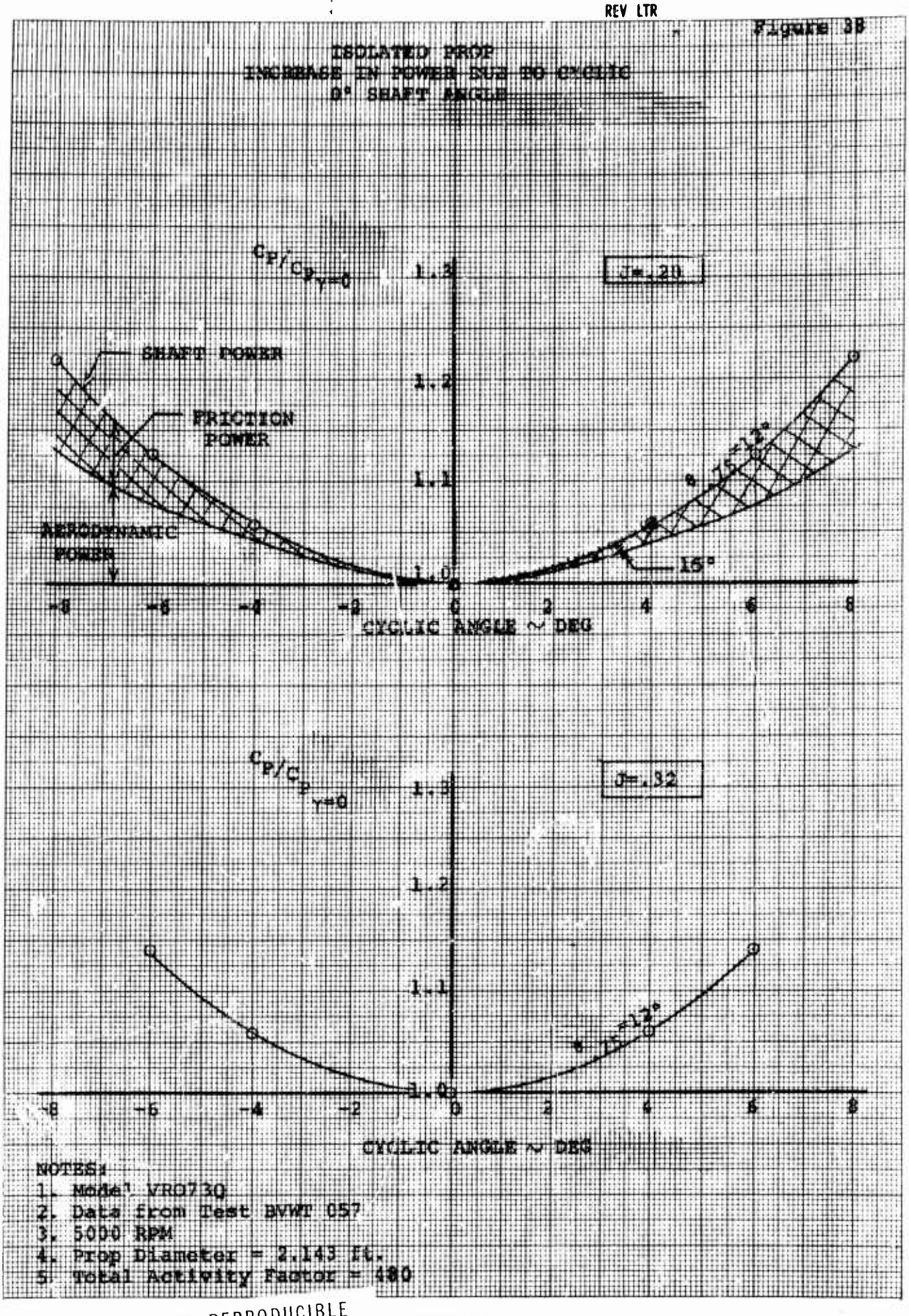

NOTES:
1. Model VRO730
2. Data from Test BVWT 057
3. 5000 RPM
4. Prop Diameter = 2.143 FT.
5. Total Activity Factor = 480

ISOLATED PROP [illegible] 60° SHAFT ANGLE

Figure 39

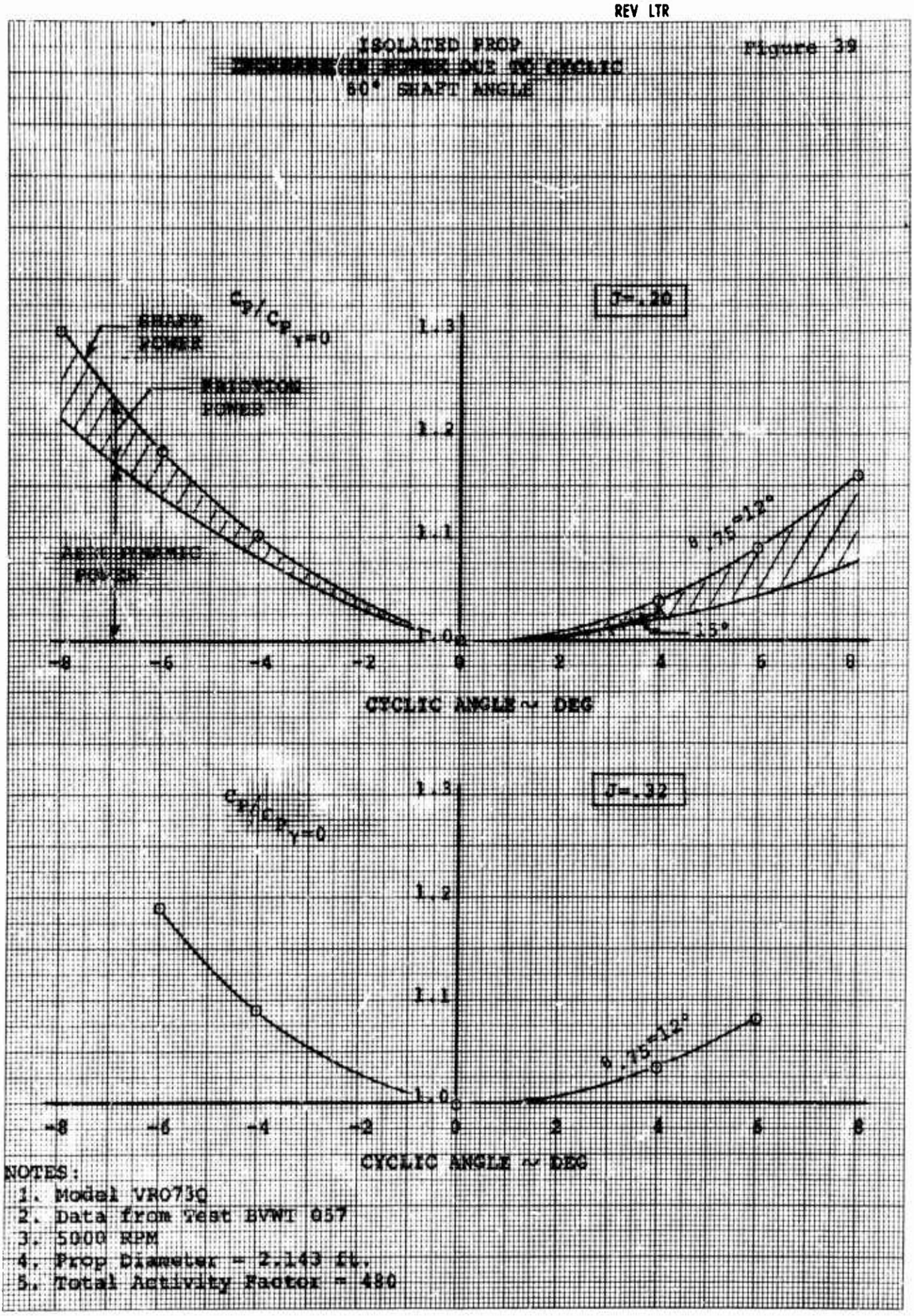

NOTES:
1. Model VRO73Q
2. Data from Test BVWT 057
3. 5000 RPM
4. Prop Diameter = 2.143 ft.
5. Total Activity Factor = 480

Figure 40

ISOLATED PROP
VARIATION OF POWER WITH CYCLIC
HOVER

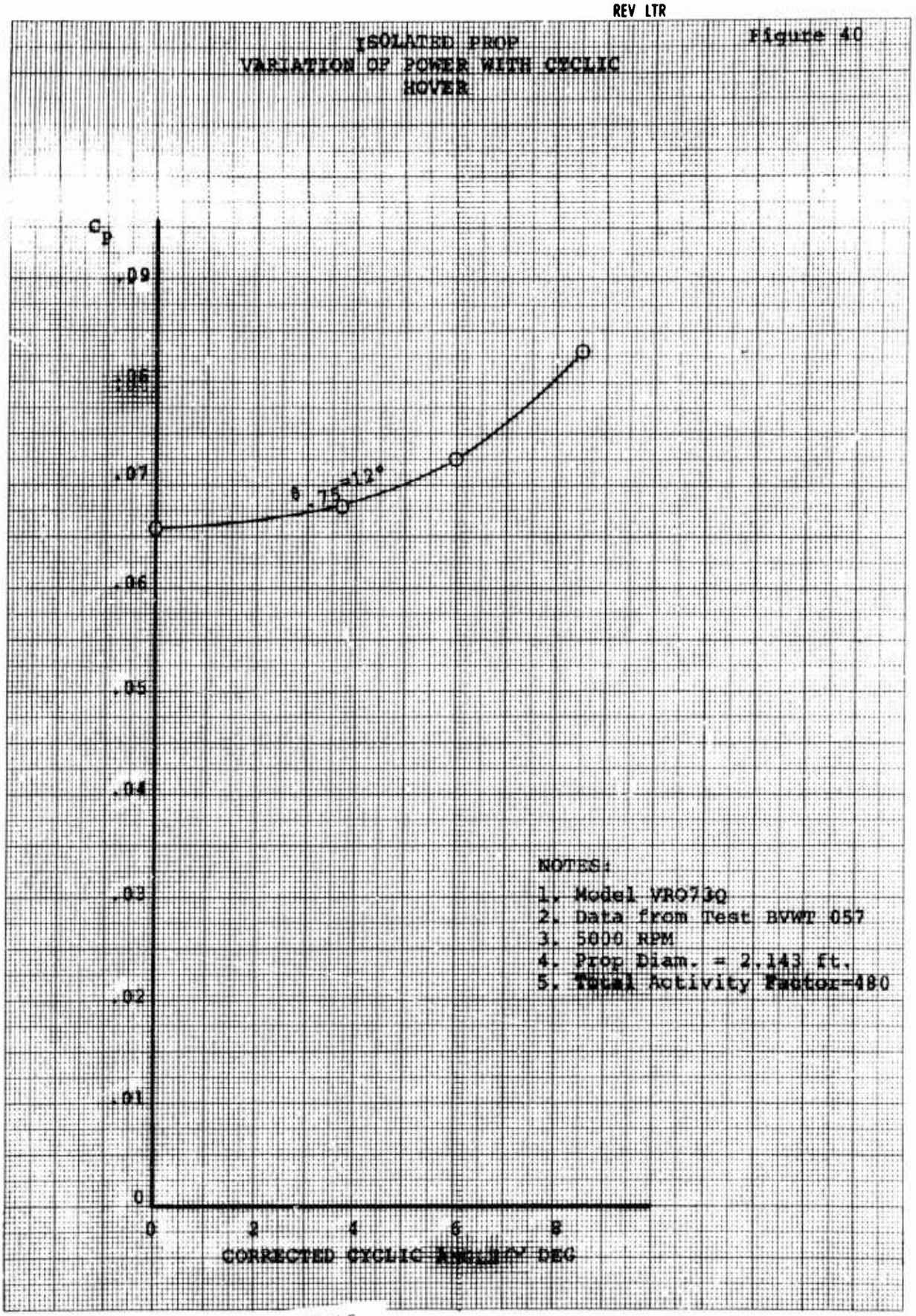

NOTES:
1. Model VRO730
2. Data from Test BVWT 057
3. 5000 RPM
4. Prop Diam. = 2.143 Ft.
5. Total Activity Factor=480

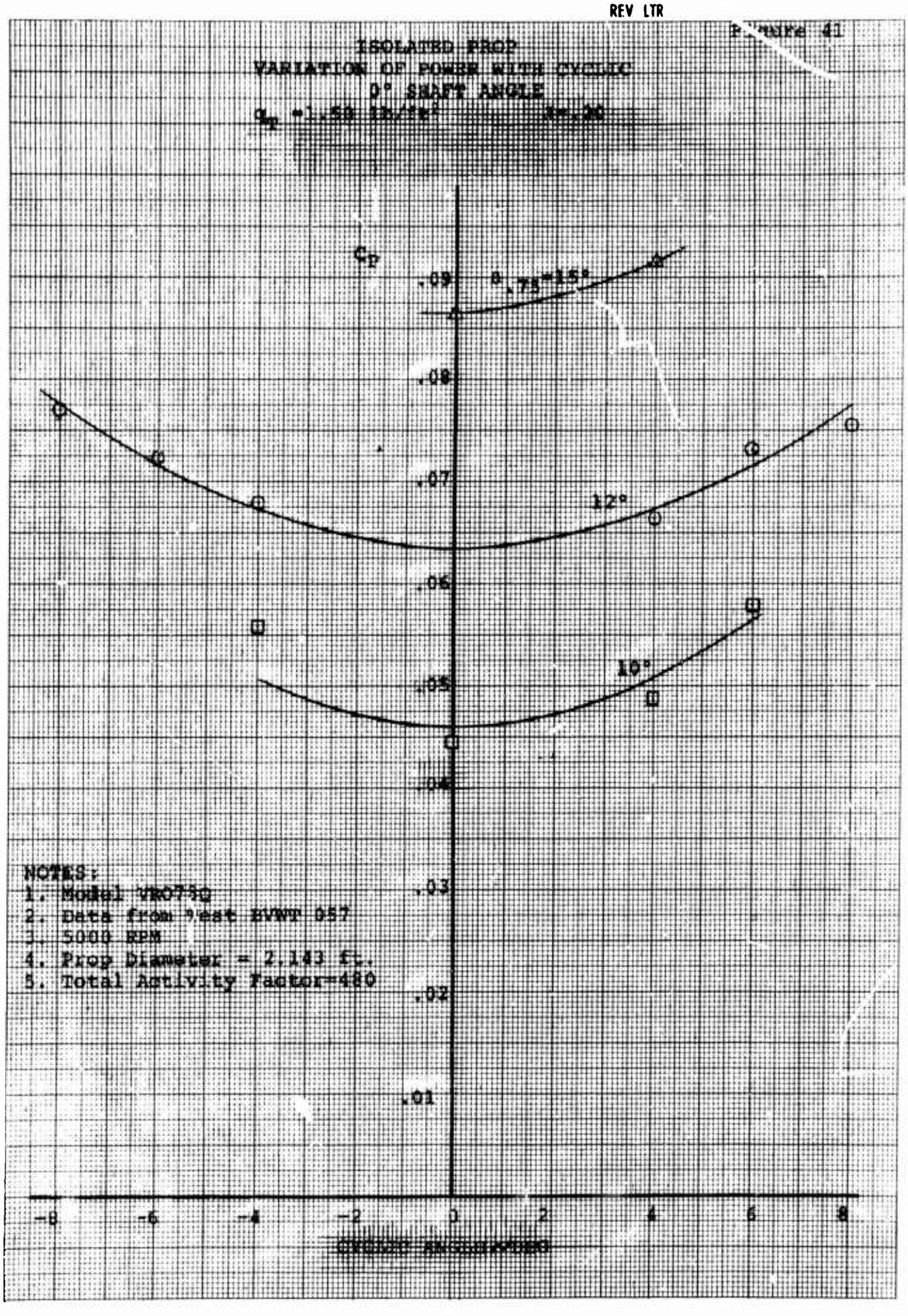

Figure 42

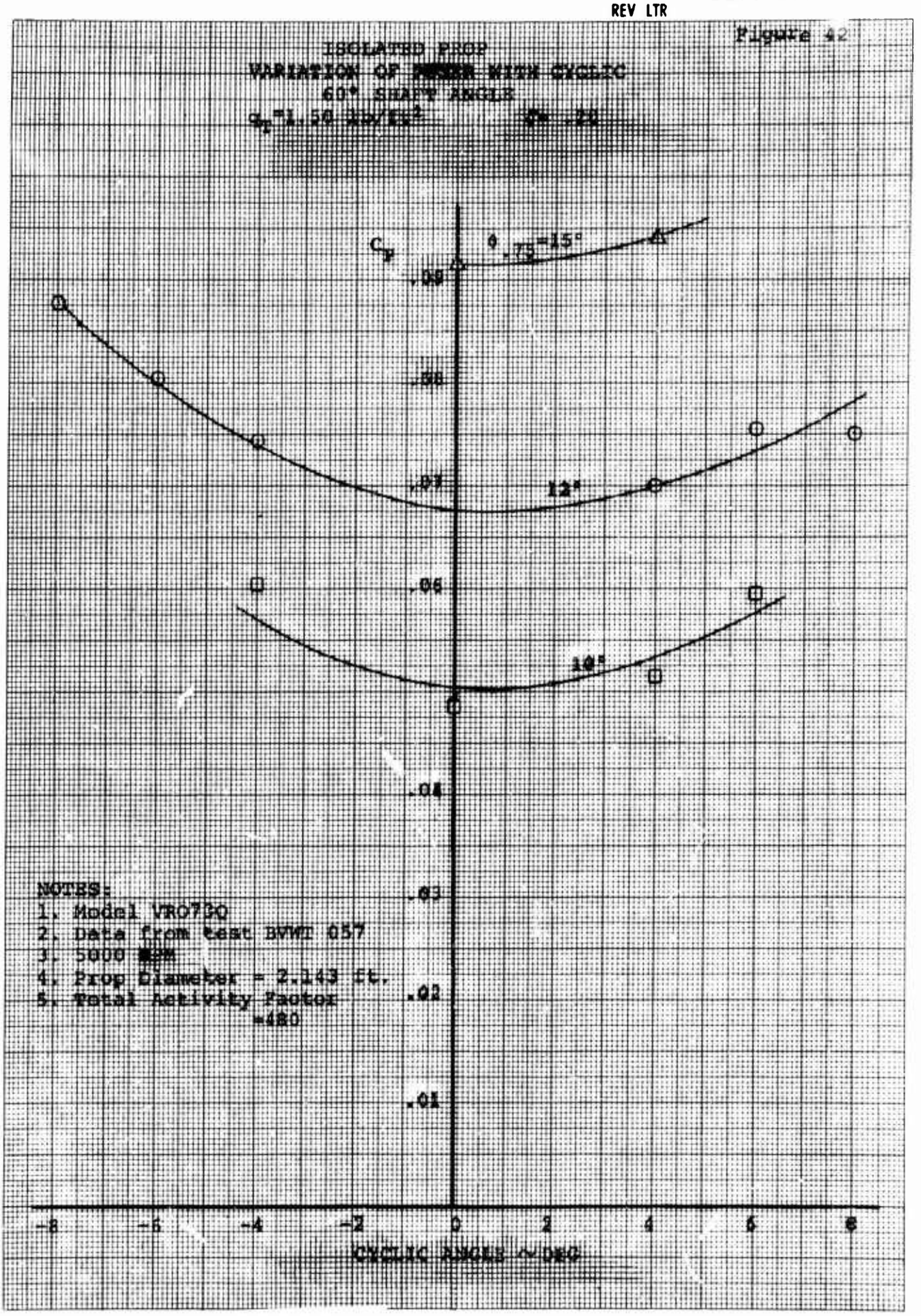

Figure 43

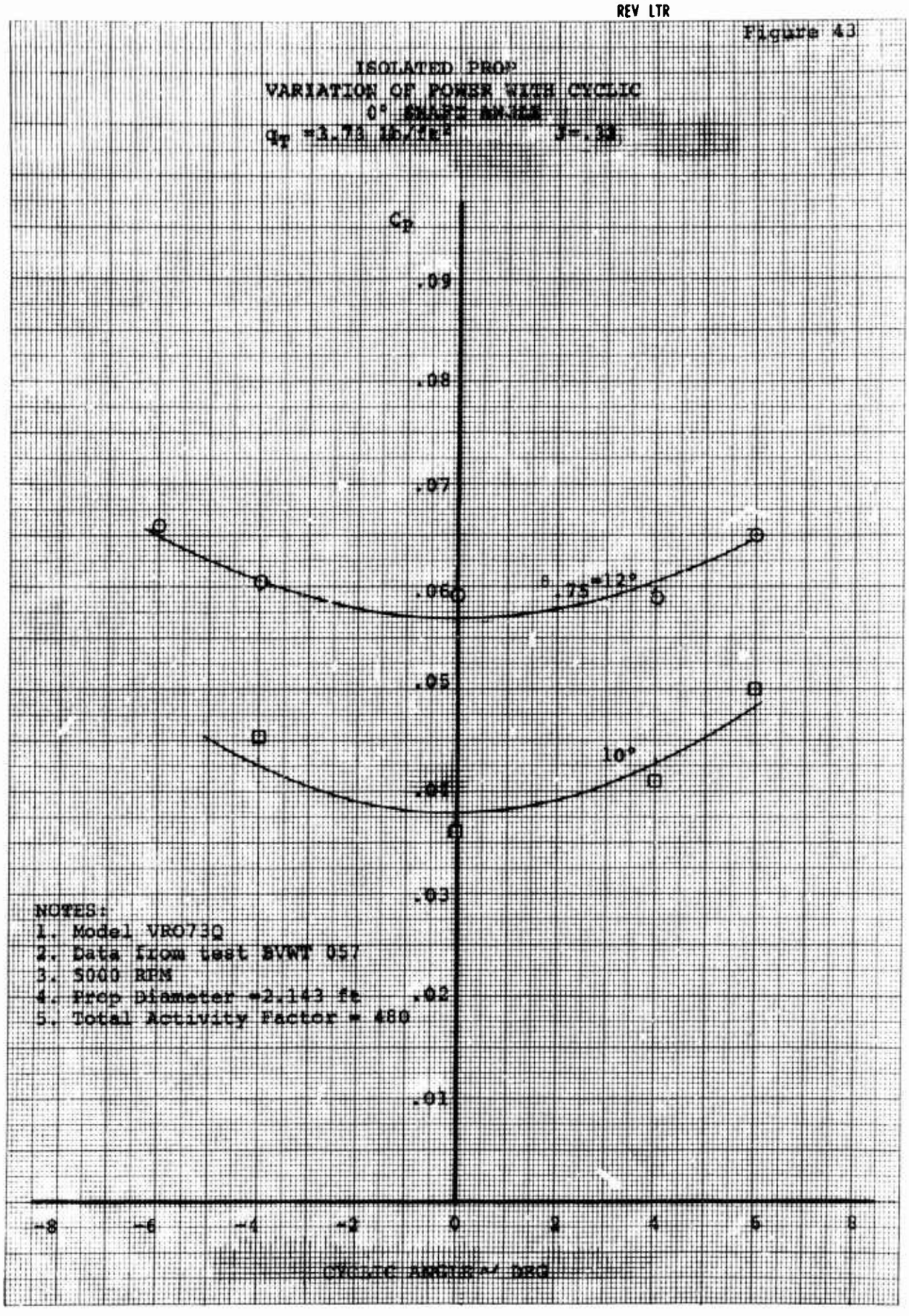

Figure 41

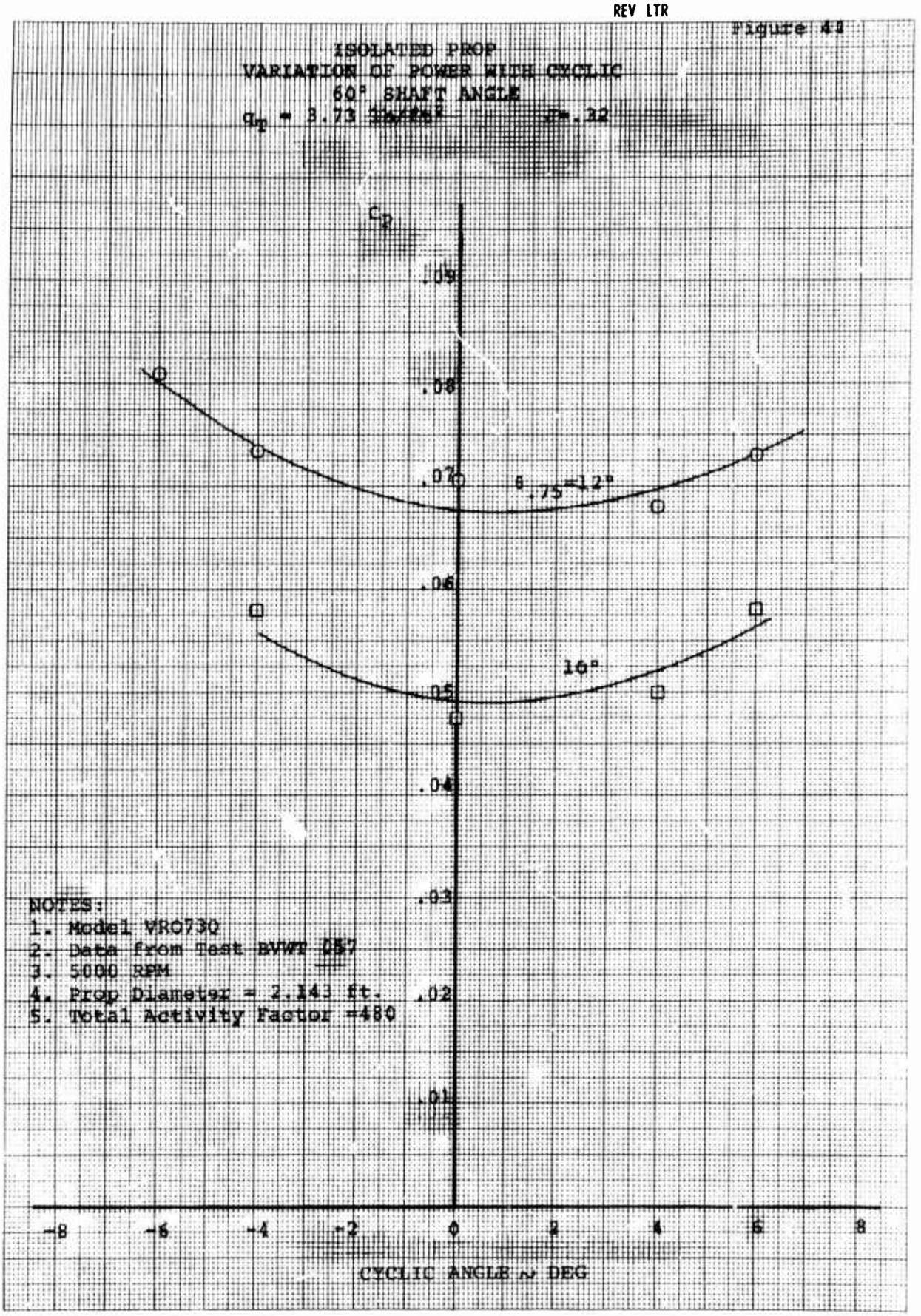

SHROUDED PROP
VARIATION OF FRICTION POWER WITH CYCLIC
0° / 60° SHAFT ANGLE
q_T = 1.50 lb/ft² J=.20
ADD MOTOR

Figure 45

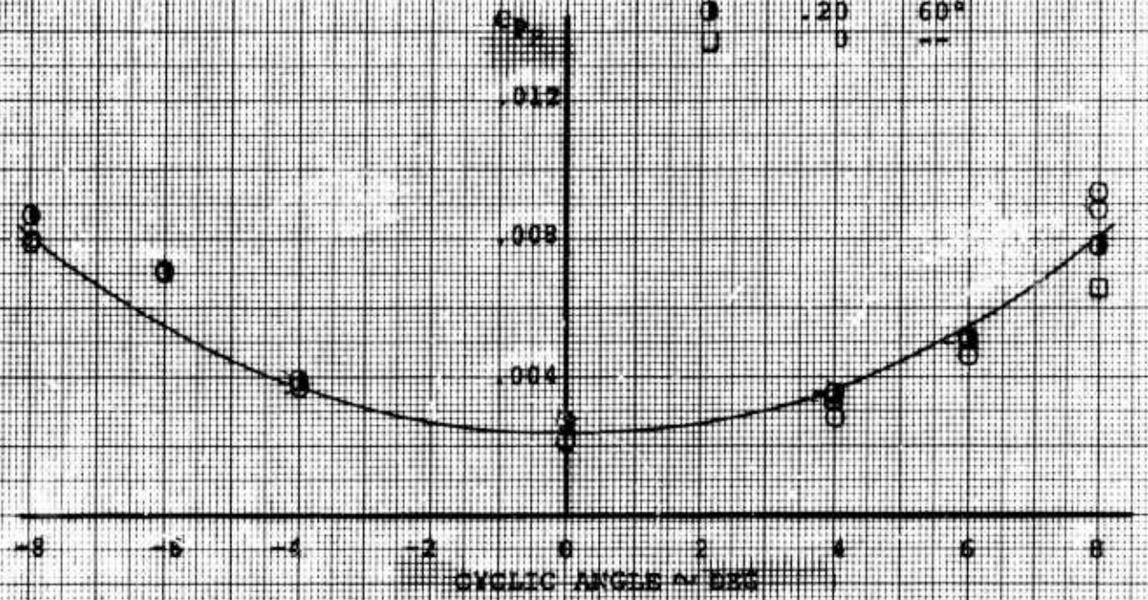

NOTES:
1. Model VRO73Q
2. Data from BVWT 057
3. 5000 RPM
4. Prop Diameter = 2.143 ft.
5. Ttoal Activity Factor =480

Figure 46

ISOLATED PROP
INCREASE IN POWER DUE TO CYCLIC
[illegible] and 60° SHAFT ANGLE

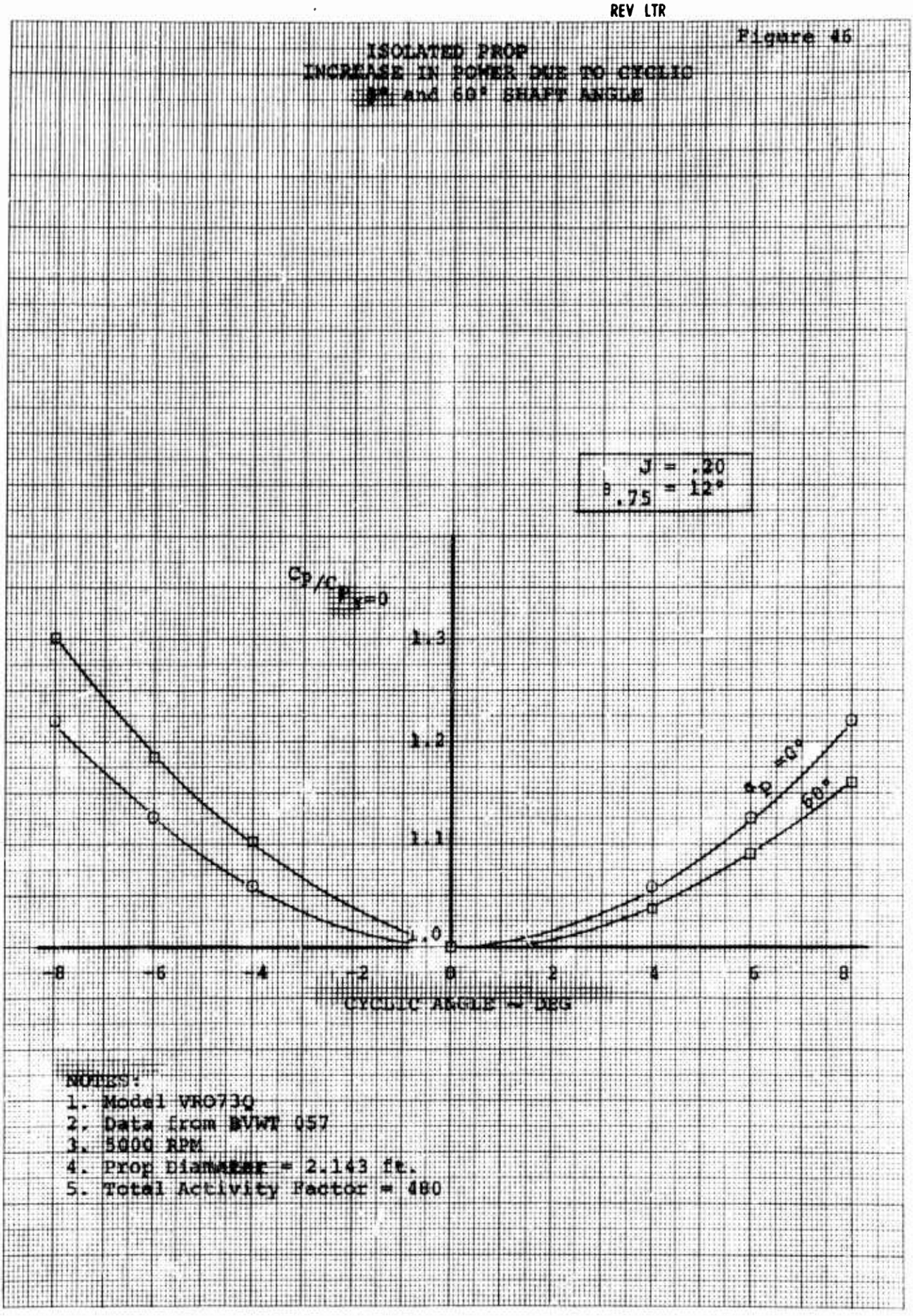

NOTES:
1. Model VRO73Q
2. Data from BVWT 057
3. 5000 RPM
4. Prop Diameter = 2.143 ft.
5. Total Activity Factor = 480

Figure 47

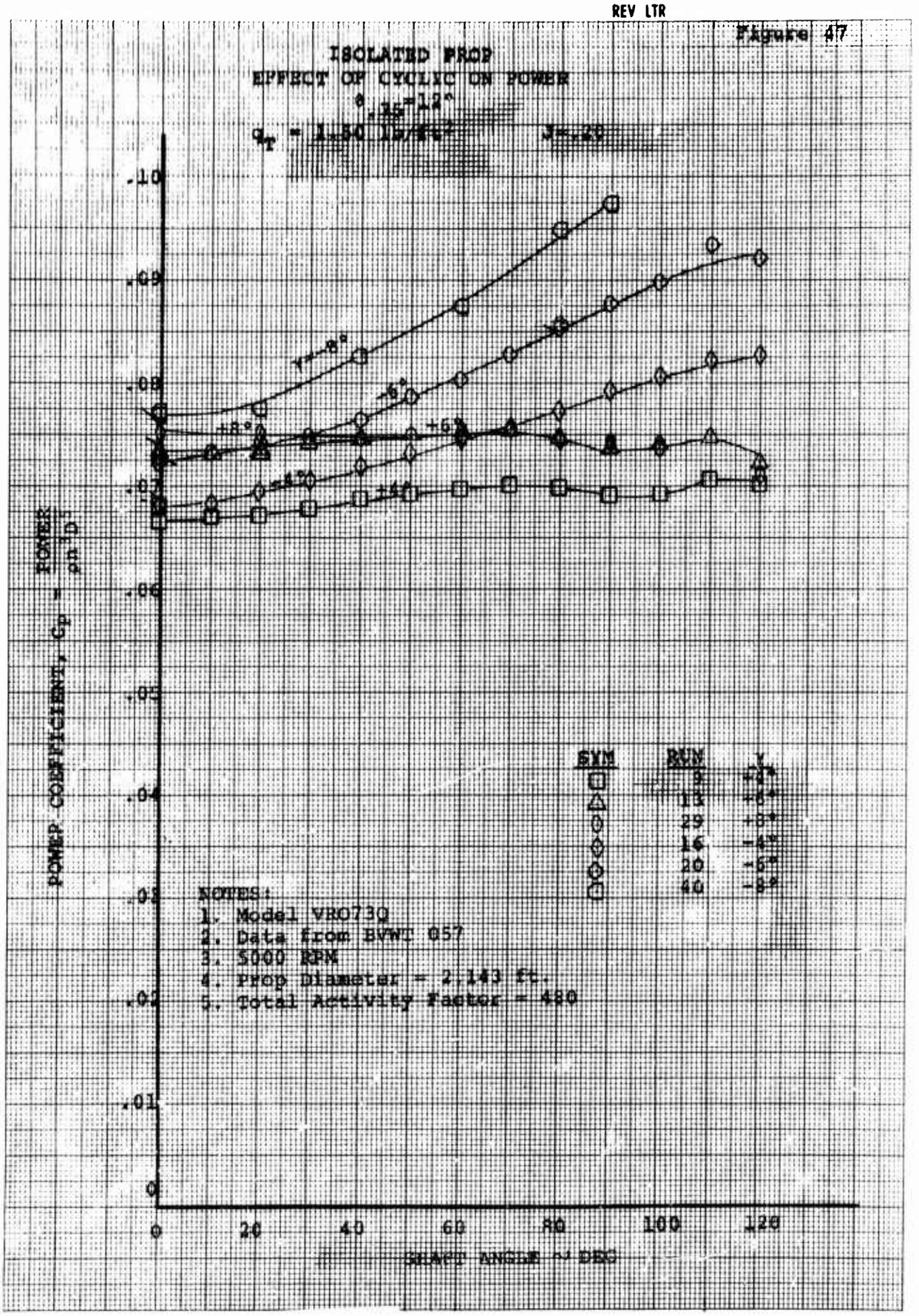

Figure 48

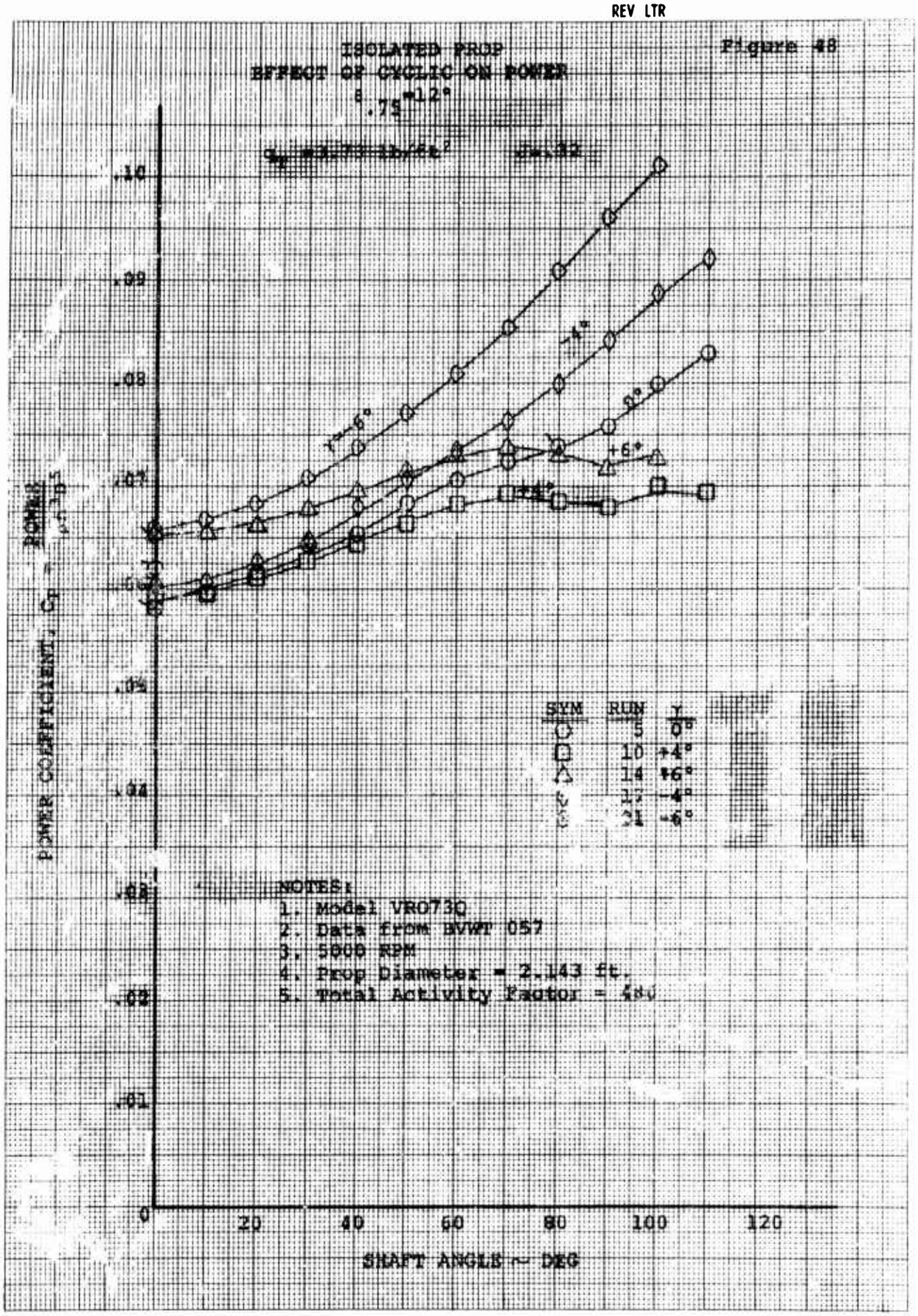

Figure 48

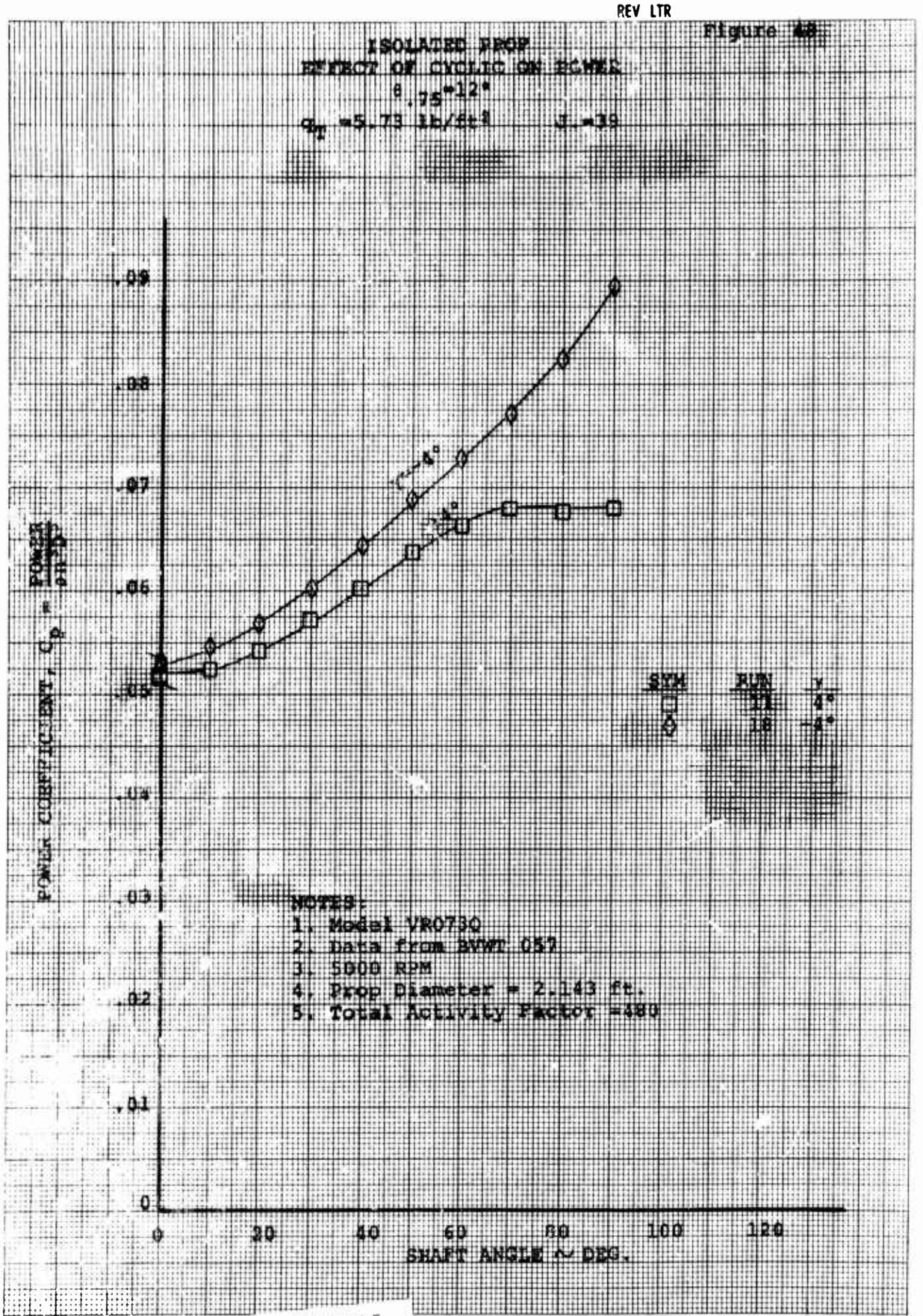

Figure 50

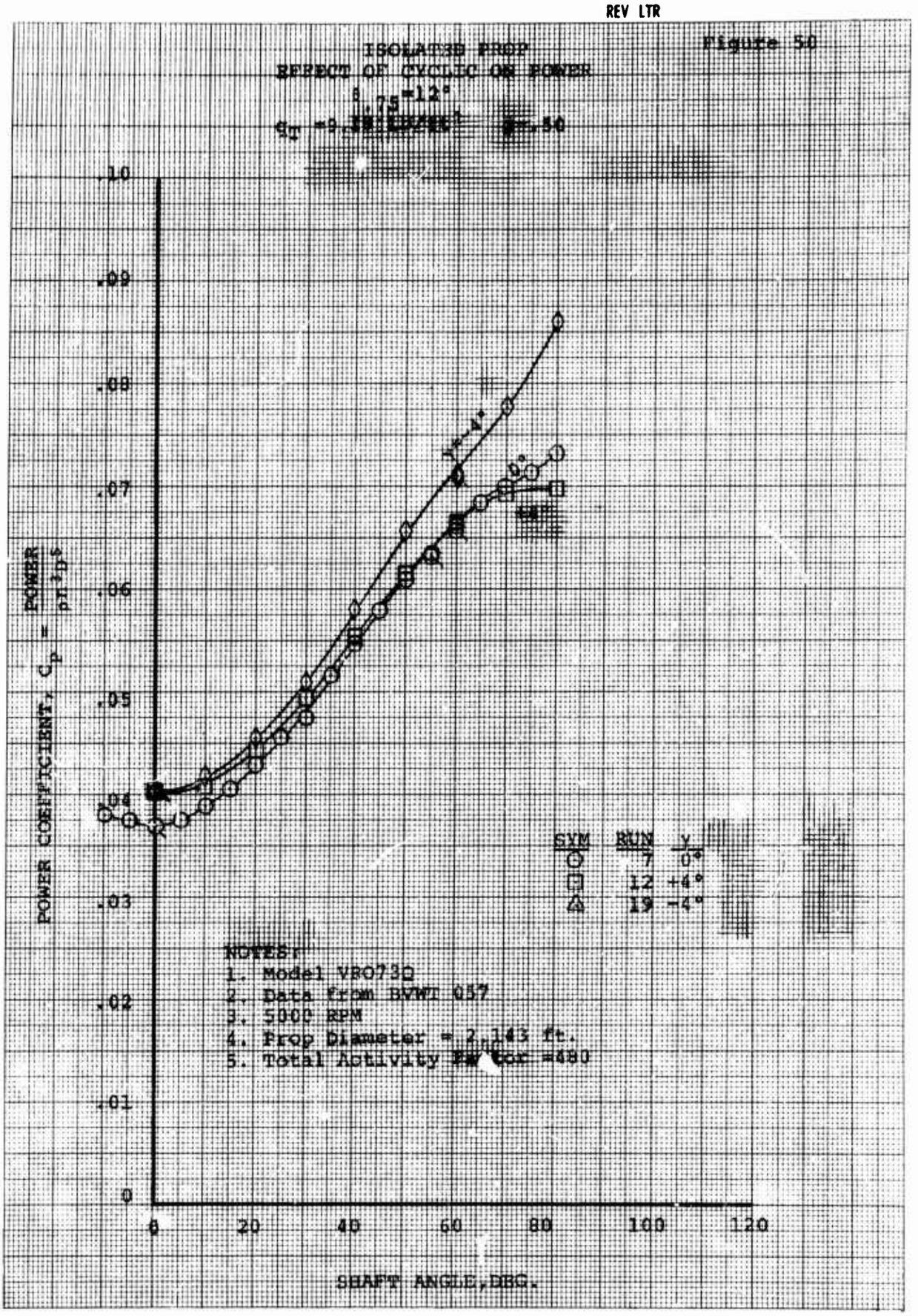

Figure 51

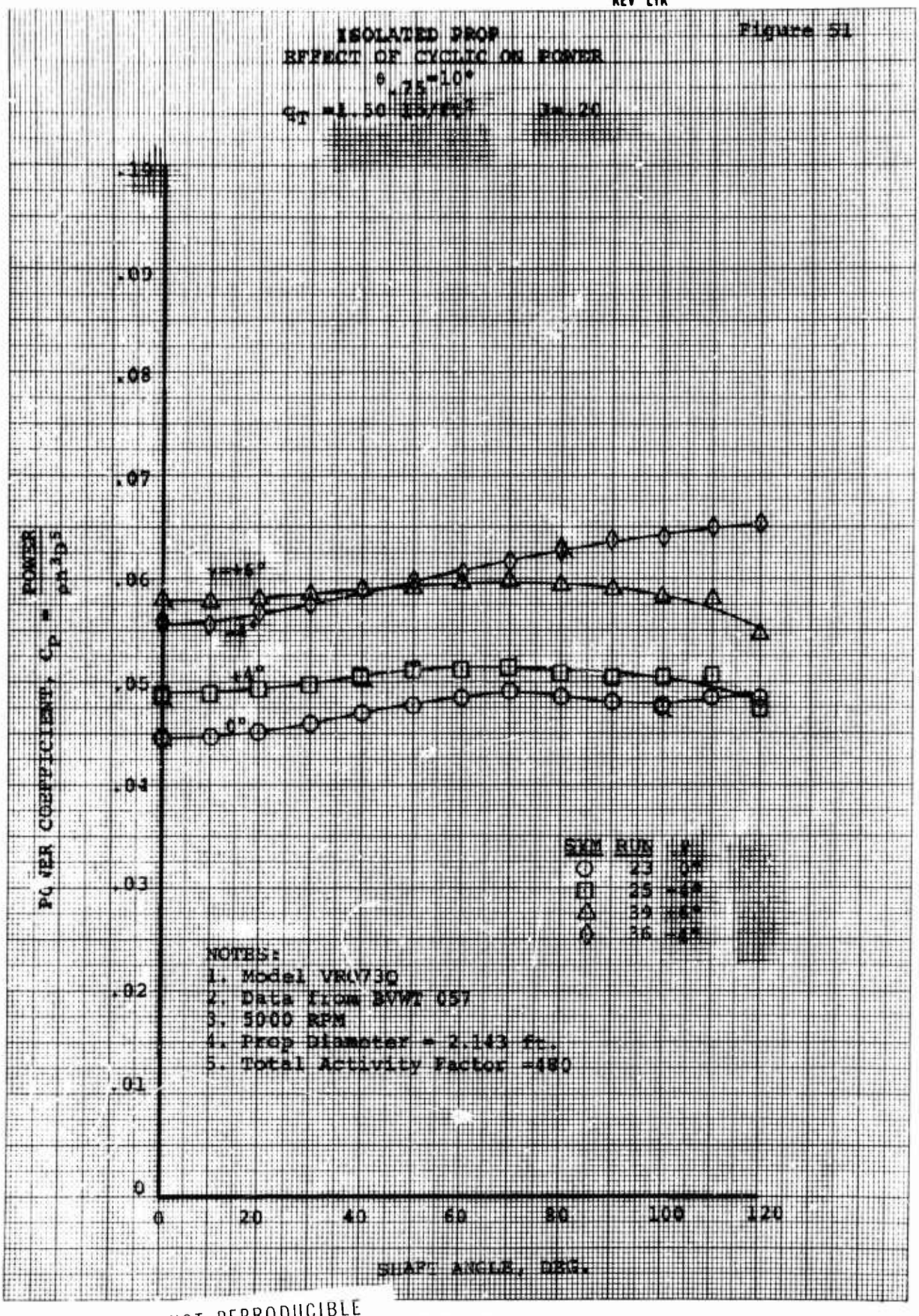

Figure 52

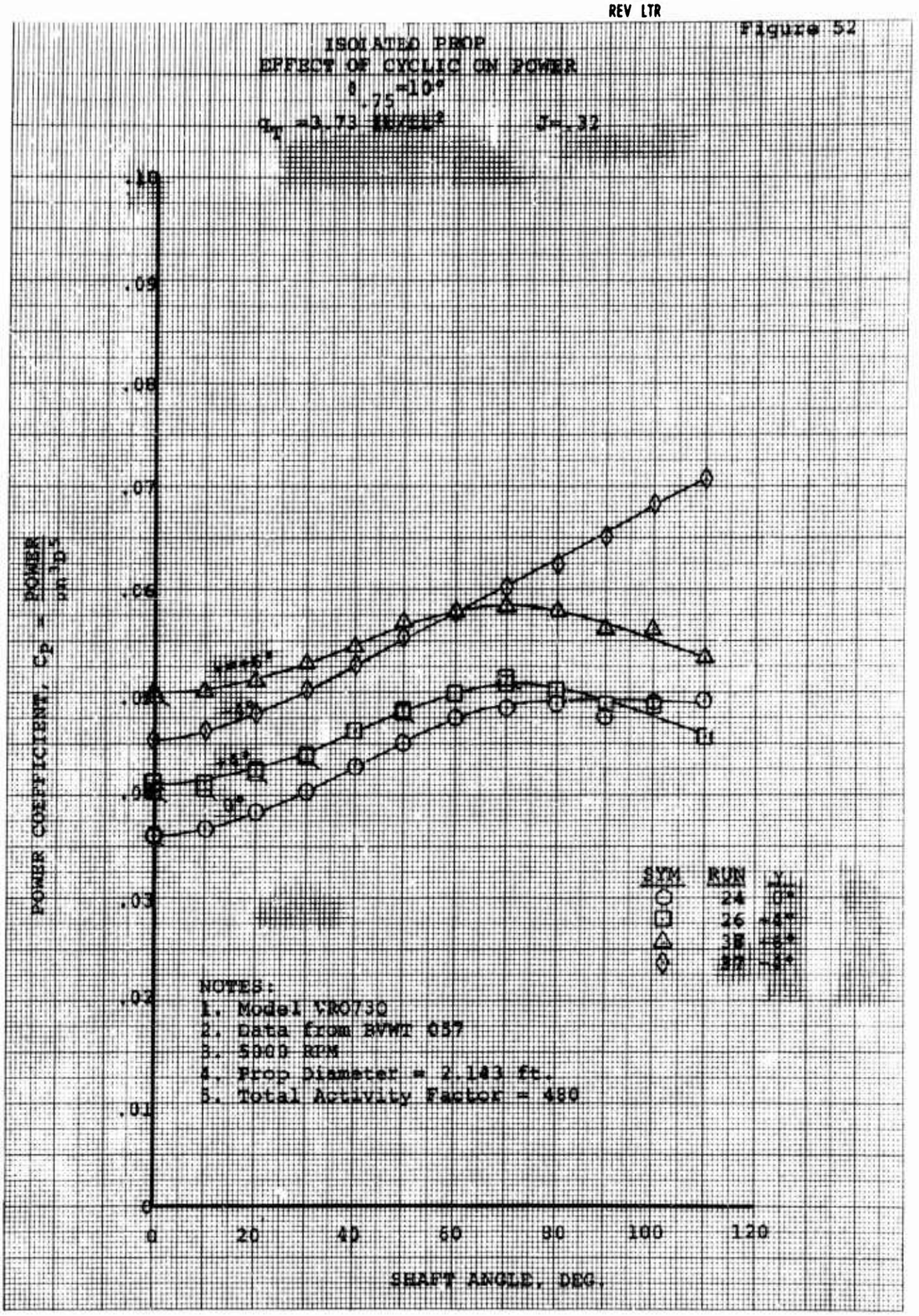

Figure 53

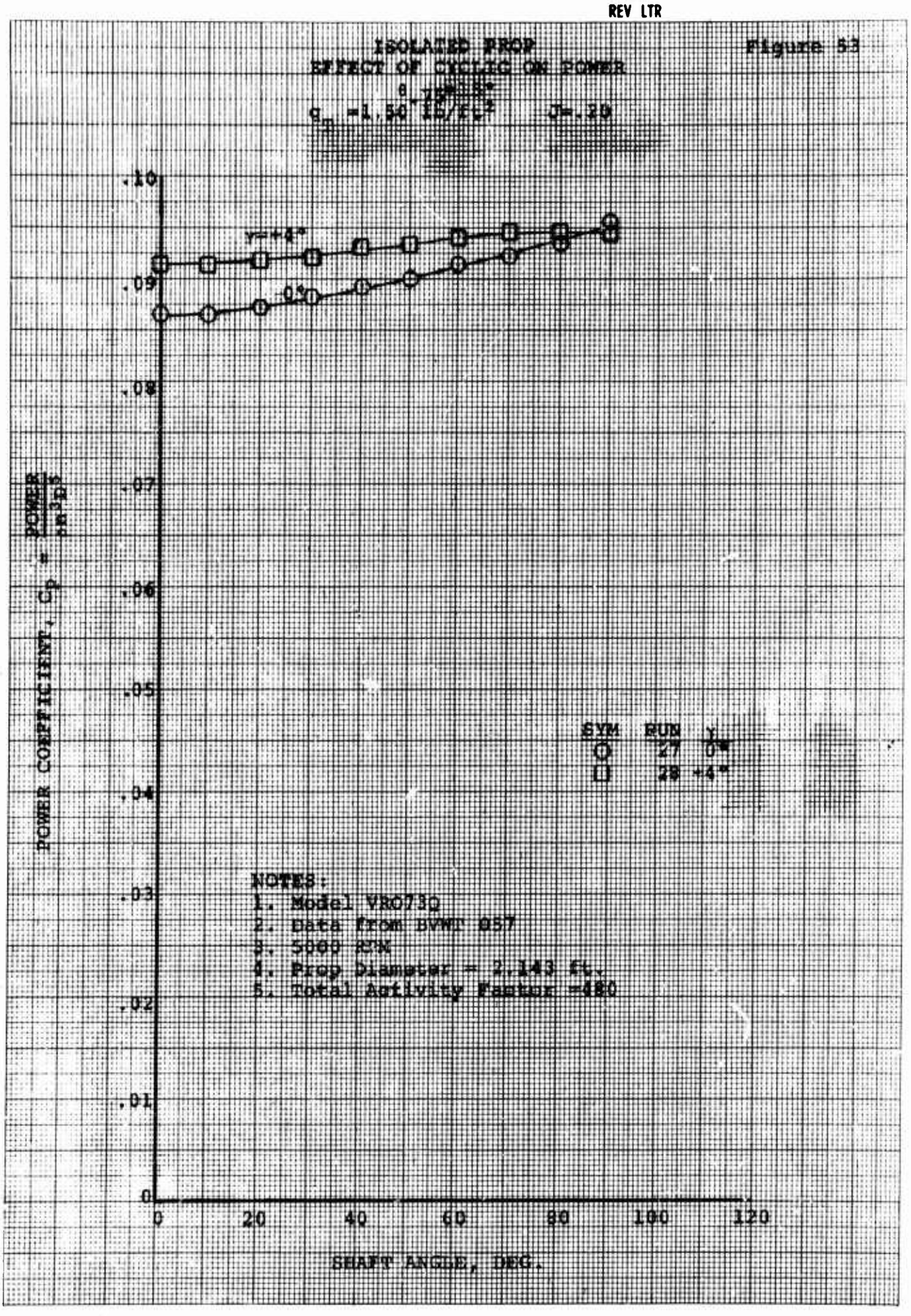

6.4 EFFECT OF CYCLIC ON THRUST

The variation of thrust with cyclic angle is depicted in Figures 54 and 55 for the 1.50 tunnel q or 0.2 J case and the collective angles evaluated. The two figures present zero shaft angle data and 60° shaft angle data, respectively. Figure 54 also includes data from the hover runs. Similar information is shown in Figure 56 for the 3.73 tunnel q or 0.32 J case. The data in these figures indicate that with application of cyclic pitch the thrust increases a small amount (approximately 5%) prior to decreasing at conditions with larger amounts of cyclic applied(6° to 8°).

Figures 54 through 56 were developed from the thrust vs shaft angle curves presented in Figures 57 through 63 . Each plot presents the data from the various cyclic pitch runs acquired with a particular collective setting and at a constant tunnel q or J. These plots show that with cyclic applied the resultant thrust/shaft angle curve has the same general shape as the case with no cyclic. Also, at the speed conditions where a tilt wing aircraft could be flying at high shaft angles with larger amounts of cyclic being utilized for control (for example, 0.2J on Figure 57), cyclic does not have a large effect on thrust.

Figure 54

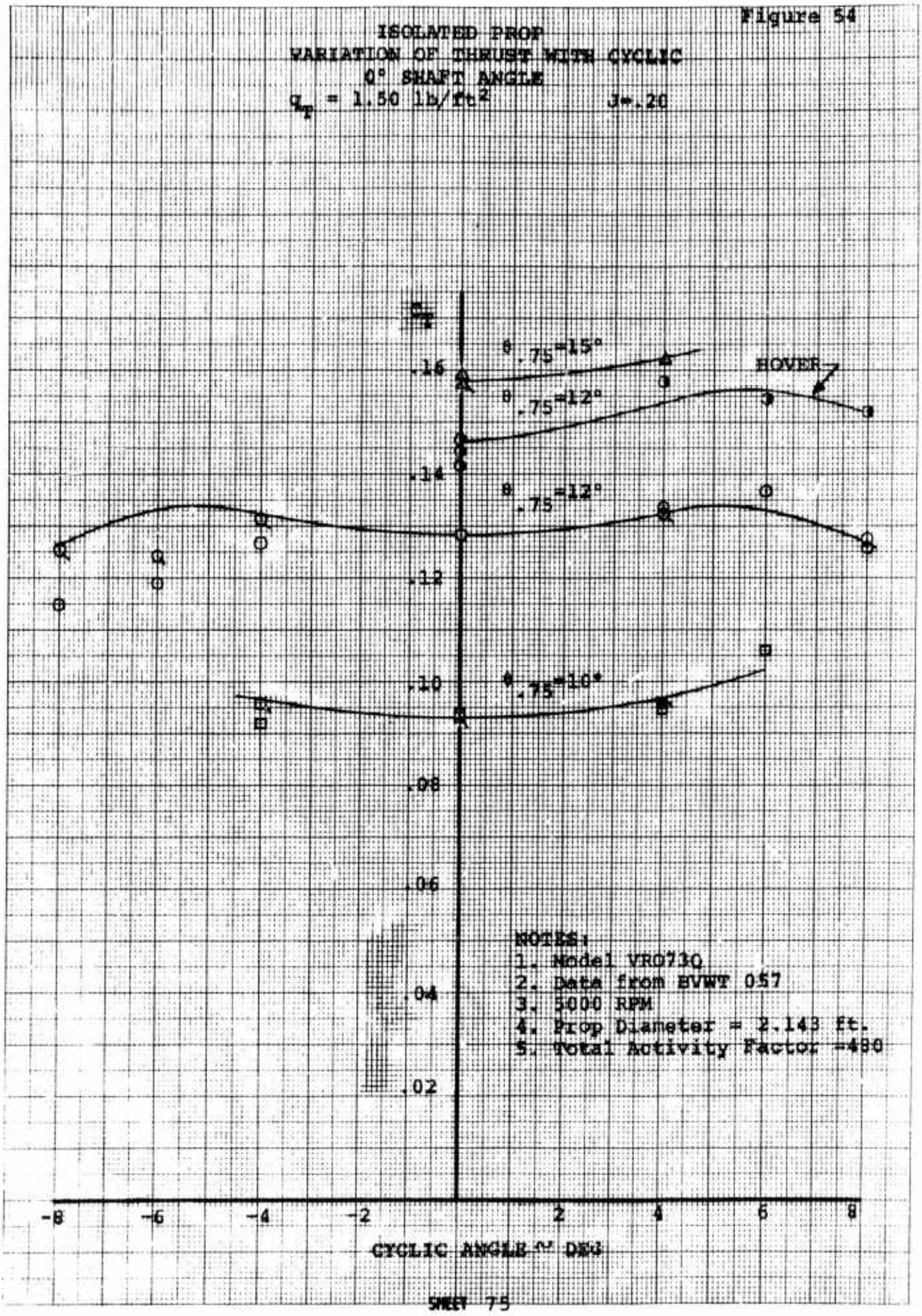

Figure 55

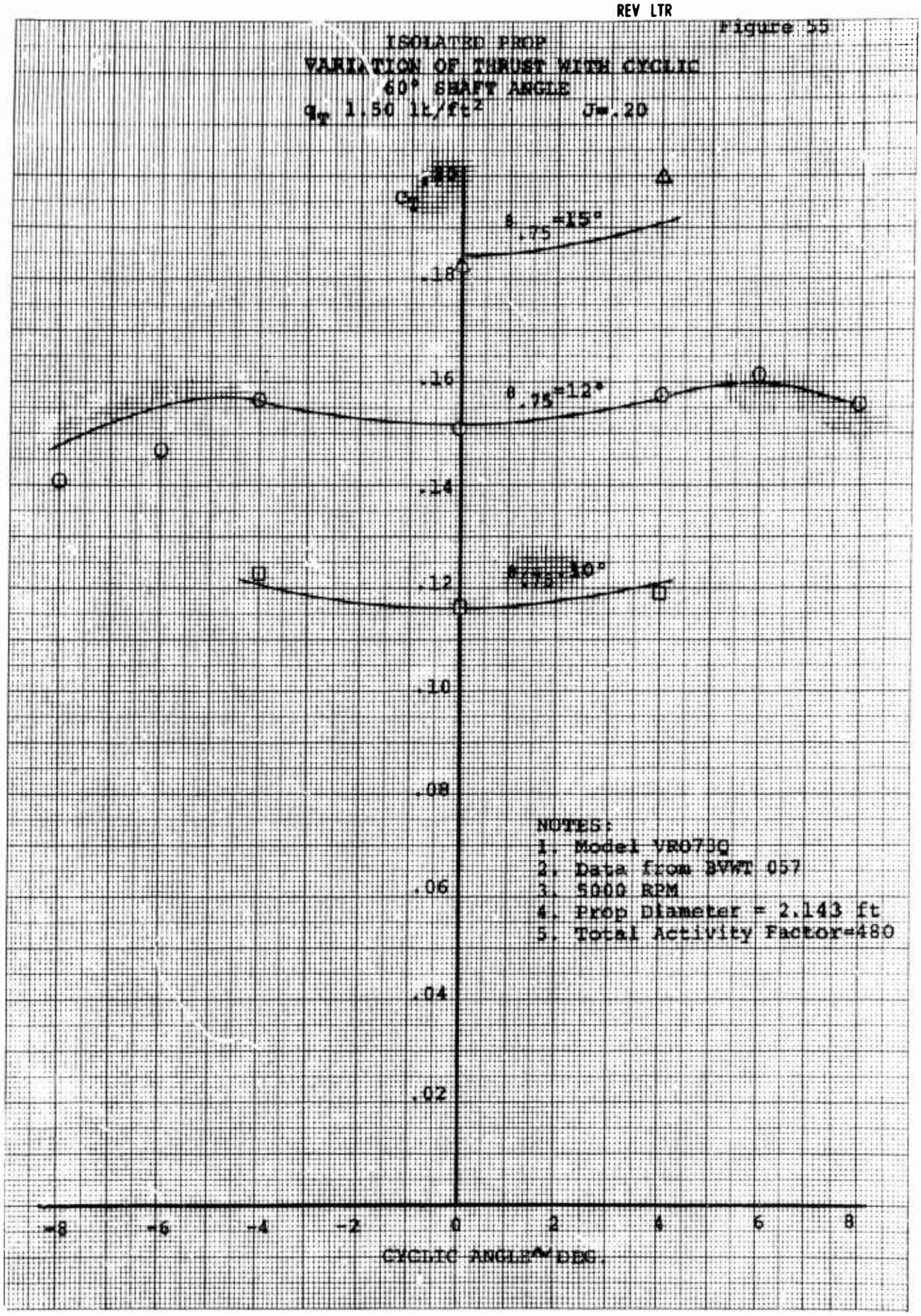

Figure 56

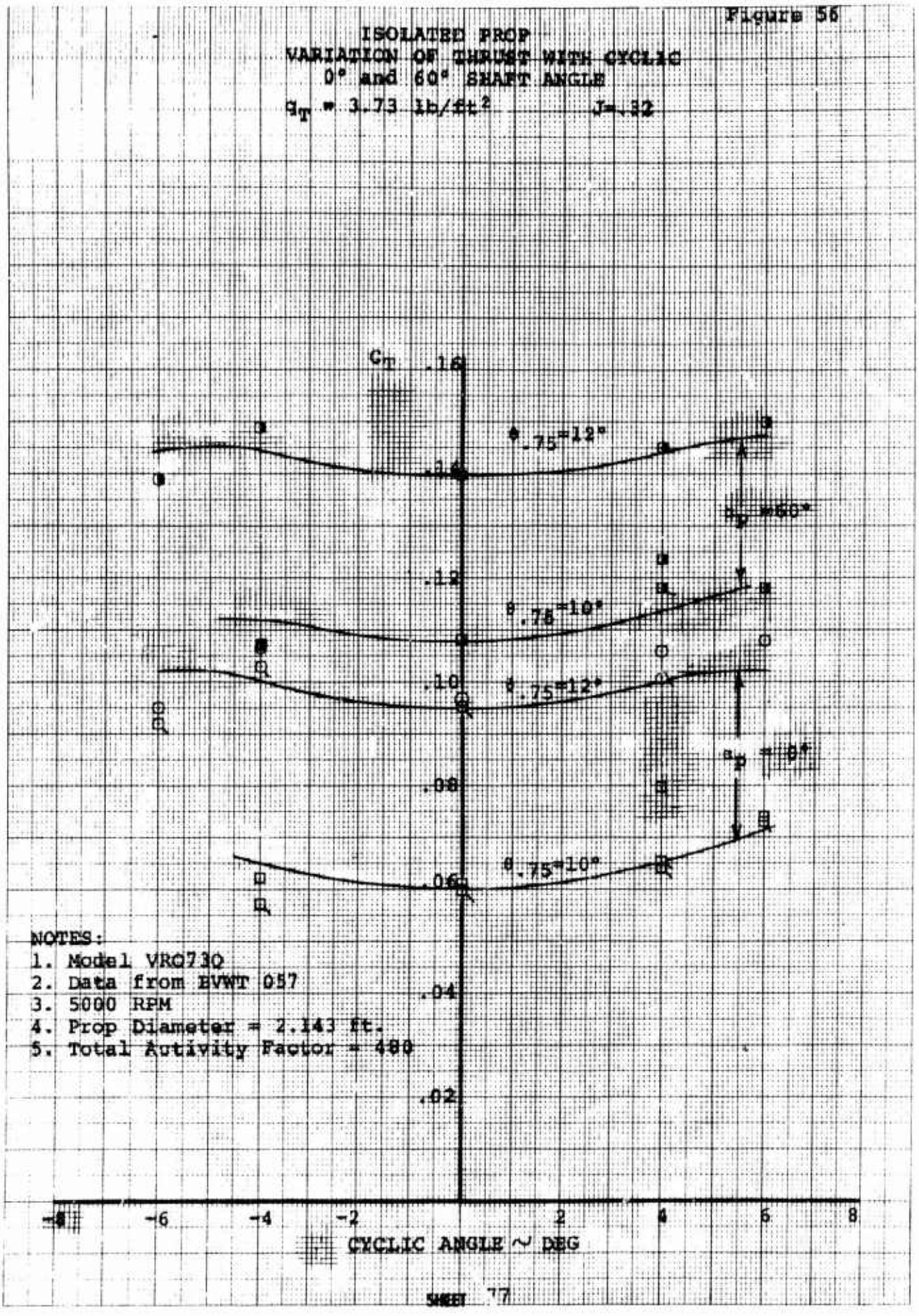

Figure 57

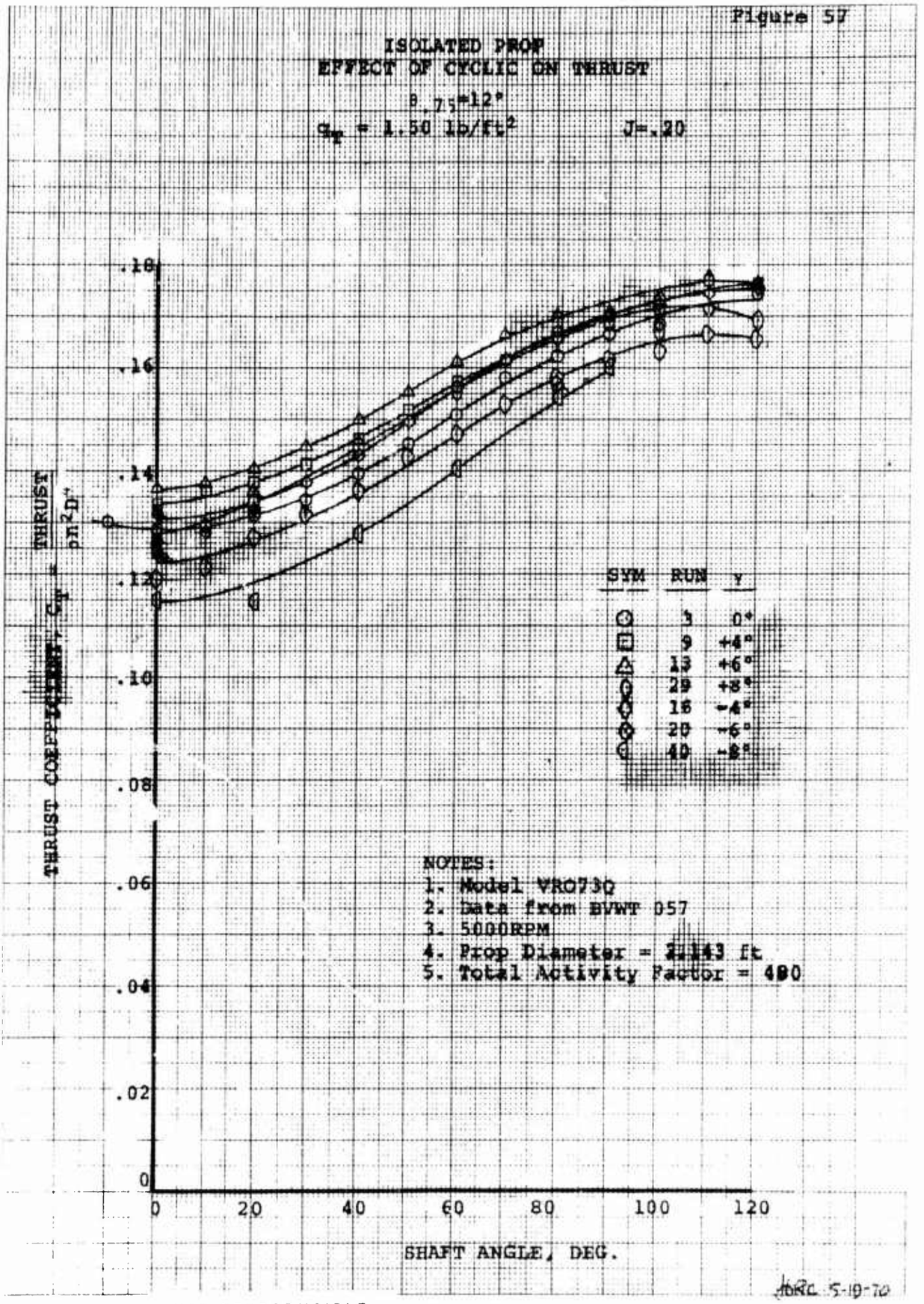

Figure 58

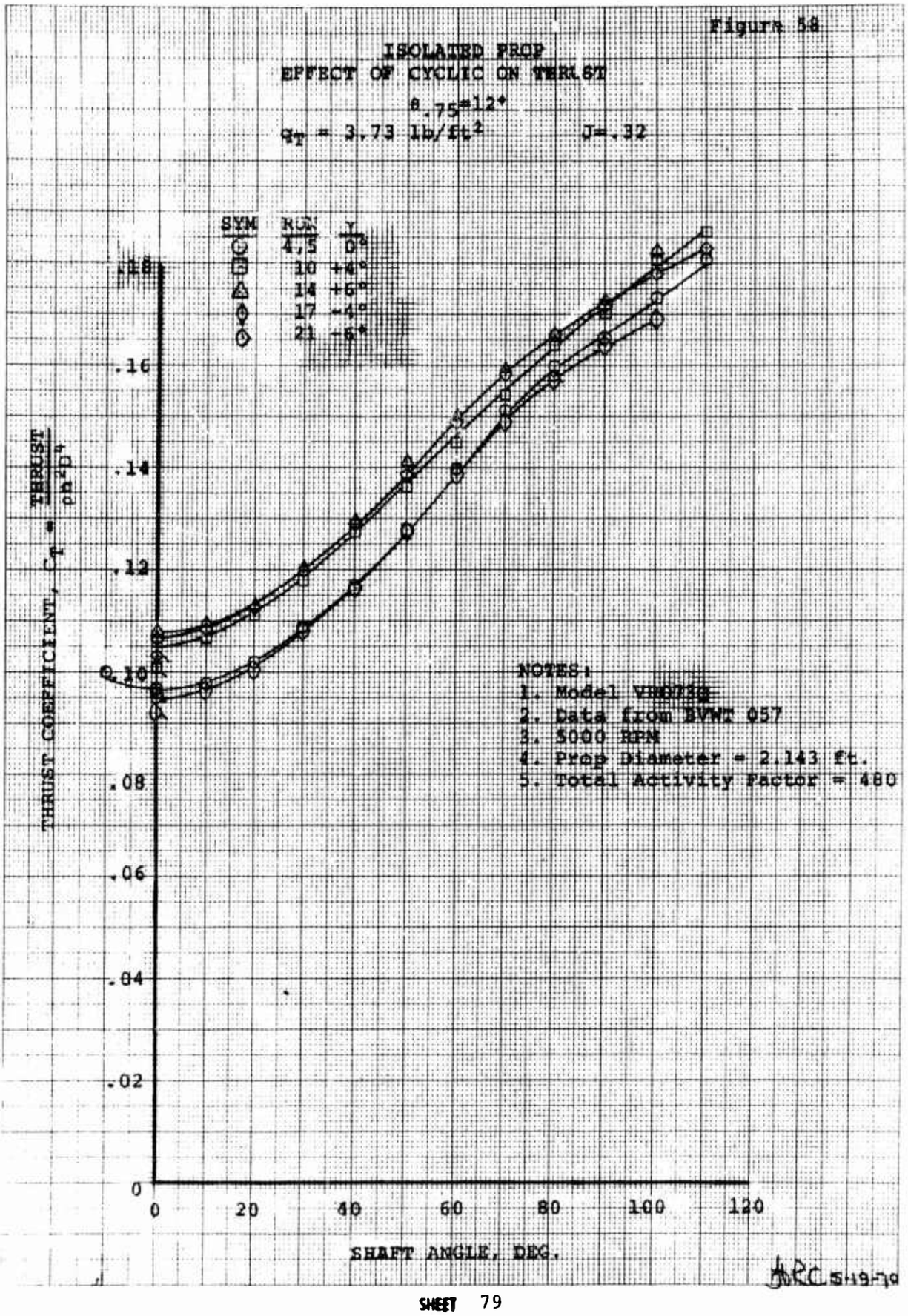

Figure 59

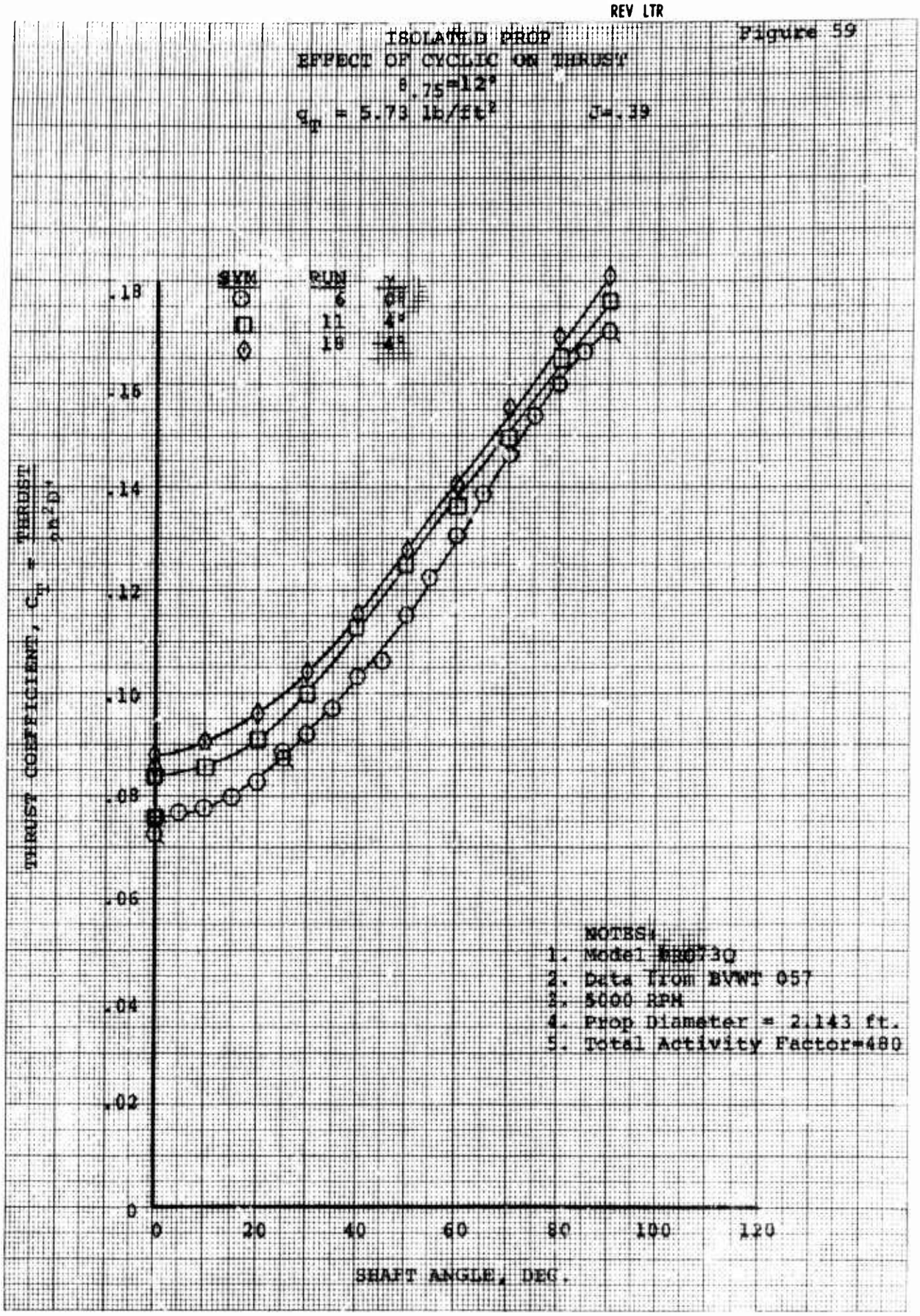

Figure 60

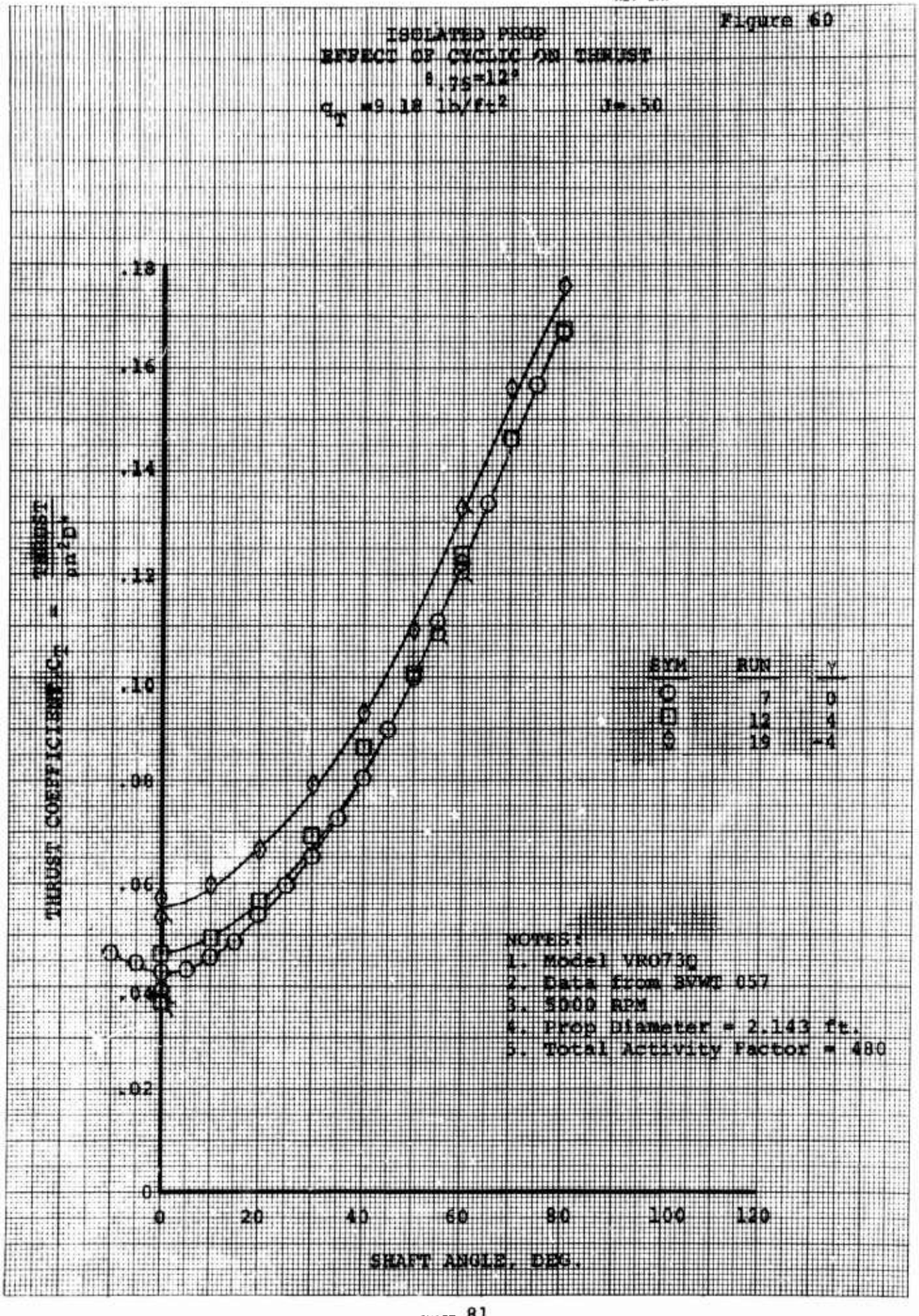

Figure 81

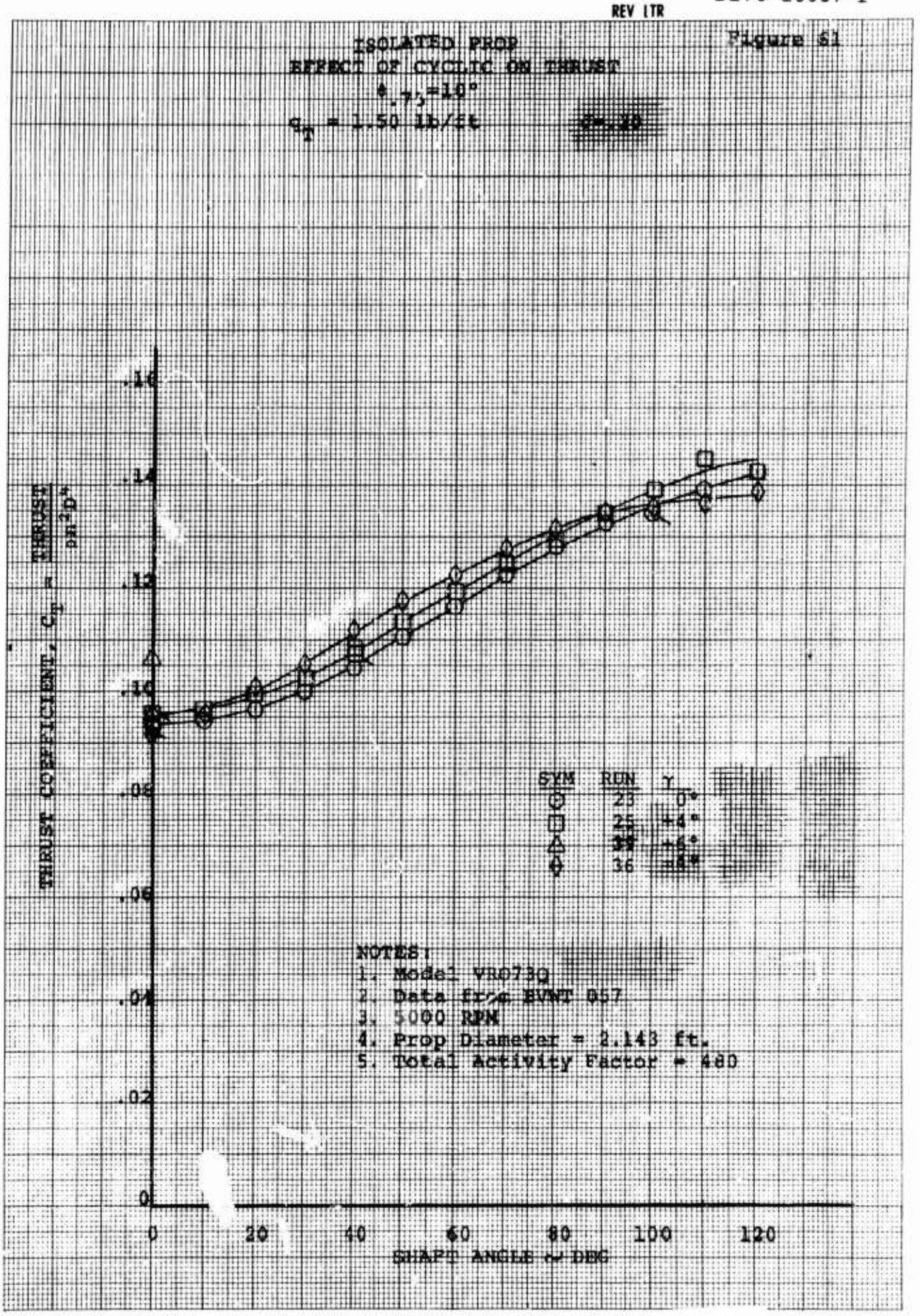

Figure 62

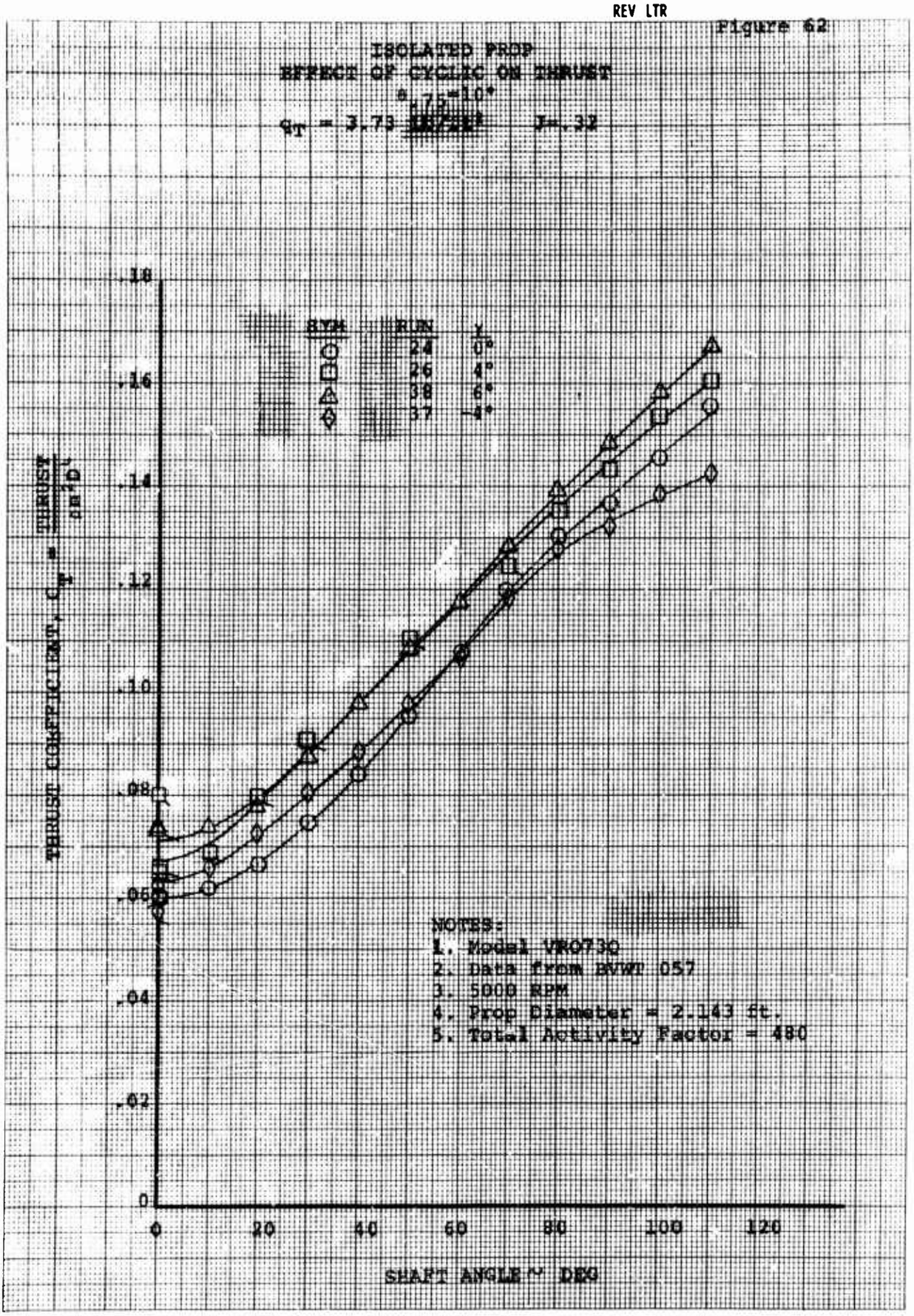

NUMBER
REV LTR

Figure 63

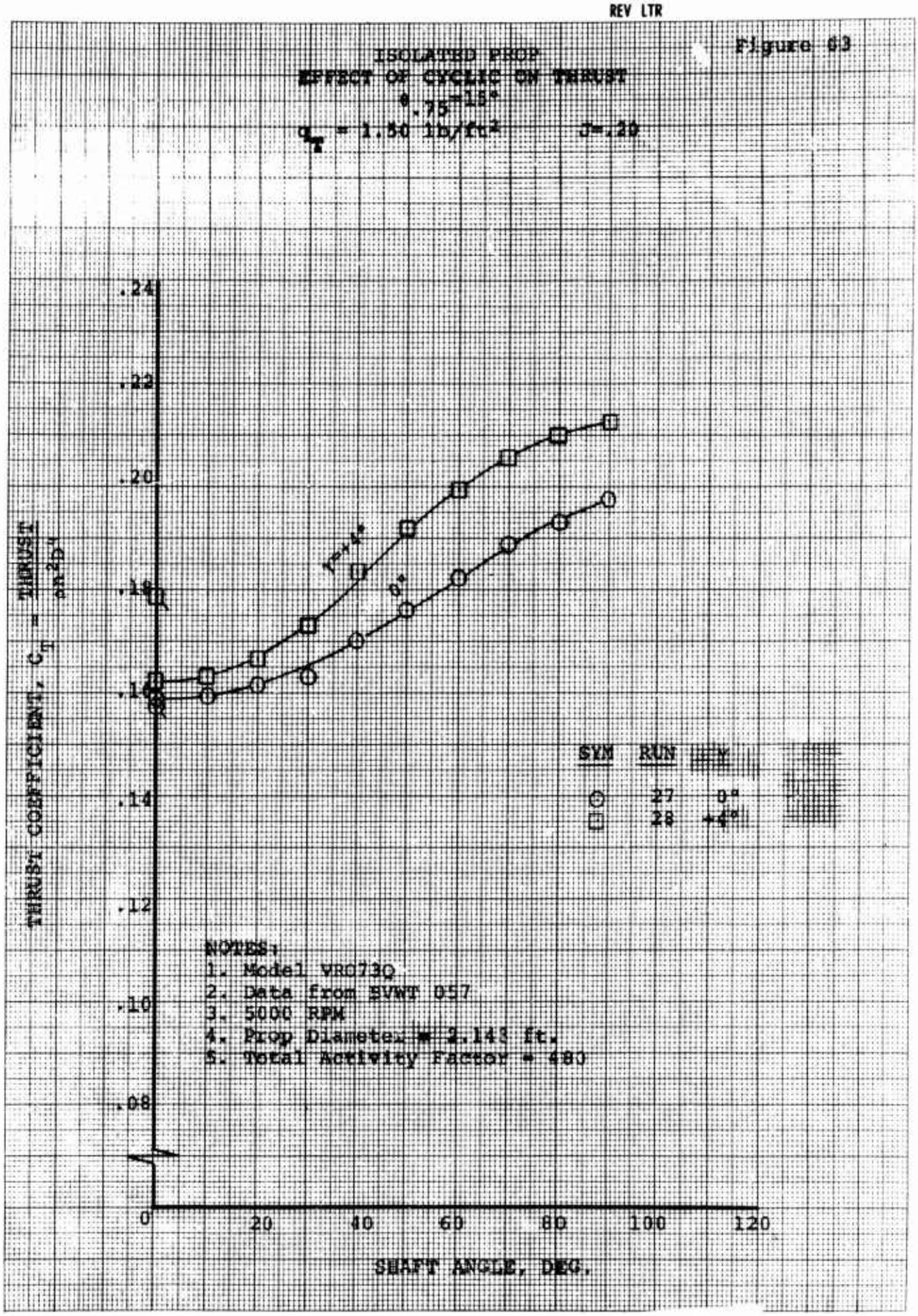

6.5 EFFECT OF CYCLIC ON PROP NORMAL FORCE

An examination of the prop normal force vs shaft angle curves presented in Figures 64 and 65 for 12° of collective reveals that application of a specific amount of cyclic pitch results in an incremental change in normal force. Positive cyclic decreases prop normal force and negative cyclic increases it.

Zero and 60° shaft angle data from Figure 64 was cross-plotted in Figures 66 and 67 to show prop normal force as a function of cyclic angle for the 0.2 and 0.32 advance ratio cases. It is apparent from these figures that prop normal force varies linearly with cyclic and the slope is constant for the test conditions illustrated. An explanation for the reduction in prop normal force with positive cyclic or the increase with negative cyclic, is that cyclic action produces an effective change in the propeller inflow angle.

Figure 68, which presents the variation in prop normal force with cyclic for the three collective settings tested at 0.2J, indicates that dC_{NF_p}/d_γ increases with collective angle. The 10° and 15° collective data in this figure was cross-plotted from the prop normal force vs shaft angle plots presented in Figures 69 and 70, respectively.

Figure 64

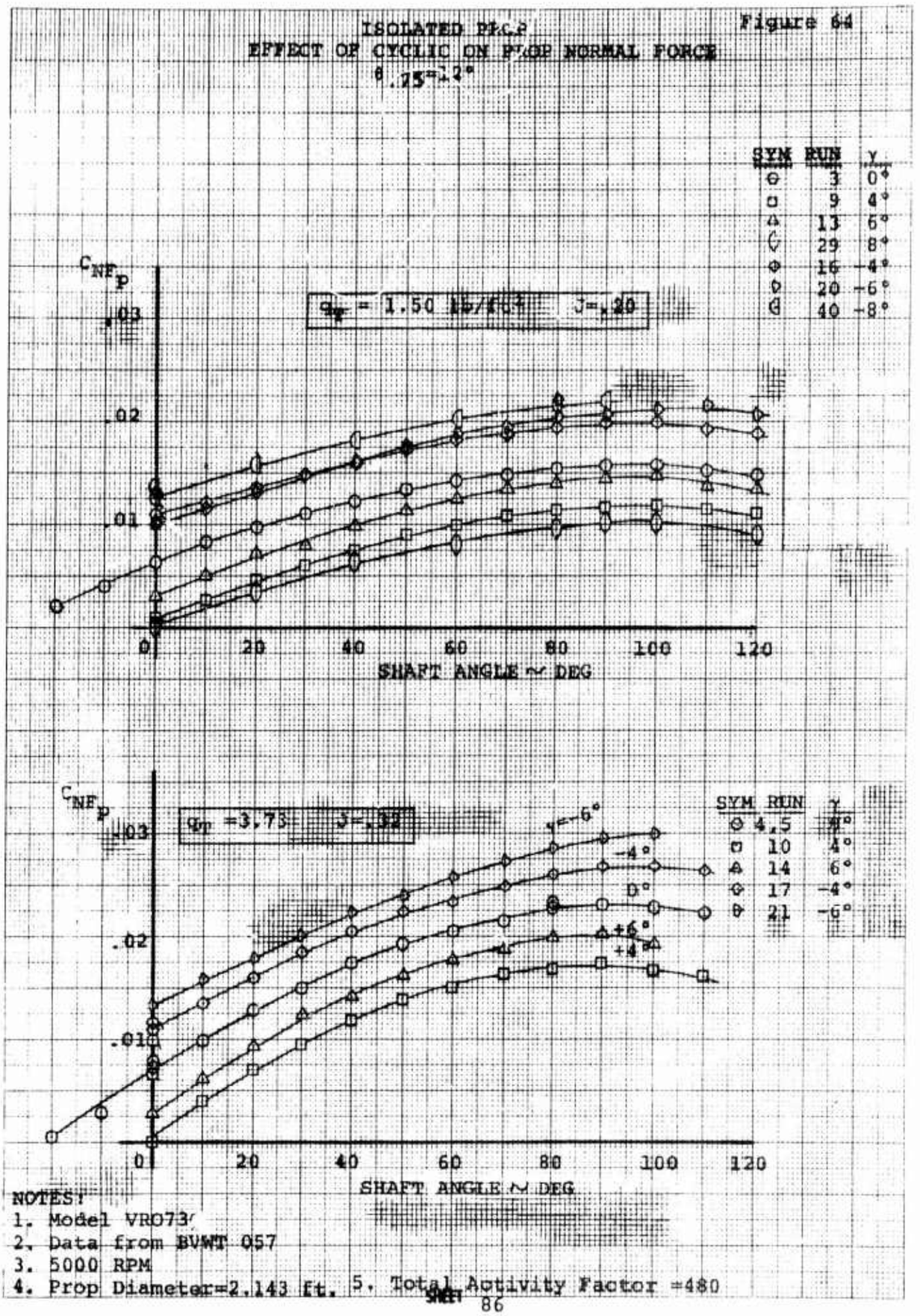

NOTES:
1. Model VRO73
2. Data from BVWT 057
3. 5000 RPM
4. Prop Diameter=2.143 ft. 5. Total Activity Factor =480

Figure 65

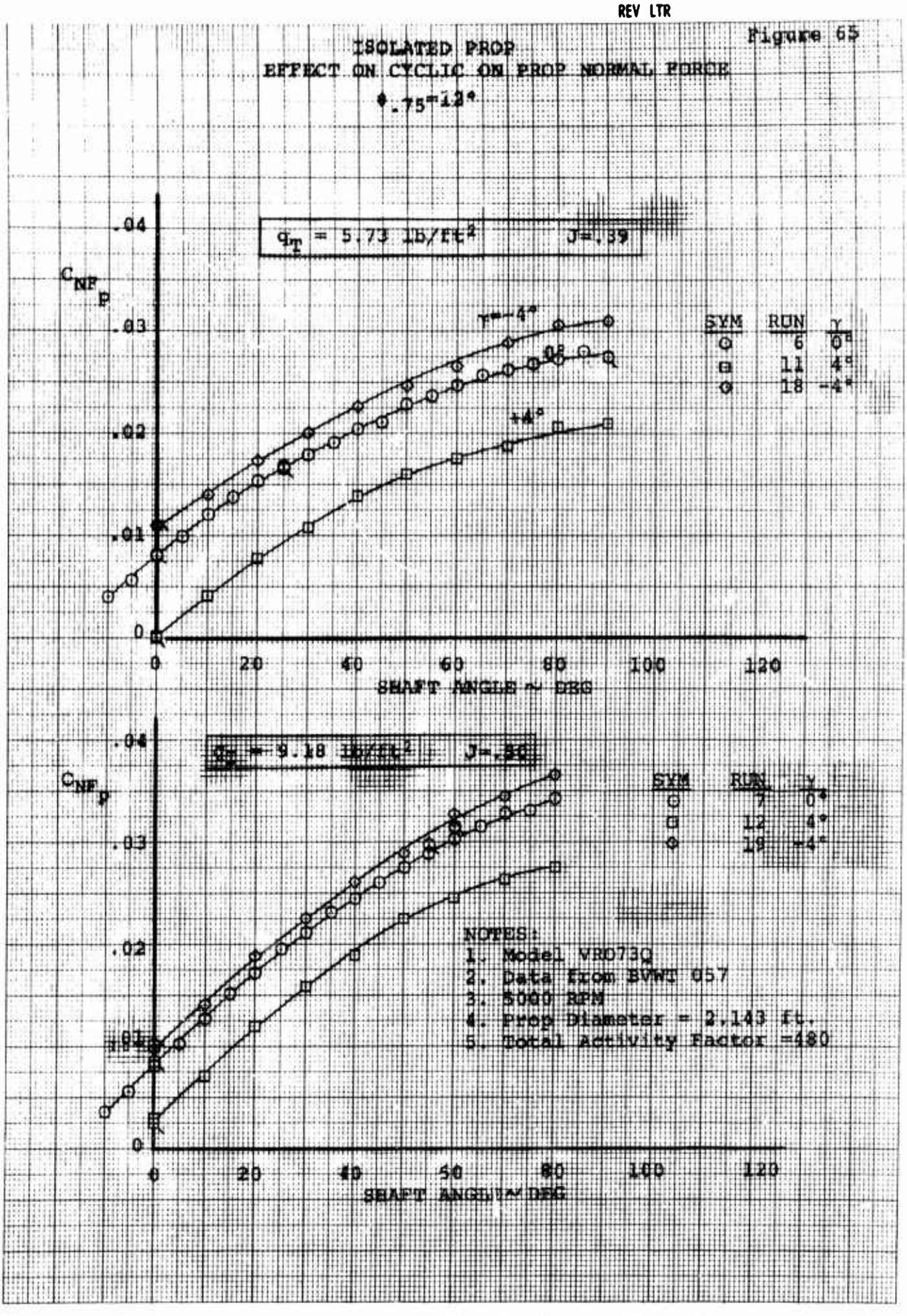

Figure 66

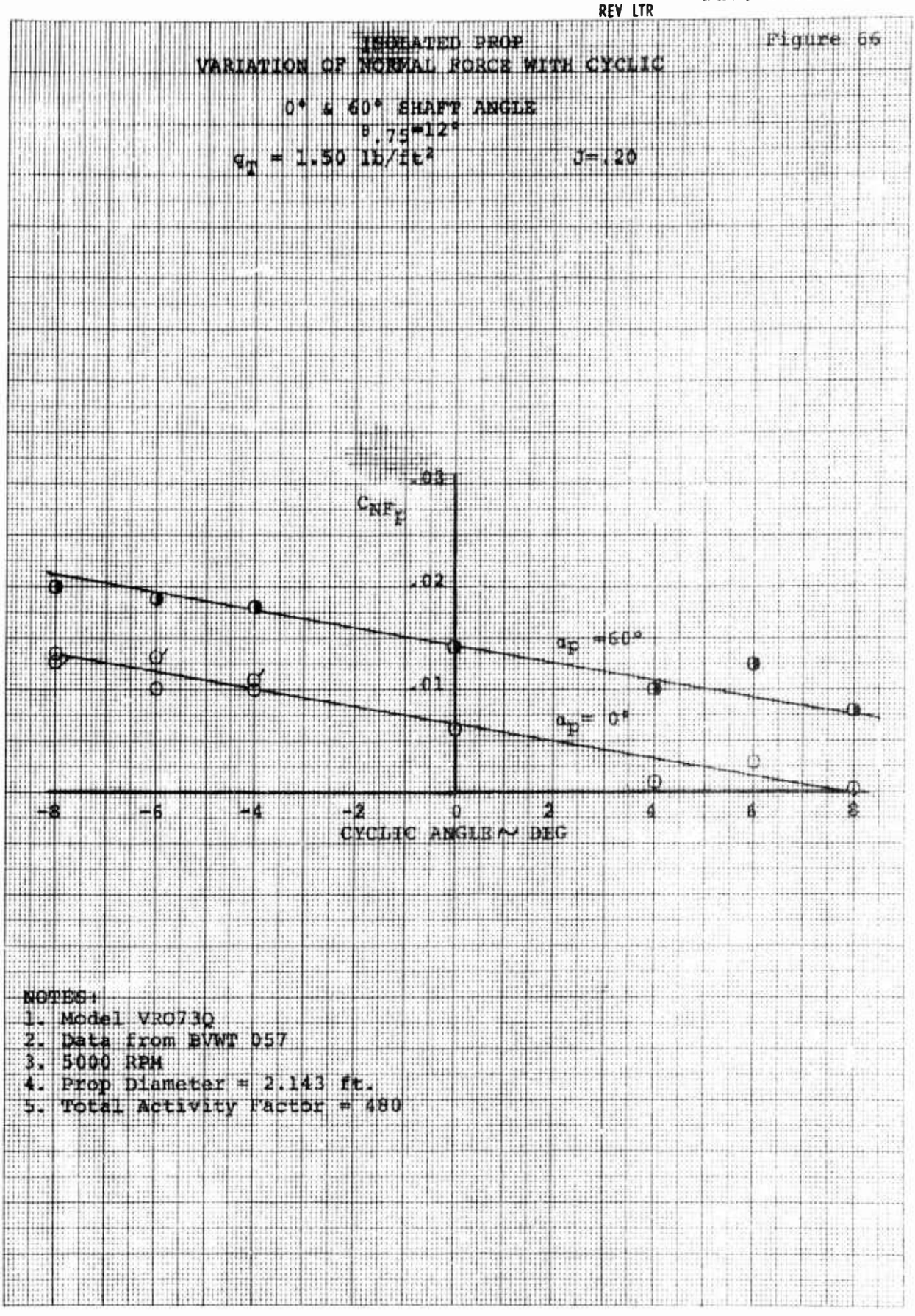

NOTES:
1. Model VRO73Q
2. Data from BVWT 057
3. 5000 RPM
4. Prop Diameter = 2.143 ft.
5. Total Activity Factor = 480

Figure 67

ISOLATED PROP
VARIATION OF NORMAL FORCE WITH CYCLIC
0° & 60° SHAFT ANGLE
$\beta_{.7R}$=12°
Φ_T = 3 [illegible] lb/ft² J=.32

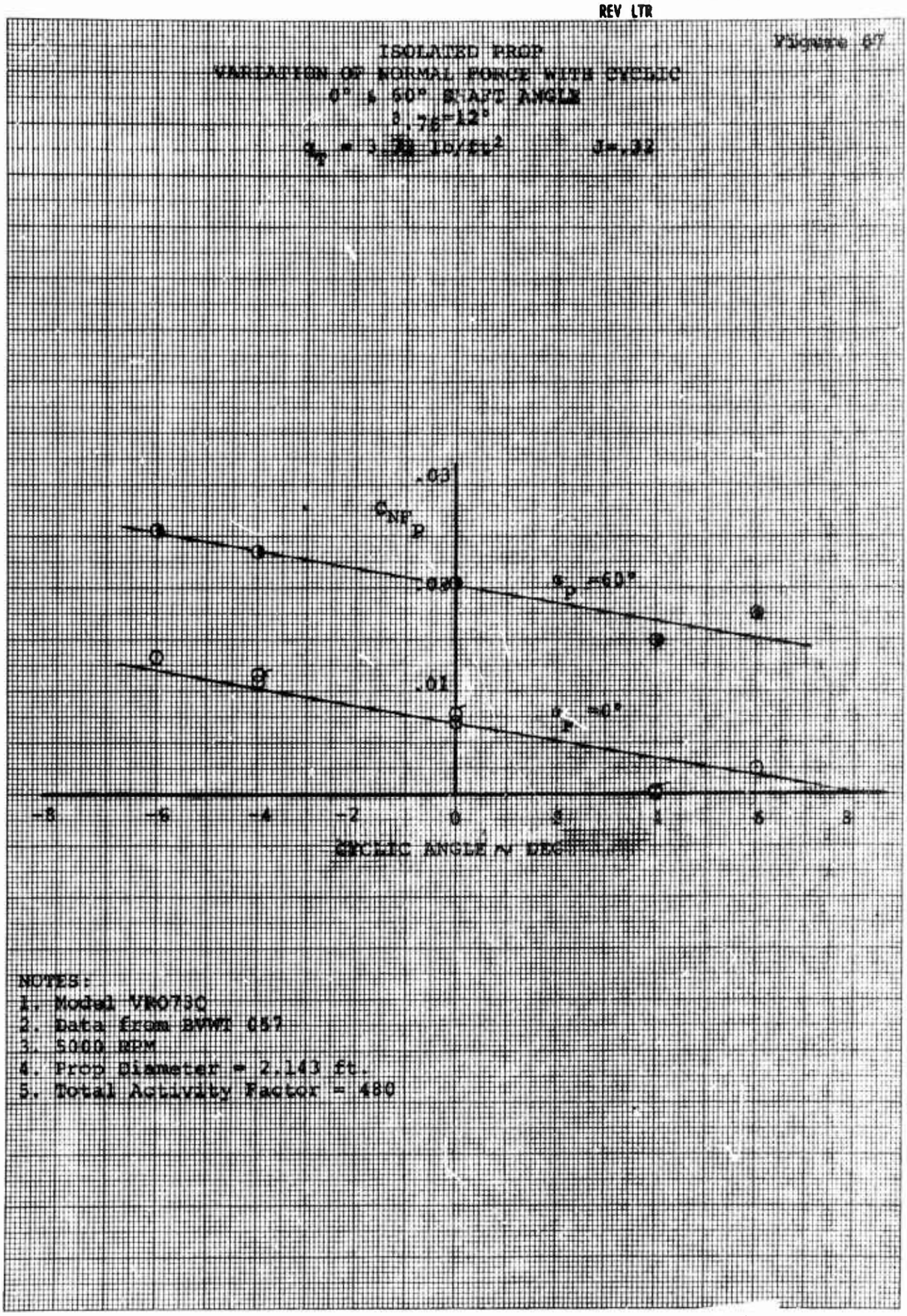

NOTES:
1. Model VK0730
2. Data from BWWT 057
3. 5000 RPM
4. Prop Diameter = 2.143 ft.
5. Total Activity Factor = 480

Figure 68

ISOLATED PROP
VARIATION OF NORMAL FORCE WITH CYCLIC AND COLLECTIVE
q_T = 1.50 lb/ft² J=0.20

NOTES:
1. Model VR073Q
2. Data from Test BVWT 057
3. 5000 RPM
4. Prop Diameter = 2.143 ft.
5. Total Activity Factor = 480

SYM	θ.75
○	12
□	10
△	15

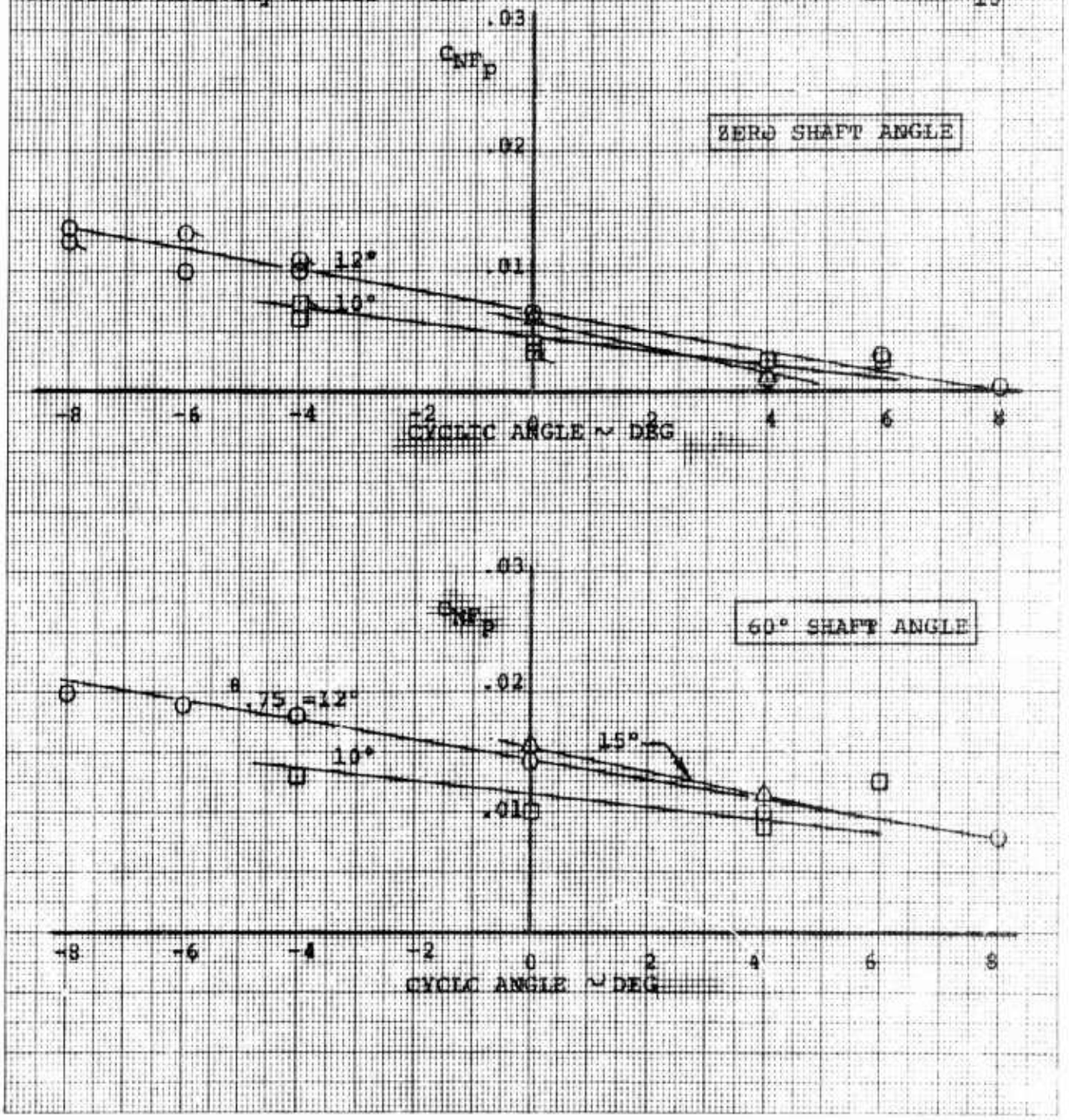

Figure 69

ISOLATED PROP
EFFECT OF CYCLIC ON PROP NORMAL FORCE
$\theta_{.75}$=10°

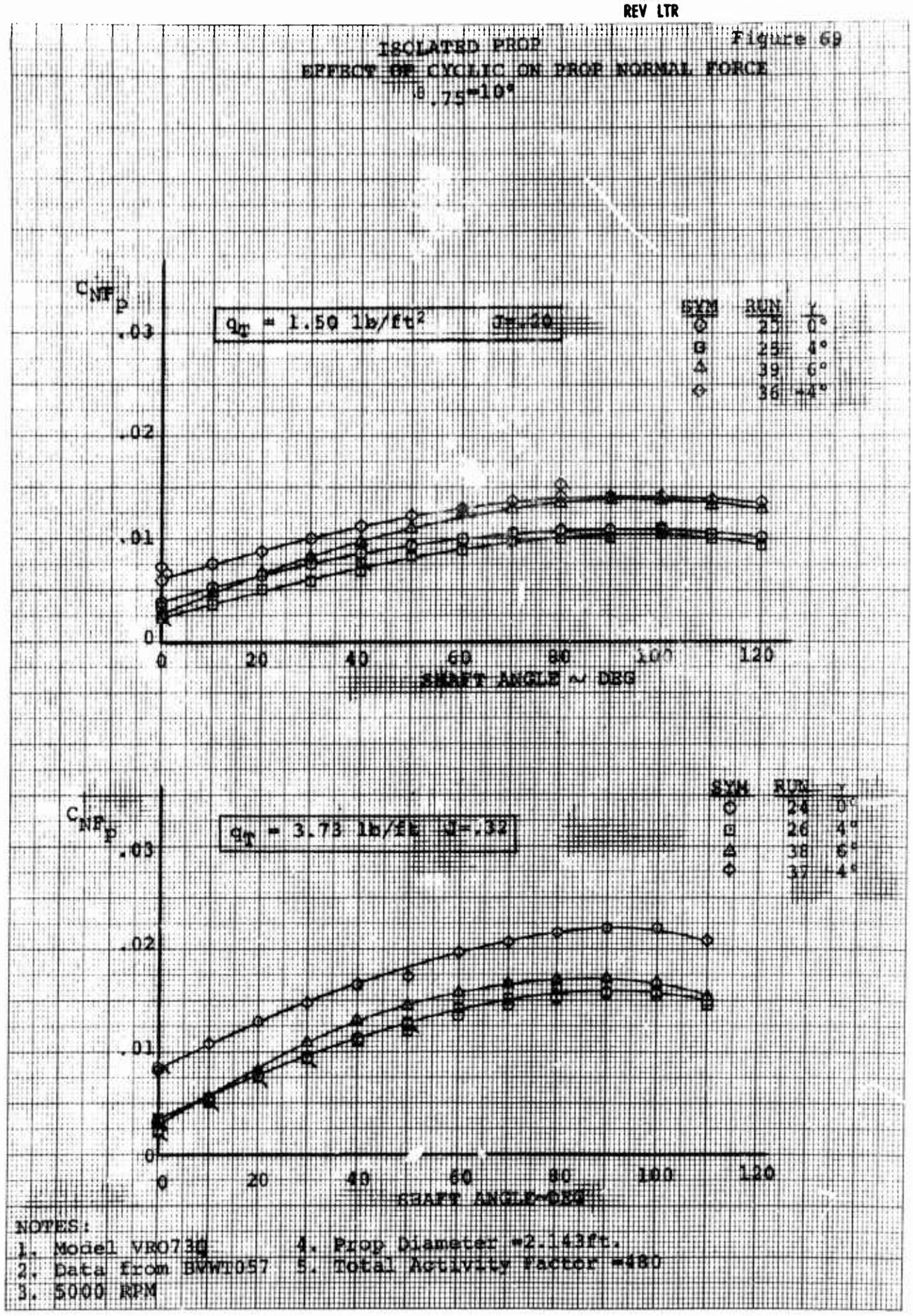

NOTES:
1. Model VRO730
2. Data from BWWT057
3. 5000 RPM
4. Prop Diameter =2.143ft.
5. Total Activity Factor =480

Figure 79

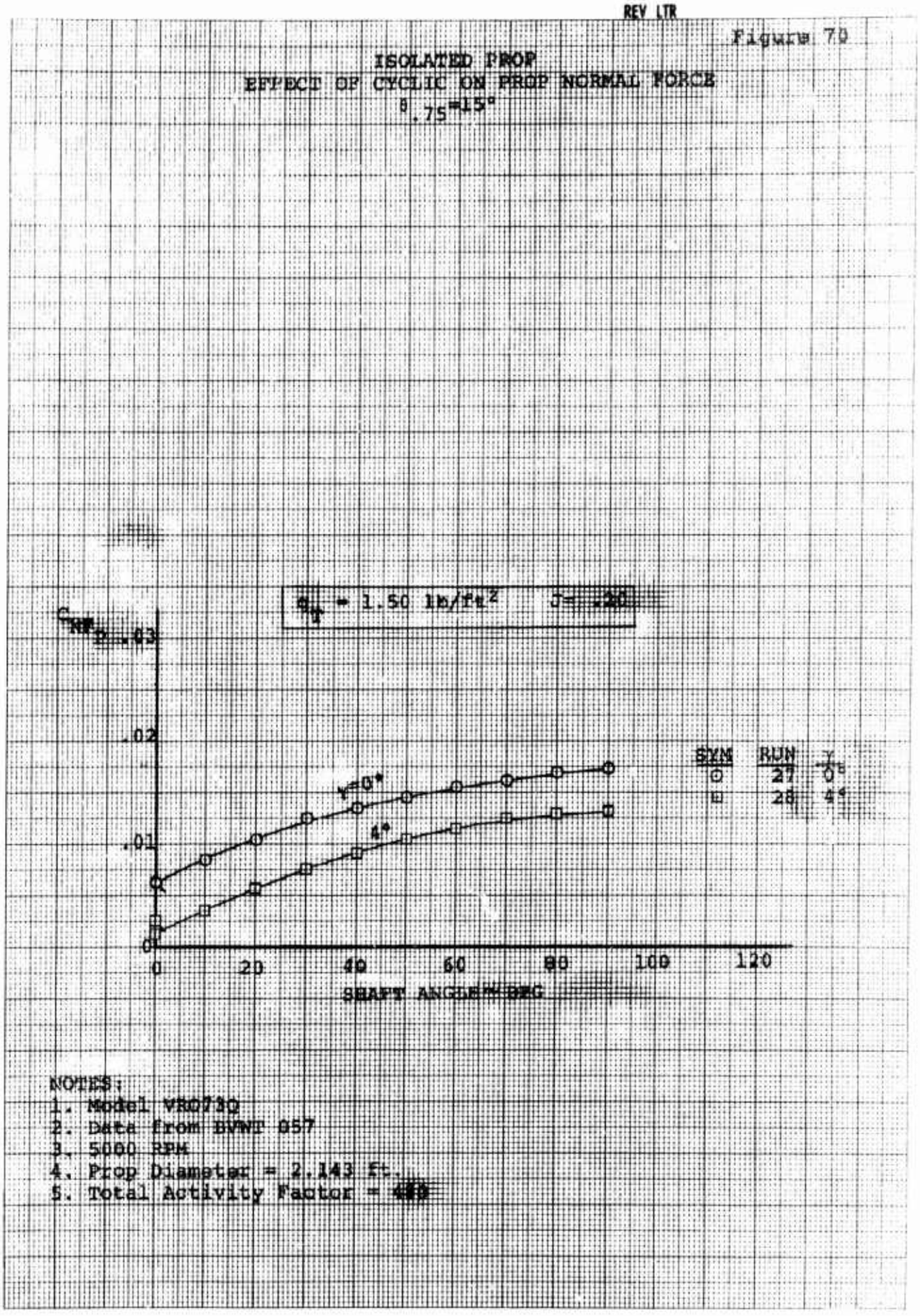

6.6 EFFECT OF CYCLIC ON PROP SIDE FORCE

Figures 71 through 74, which present the prop side force vs shaft angle data acquired at the various combinations of collective pitch setting and tunnel q or advance ratio, show that the application of cyclic pitch produces an increment in side force which is, in general, constant with shaft angle. Positive cyclic increased side force and negative cyclic decreased it.

Figure 75 illustrates the variation of prop side force with cyclic prevalent at 0.2J and 0.32J with 12° of collective. This data shows that the side force essentially, varied linearly with cyclic.

If full cyclic pitch control occurred aerodynamically at the 12 and 6 o'clock locations of the azimuth, no increment in side force should have resulted from application of cyclic. The model propeller tested was of a left hand rotation (pilot's view) and in the test, a positive side force was to the right. Consequently, the indications are that a phase lead existed, i.e., full cyclic pitch control occurred aerodynamically prior to the azimuth location desired. Phase lead is discussed further in Section 6.7 (Effect of Cyclic on Hub Yawing Moment).

Figure 71

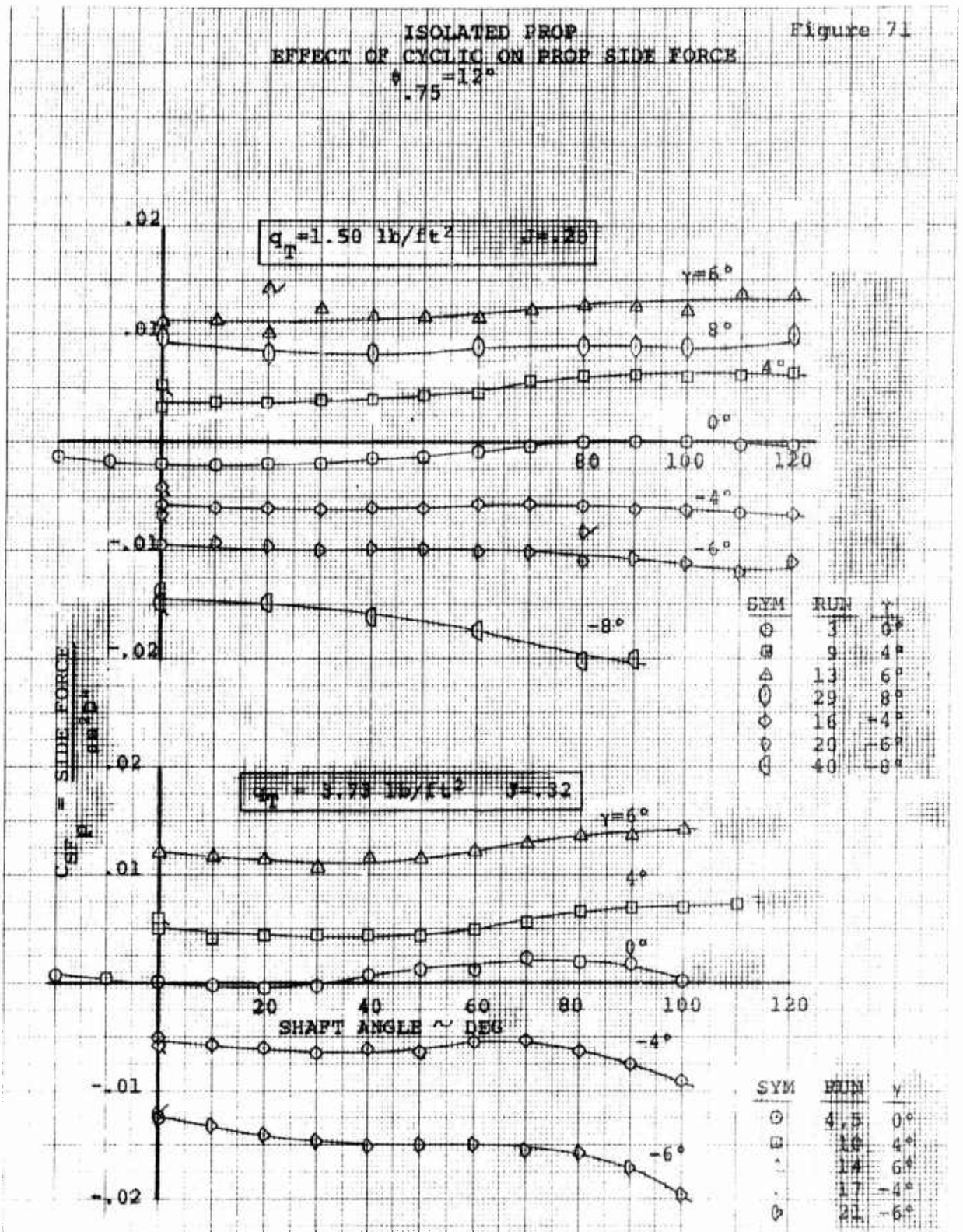

NOTES:
1. Model VRO73Q
2. Data from BVWT 057
3. 5000 RPM
4. Prop Diameter = 2.143 ft.
5. Total Activity Factor = 480

Figure 72

ISOLATED PROP
EFFECT OF CYCLIC ON PROP SIDE FORCE
$\theta_{.75}$=12°

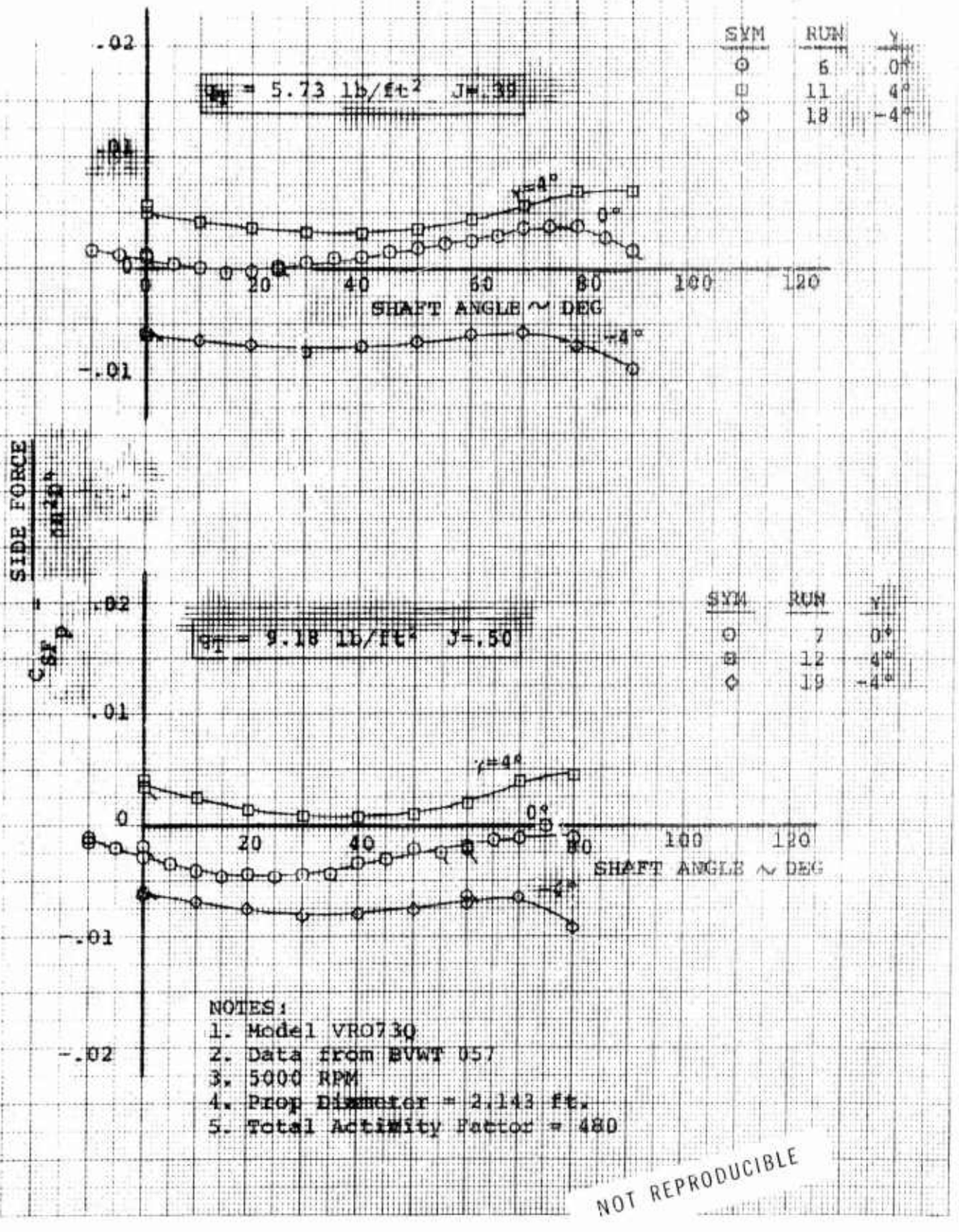

NOTES:
1. Model VRO730
2. Data from BVWT 057
3. 5000 RPM
4. Prop Diameter = 2.143 ft.
5. Total Activity Factor = 480

Figure 73

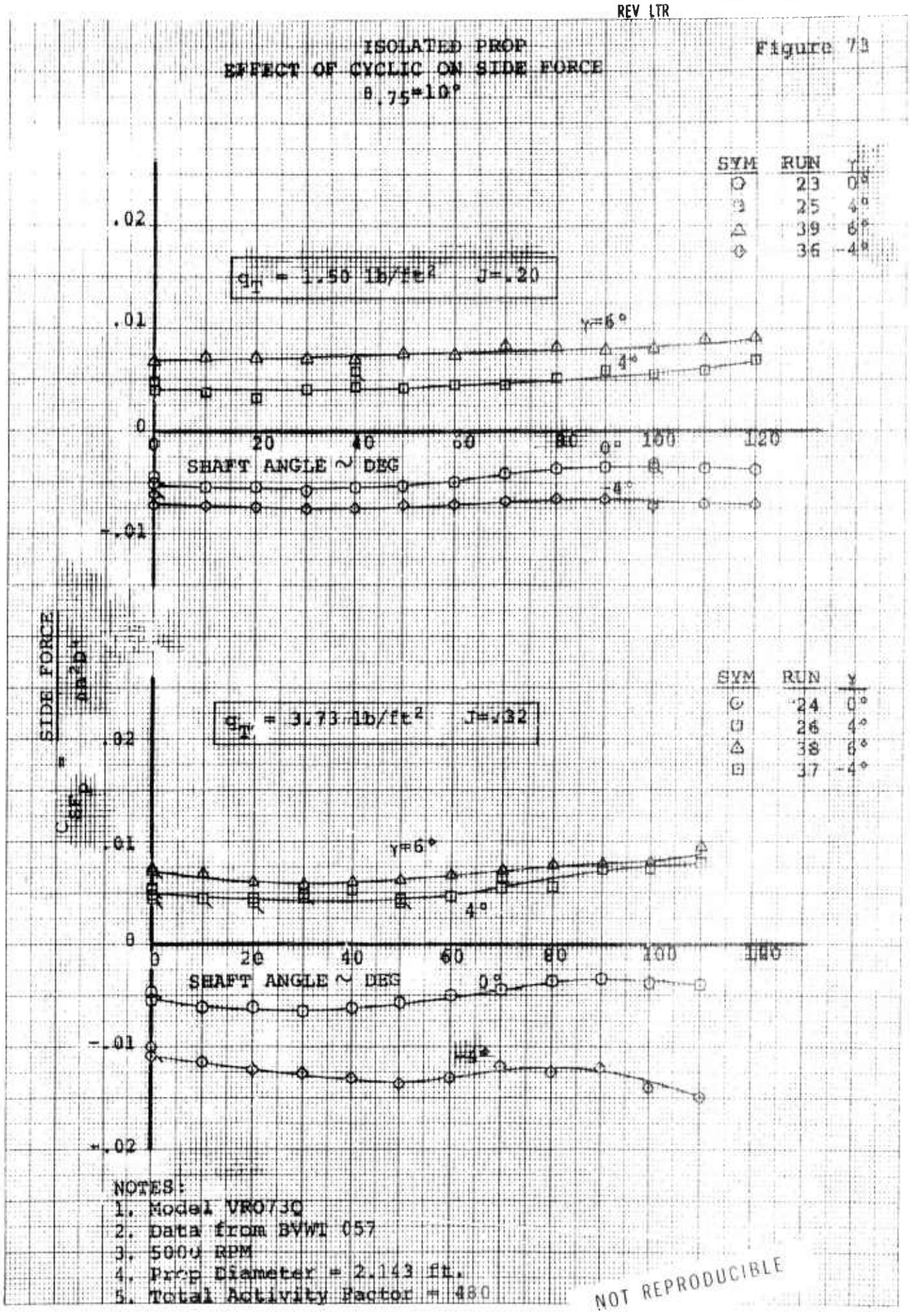

NOTES:
1. Model VRO73Q
2. Data from BVWT 057
3. 5000 RPM
4. Prop Diameter = 2.143 ft.
5. Total Activity Factor = 480

Figure 74

ISOLATED PROP
EFFECT OF CYCLIC ON SIDE FORCE
$\theta_{.75}$=15°

q_T = 1.50 lb/ft² J=.20

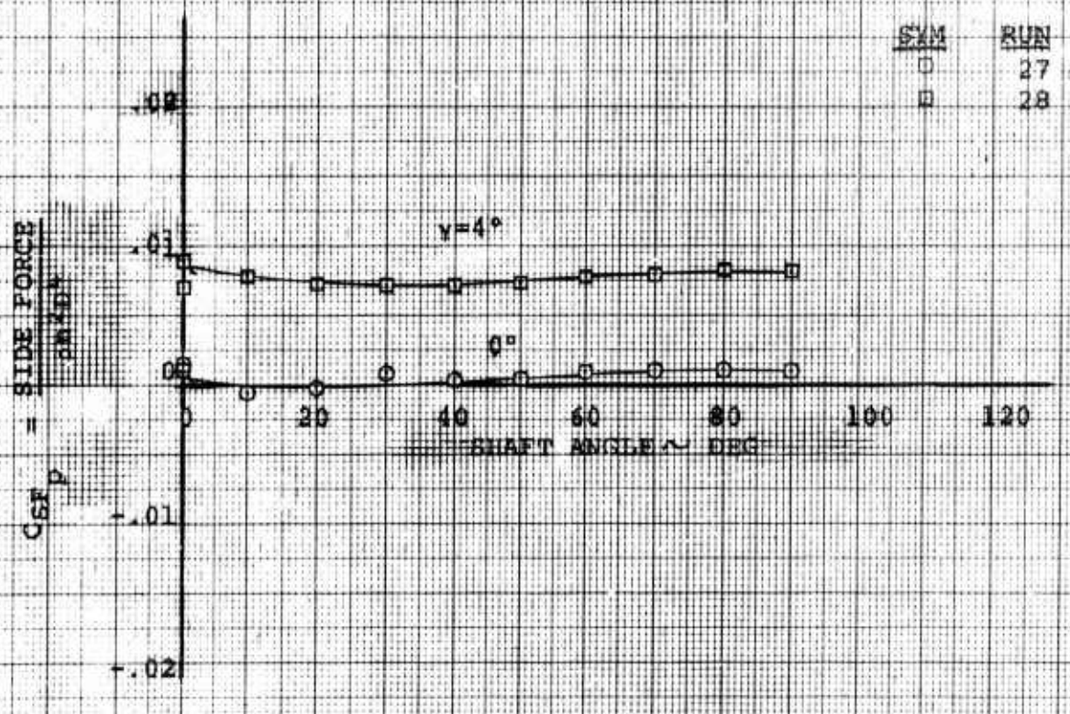

NOTES:
1. Model VRO730
2. Data from BVWT 057
3. 5000 RPM
4. Prop Diameter = 2.143 ft.
5. Total Activity Factor = 480

Figure 75

ISOLATED PROP
VARIATION OF PROP SIDE FORCE
WITH CYCLIC
$\theta_{.75}$=12°

NOTES:
1. Model VRO730
2. Data from LVWT 057
3. 5000 RPM
4. Prop Diameter=2.143ft.
5. Total Activity Factor=480

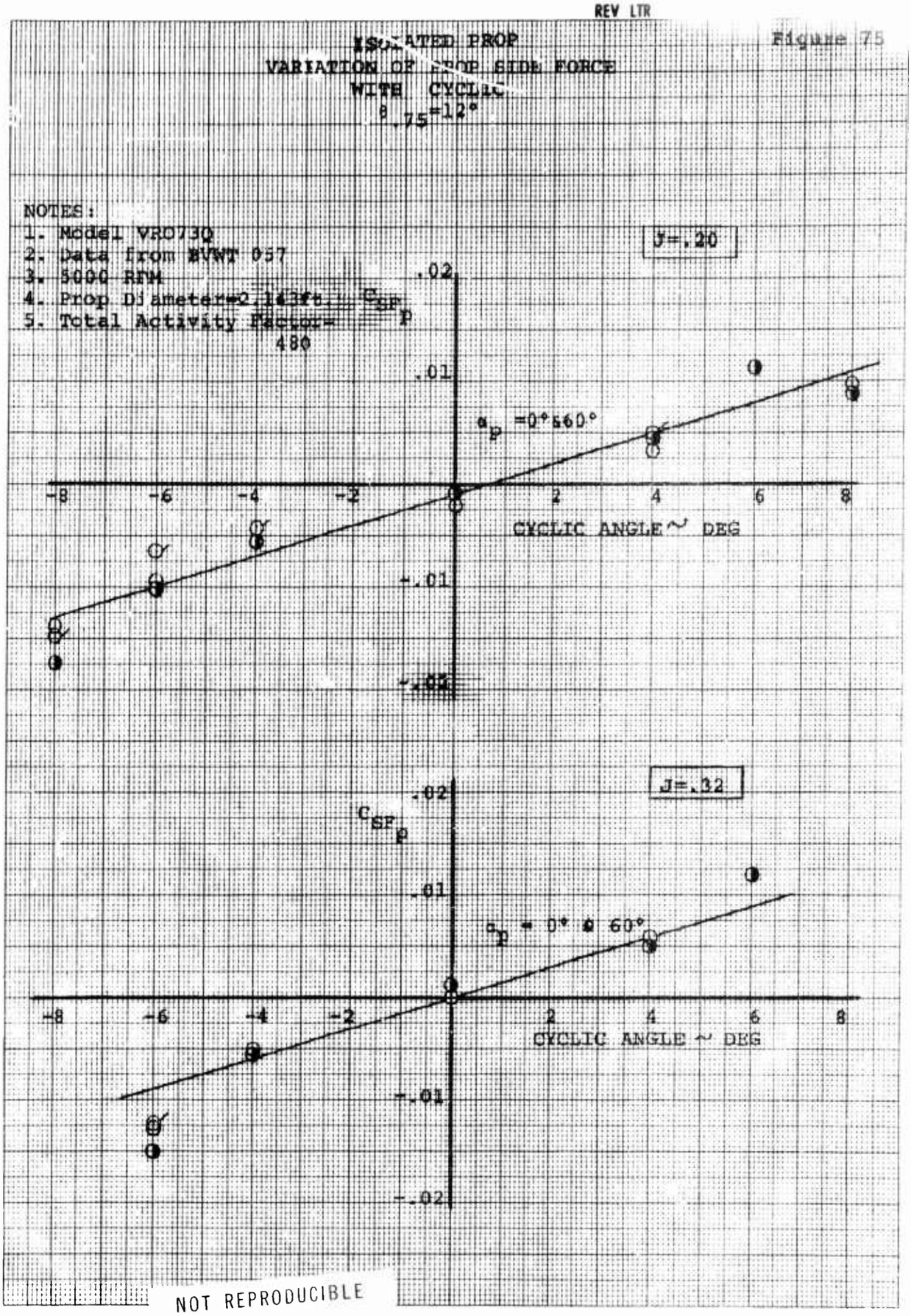

6.7 EFFECT OF CYCLIC ON HUB YAWING MOMENT

The almost linear increase in hub yawing moment with increasing shaft angle is shown in Figures 76 through 82. Each of these figures present the hub yawing moment data acquired with and without cyclic pitch at a constant tunnel q or advance ratio with a particular collective setting. During this test, a positive yawing moment was clockwise (pilot's view) or nose to the right.

The data in Figures 76 through 82 indicate an incremental change in hub yawing moment over the shaft angle range when cyclic pitch was introduced. Positive cyclic produced a negative increment and negative cyclic a positive increment.

The moment data at zero shaft angle and 60° shaft angle from Figures 76 and 77 were crossplotted in Figures 83 and 84 to show the variation in hub yawing moment with cyclic. A linear variation with essentially a constant slope can be ascertained. This characteristic indicates a constant phase lead angle existed, i.e., (1) the cyclic pitch effectiveness (dC_{M_p}/d_γ) has been previously determined to be essentially constant over a wide range of shaft angles and over a range of advance ratios from zero (hover) to 0.4, and (2) positive cyclic introduced a negative yawing moment in conjunction with its normal increment of negative pitching moment.(1)

An average phase lead angle of 15° was calculated using the hub yawing moment data (ΔC_{YM_p}) from Figures 76 and 77 in combination with the hub pitching moment data (ΔC_{M_p}) from Figures 23 and 24. The mathematical expression used for the calculation is as follows:

$$\text{Phase angle} = \tan^{-1}\left[\frac{\Delta C_{YM_p} \text{ (due to cyclic)}}{\Delta C_{M_p} \text{ (due to cyclic)}}\right]$$

A previous 2.14 ft. diameter isolated propeller test with three lower Activity Factor blades (91 per blade) and a similar cyclic hub (subsequently modified for the higher Activity Factor propeller of test BVWT 057) indicated a 15° phase lag angle existed between the mechanical application of and the resultant effect of cyclic. Based on this information, cyclic pitch angles were manually set during test BVWT 057, with a 15° phase lead angle. The data from this test would indicate a set of highly rigid propeller blades and a close tolerance cyclic input system, with high rigidity.

(1) The left hand rotation of the model prop was previously mentioned.

Figure 76

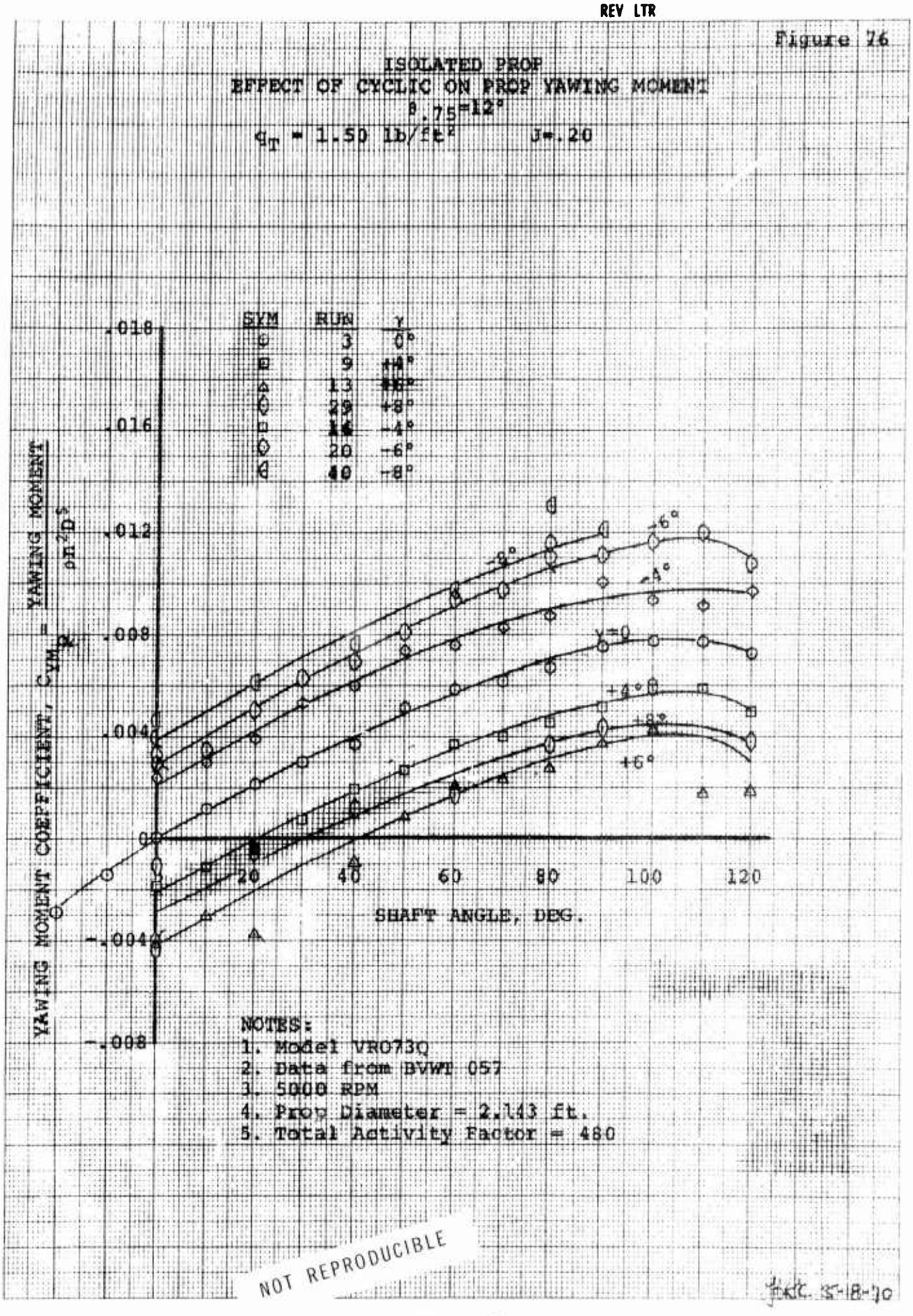

Figure 77

ISOLATED PROP
EFFECT OF CYCLIC ON PROP YAWING MOMENT
$\theta_{.75}$=12°
q_T = 3.73 lb/ft² J=.32

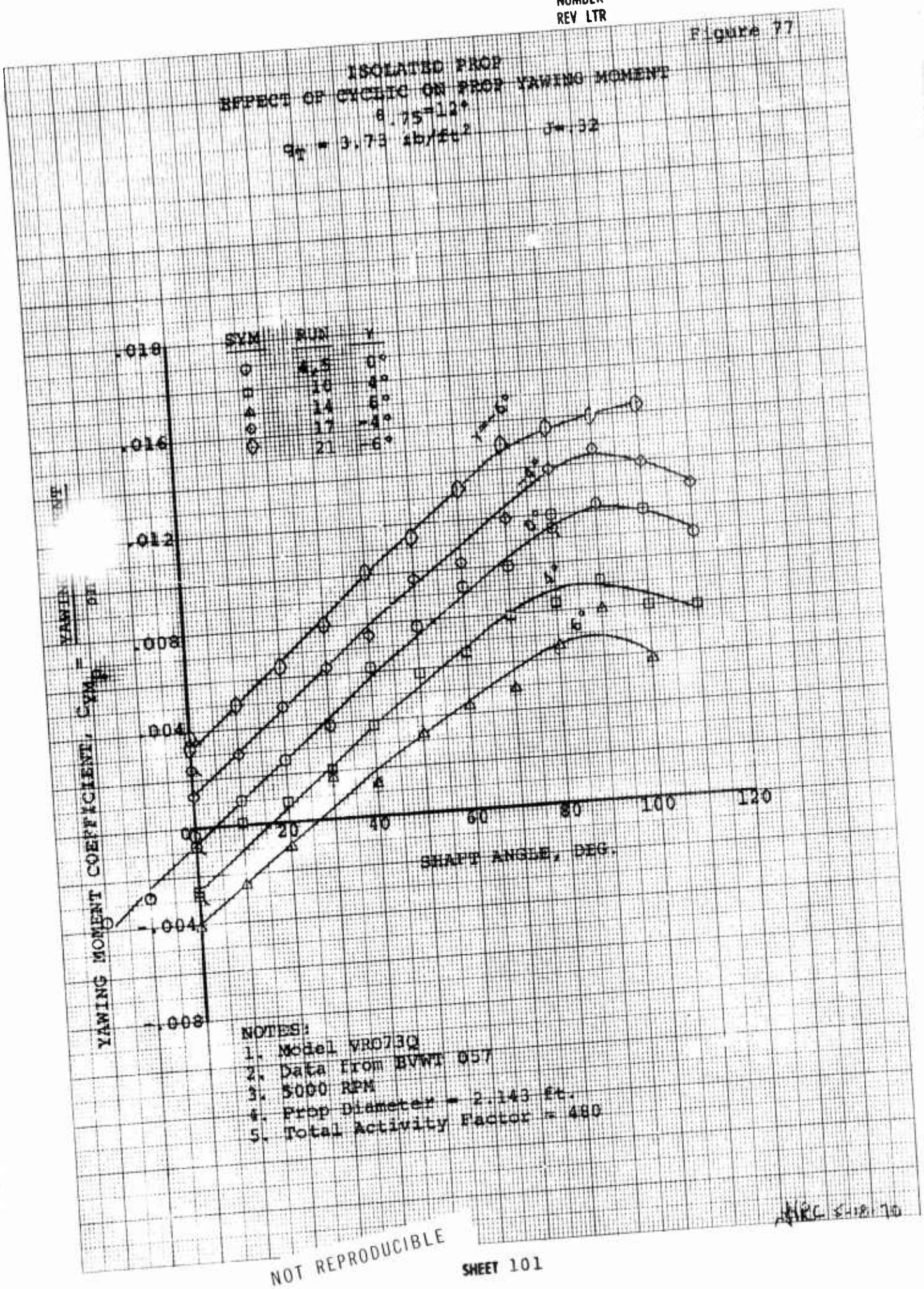

Figure 78

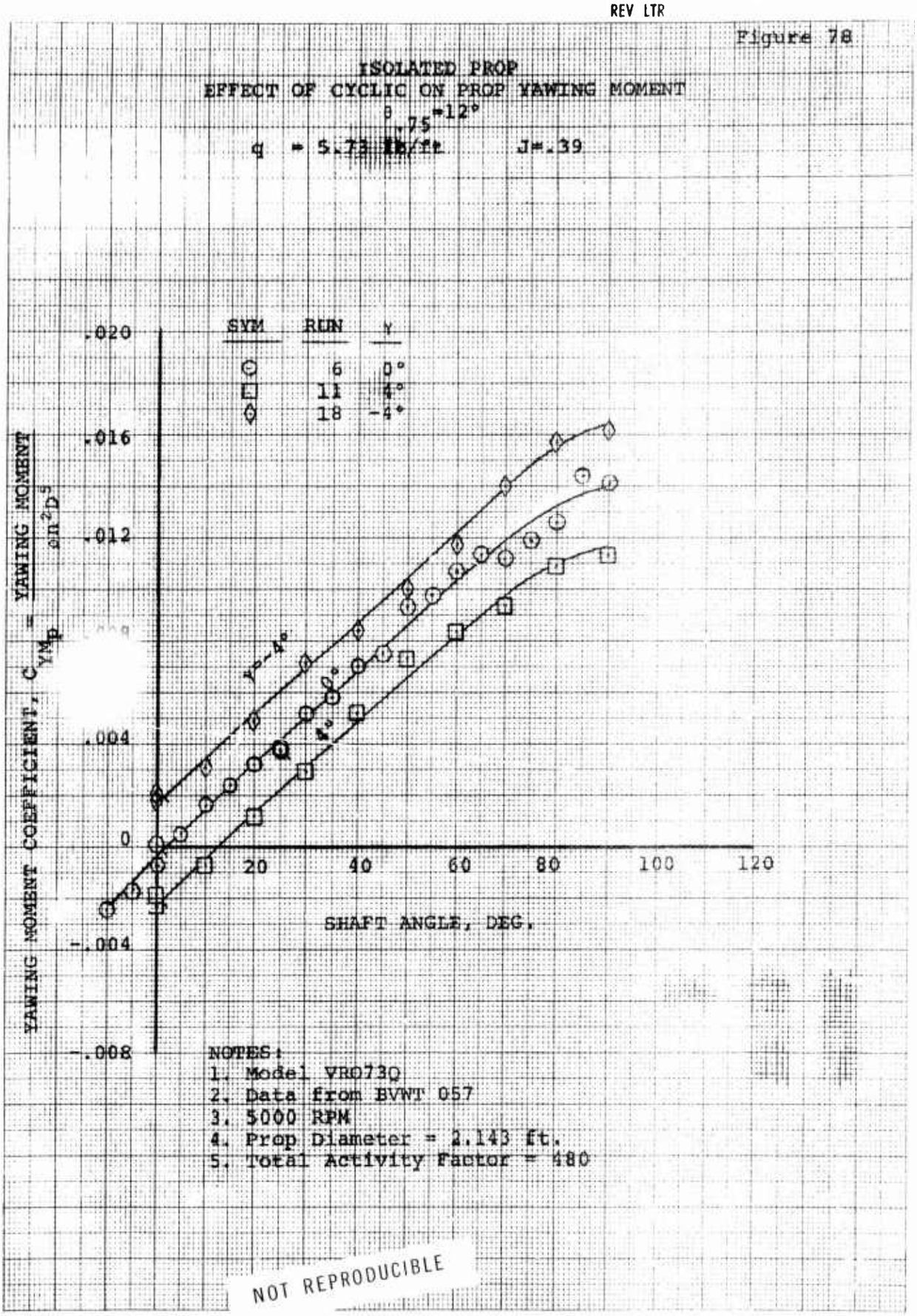

Figure 79

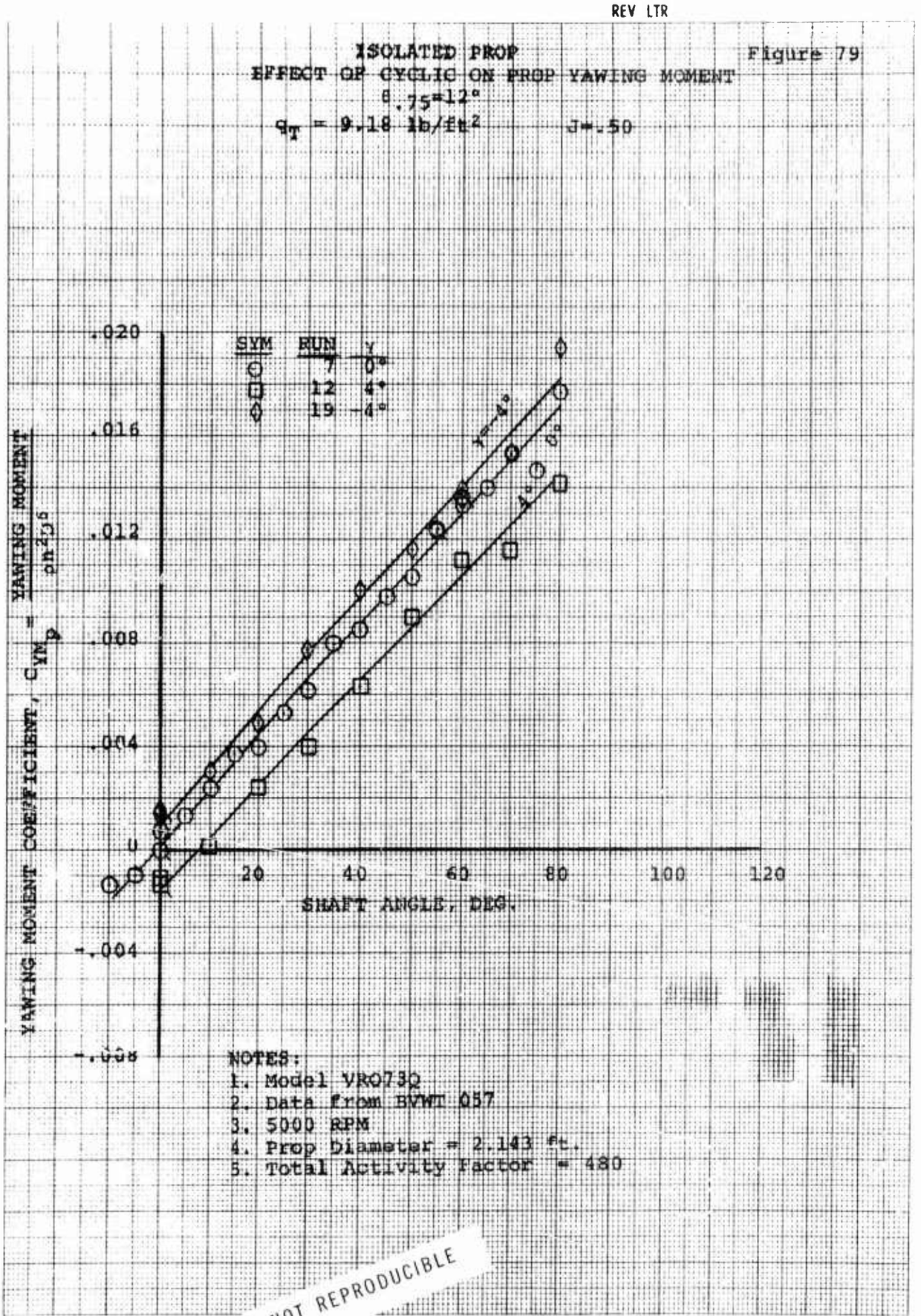

NOTES:
1. Model VRO73Q
2. Data from BVWT 057
3. 5000 RPM
4. Prop Diameter = 2.143 ft.
5. Total Activity Factor = 480

Figure 80

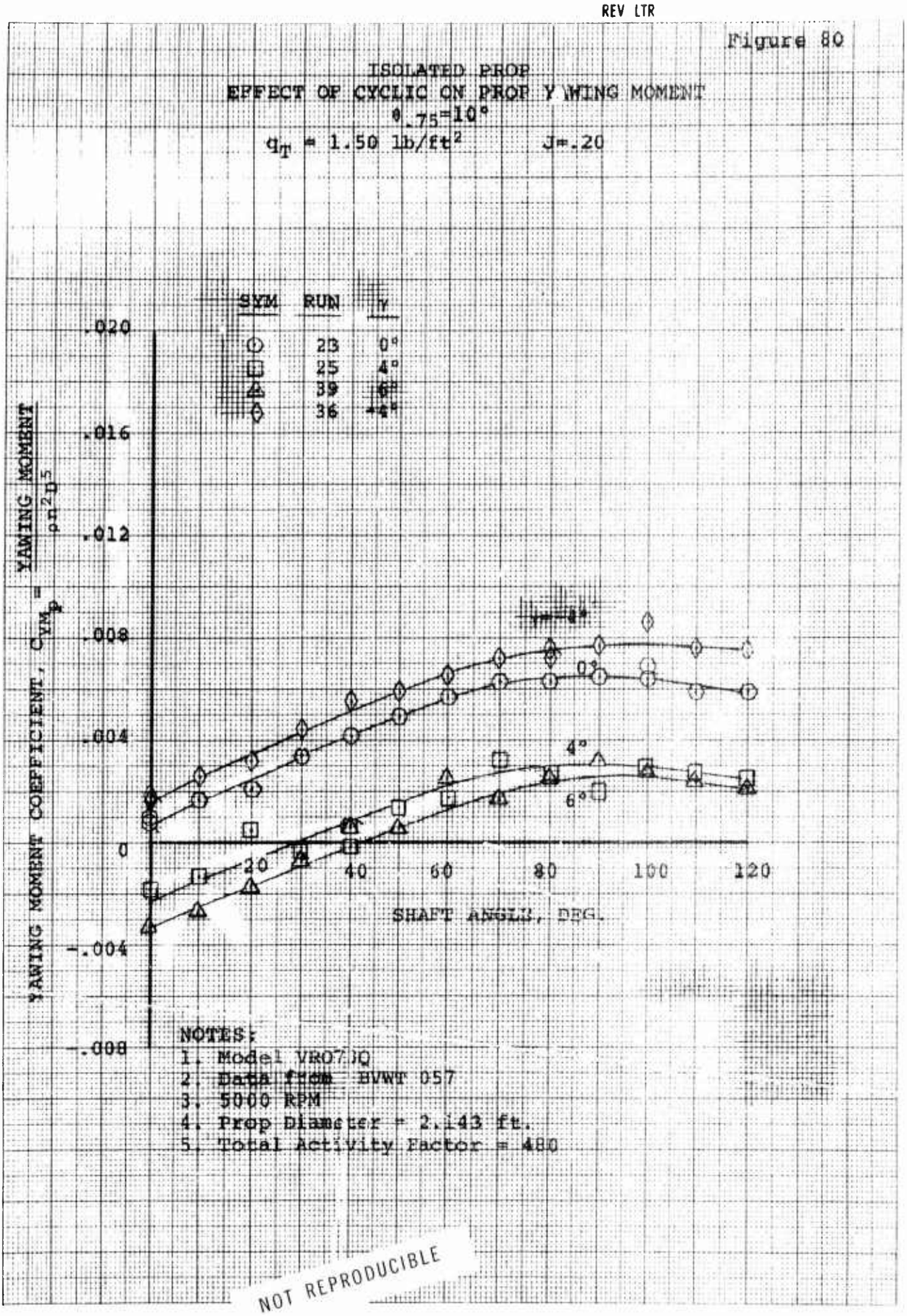

Figure 81

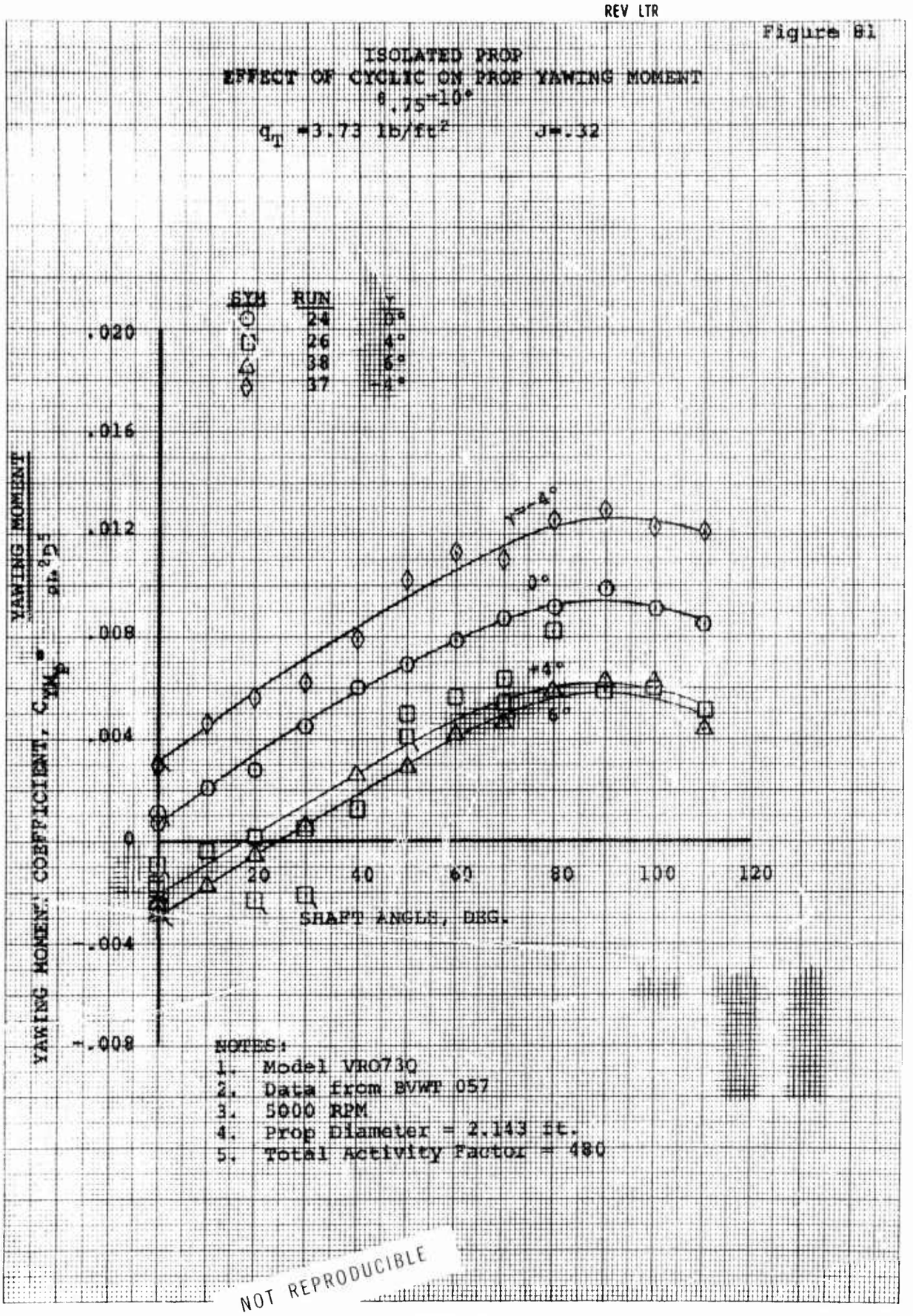

Figure 82

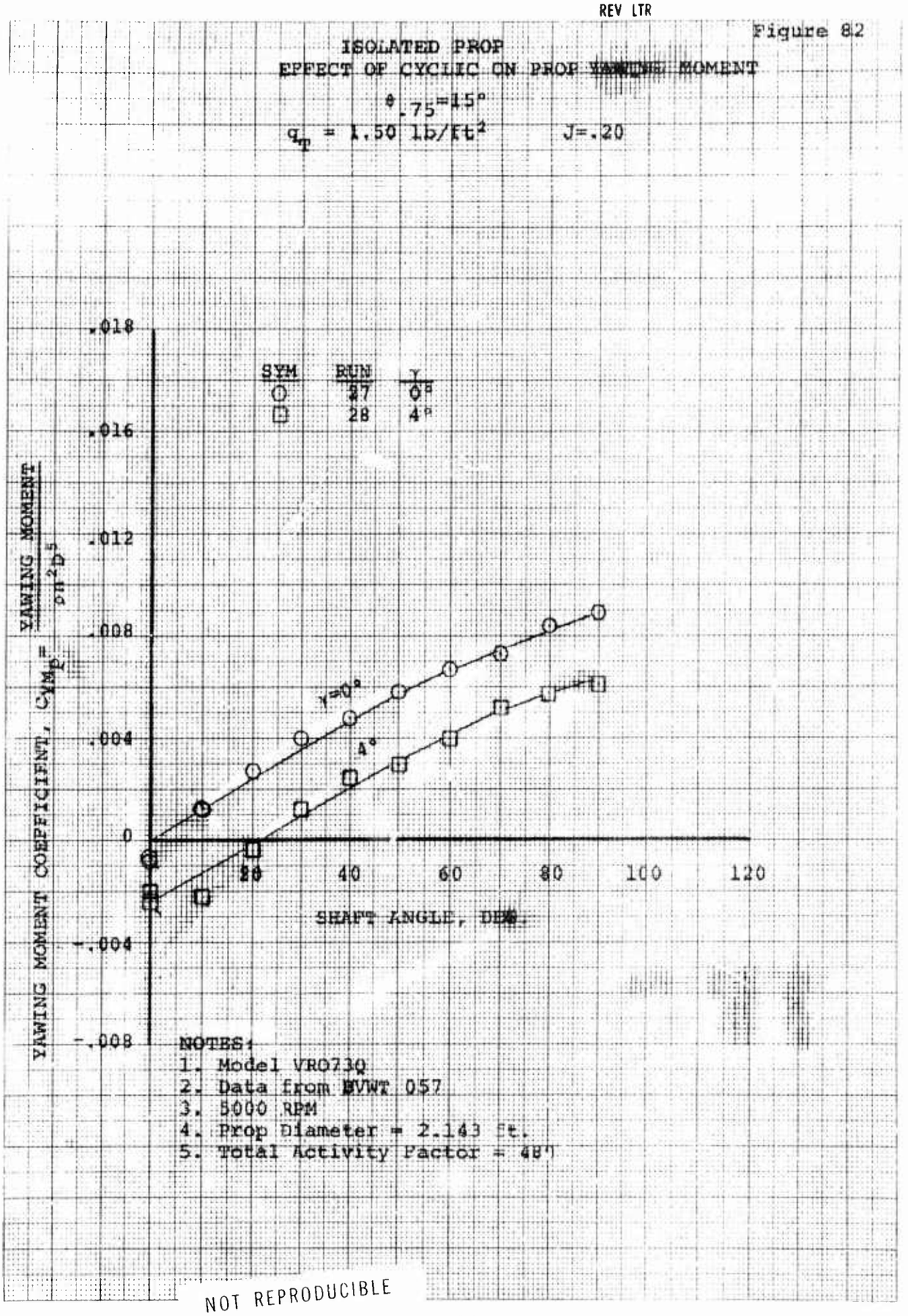

Figure 83

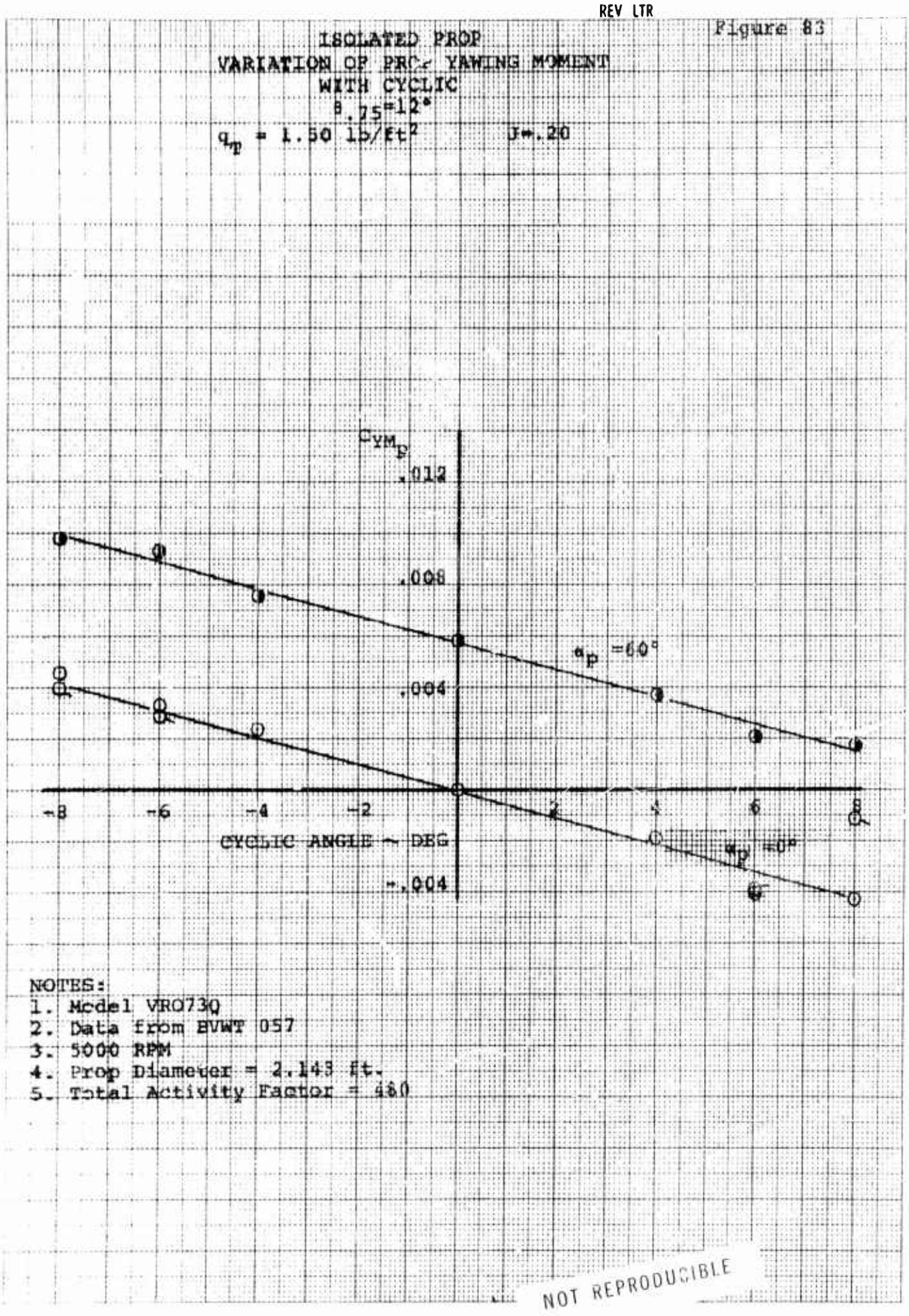

NOTES:
1. Model VRO730
2. Data from BVWT 057
3. 5000 RPM
4. Prop Diameter = 2.143 ft.
5. Total Activity Factor = 460

Figure 84

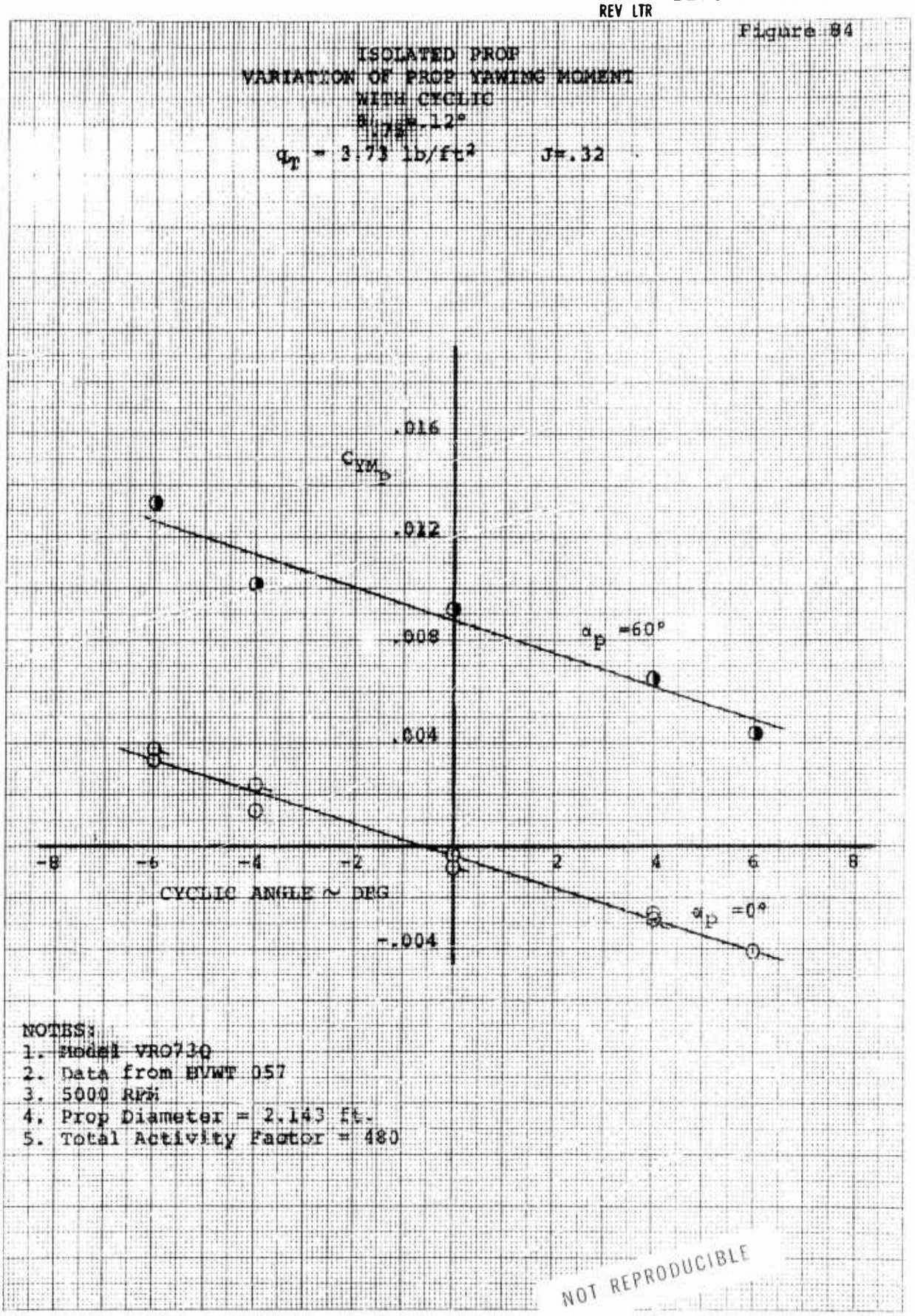

NOTES:
1. Model VRO730
2. Data from BVWT 057
3. 5000 RPM
4. Prop Diameter = 2.143 ft.
5. Total Activity Factor = 480

6.8 CYCLIC PITCH EFFECTIVENESS (SLIPSTREAM NOTATION)

This section corresponds to Section 6.2 of this report. Here, the coefficients are presented in slipstream notation, as compared to the propeller notation of Section 6.2 Cyclic effectiveness in slipstream notation is of interest since it is the practice to reduce tilt wing model data in slipstream notation and consequently pitching moments introduced from the propeller should also be understood in slipstream notation in order to ascertain the effect of the propeller on stability and control.

Figure 85 presents the hub pitching moment produced per degree of cyclic ($\Delta C_{M_S}/\Delta\gamma$) as a function of forward speed in terms of slipstream thrust coefficient (C_{T_S}). Data is shown for the three collective settings tested at a shaft angle of 60°. This figure shows that cyclic pitch effectiveness in terms of $\Delta C_{M_S}/\Delta\gamma$ is constant for the speed range evaluated excluding hover. In propeller terminology $\Delta C_{M_P}/\Delta\gamma$ increased slightly with speed.

Figure 85 also indicates that $\Delta C_{M_S}/\Delta\gamma$ increases with a decrease in collective angle. This is logical when one considers that $\Delta C_{M_S}/\Delta\gamma$ did not materially change with collective setting and that slipstream q (q_S) increases with an increase in collective and vice versa.

A cyclic pitch effectiveness ($\Delta C_{M_S}/\Delta\gamma$) of -.0475 was measured in hover per Figure 86.

The primary difference between hub pitching moment produced by cyclic when presented in slipstream notation as compared to a presentation in propeller notation, is the variation with shaft angle. An example of ΔC_{M_S} due to cyclic at various shaft angles is presented in Figure 87 for the 1.50 tunnel q and 12° collective case. This figure shows a sizeable decrease in cyclic hub pitching moment with shaft angle whereas in propeller terminology the cyclic effectiveness was essentially constant for a range of shaft angles from 0° to 90°. See Figure 23 for corresponding data in propeller terminology. The decrease of ΔC_{M_S} in slipstream notation is a result of the increase in slipstream q (q_S) with shaft angle that occurred during the constant propeller RPM/collective setting runs.

Figure 85

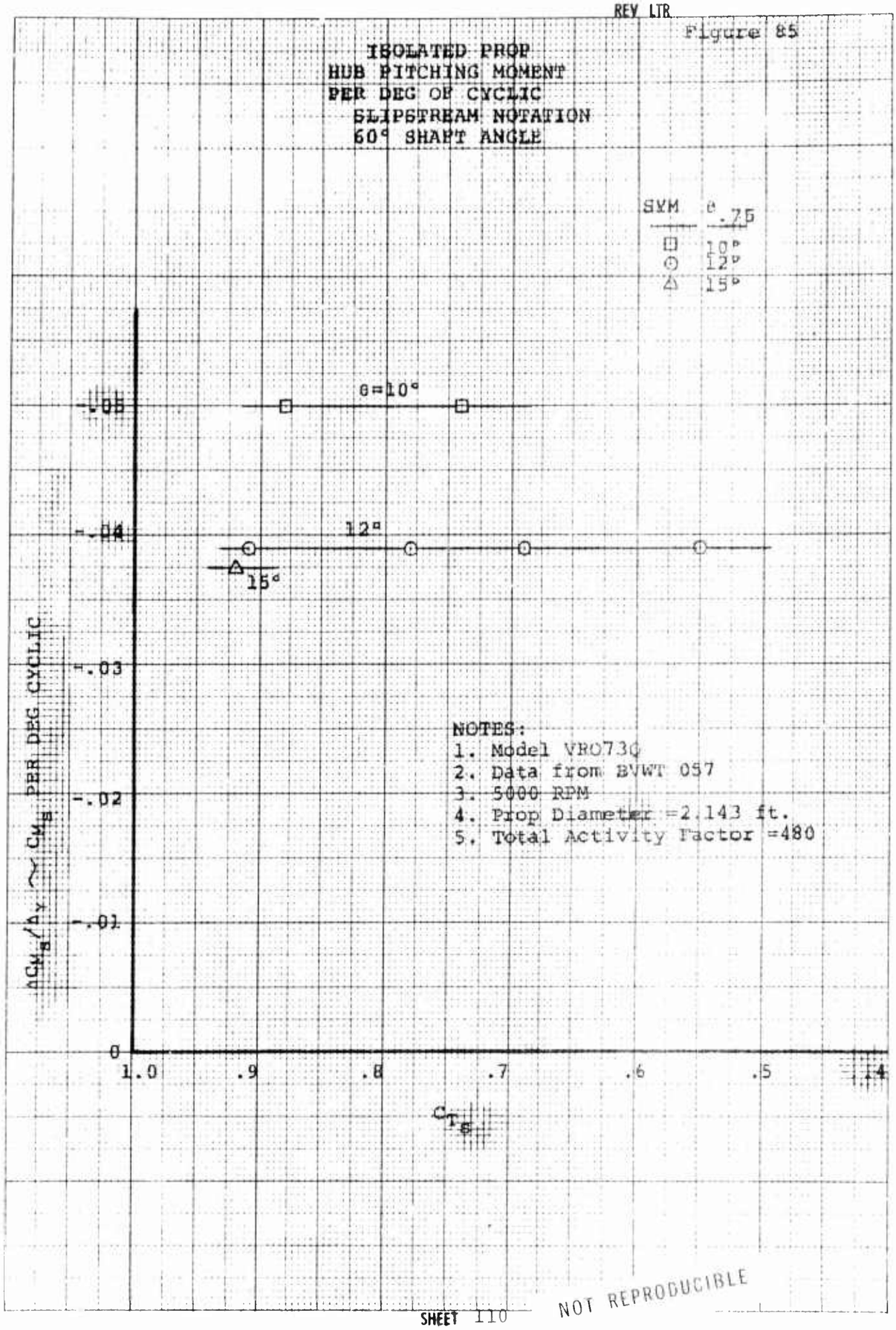

Figure 86

ISOLATED PROP
INCREMENTAL HUB PITCHING MOMENT
DUE TO CYCLIC
SLIPSTREAM NOTATION
HOVER

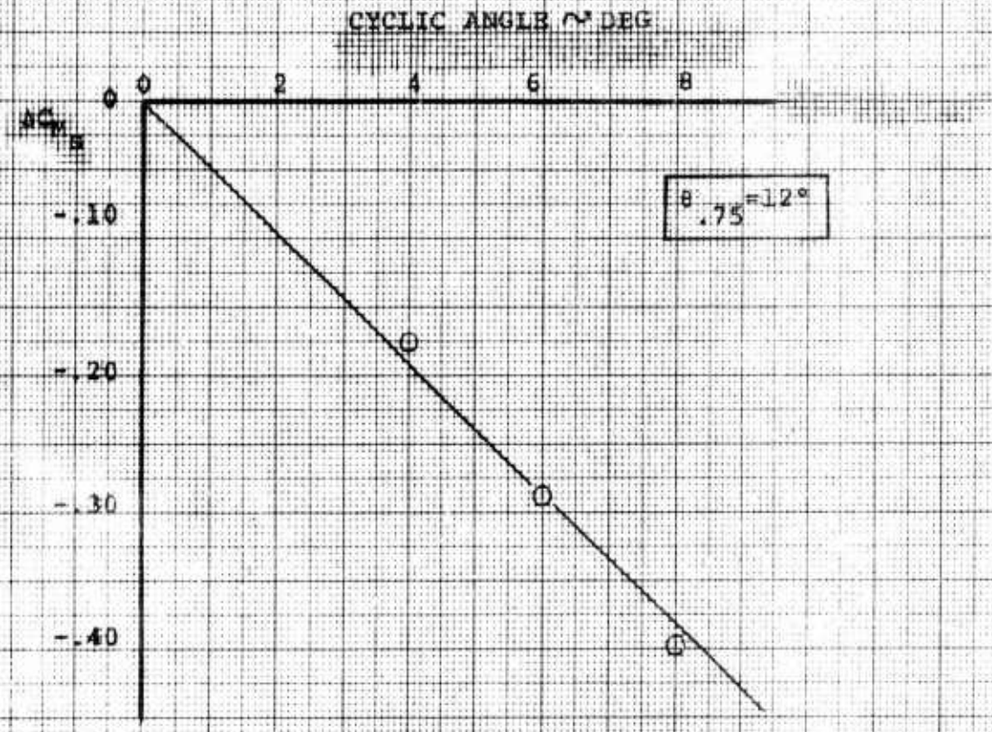

NOTES:
1. Model VRO73Q
2. Data from BVWT 057
3. 5000 RPM
4. Prop Diameter = 2.143 ft.
5. Total Activity Factor = 490
6. Data from Runs 32-35

Figure 87

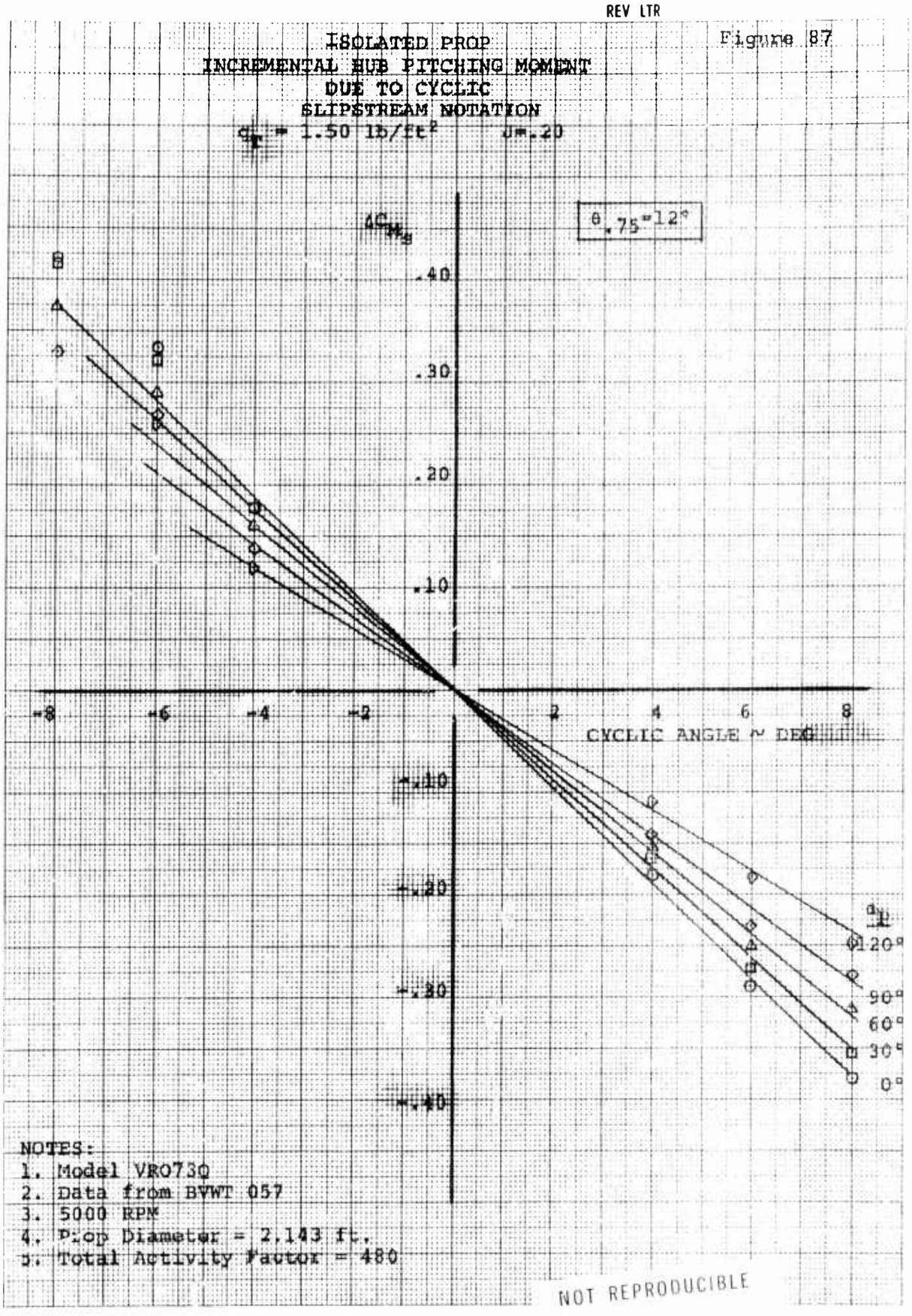

Figure 88

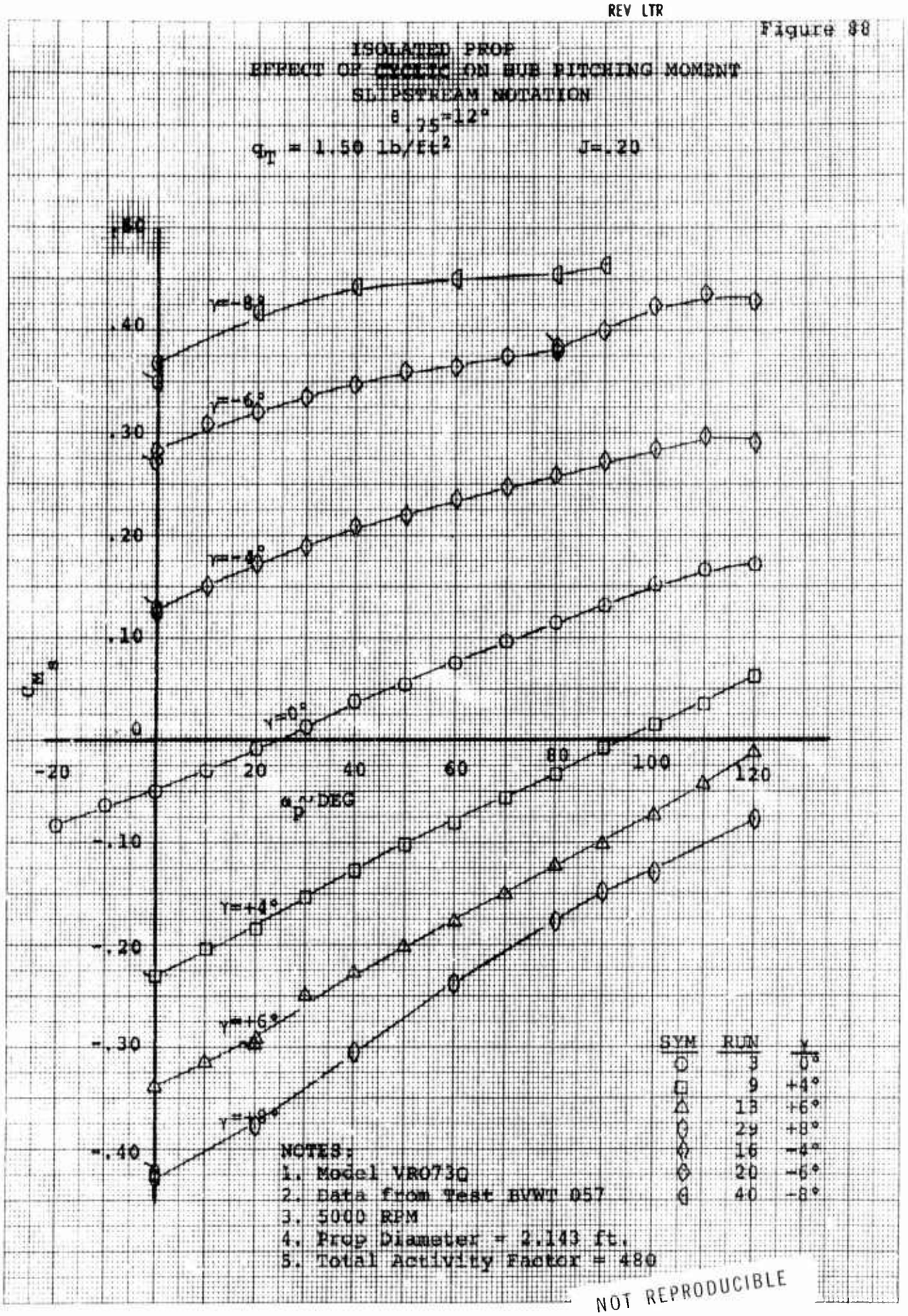

Figure 89

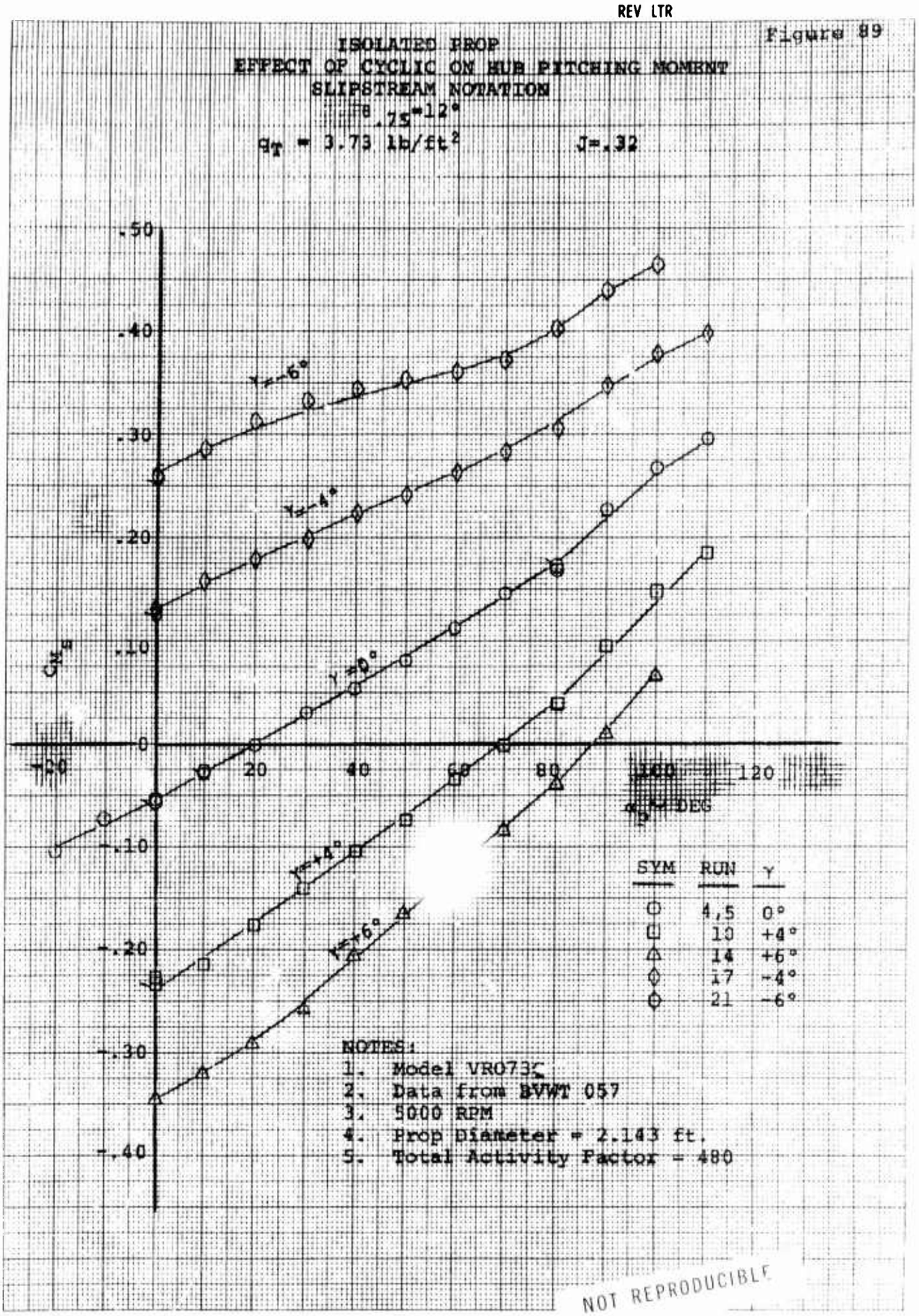

Figure 90

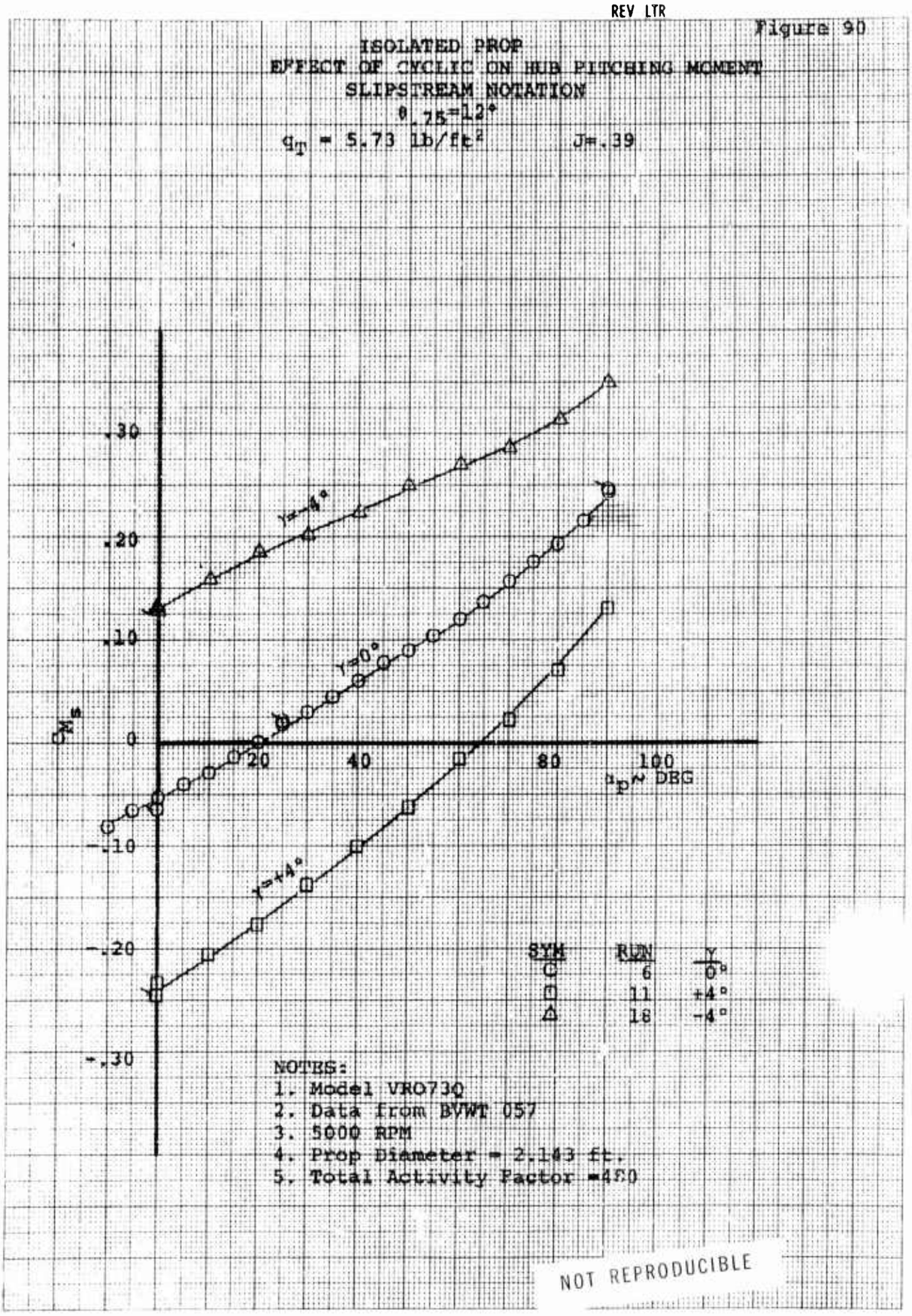

Figure 91

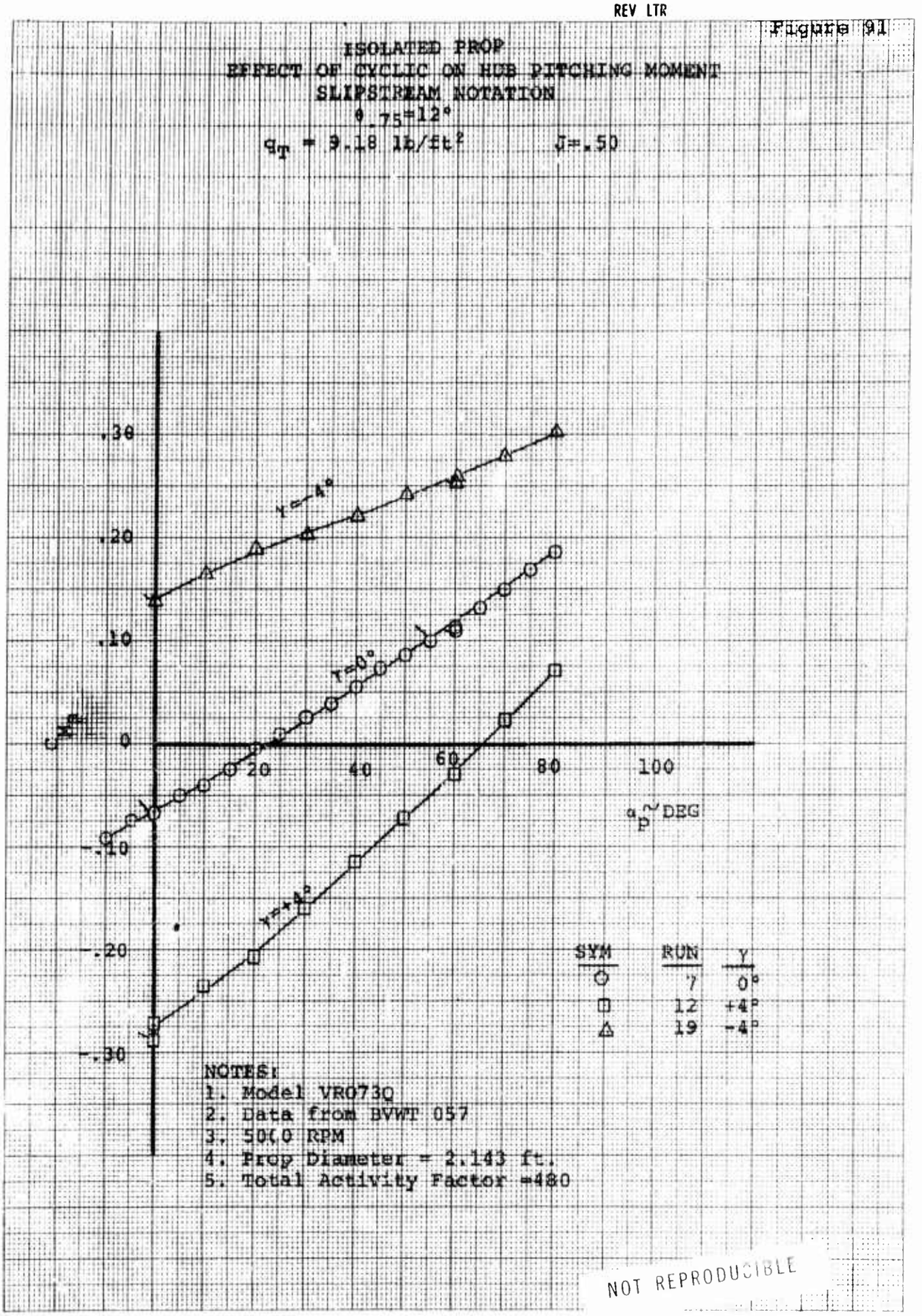

Figure 92

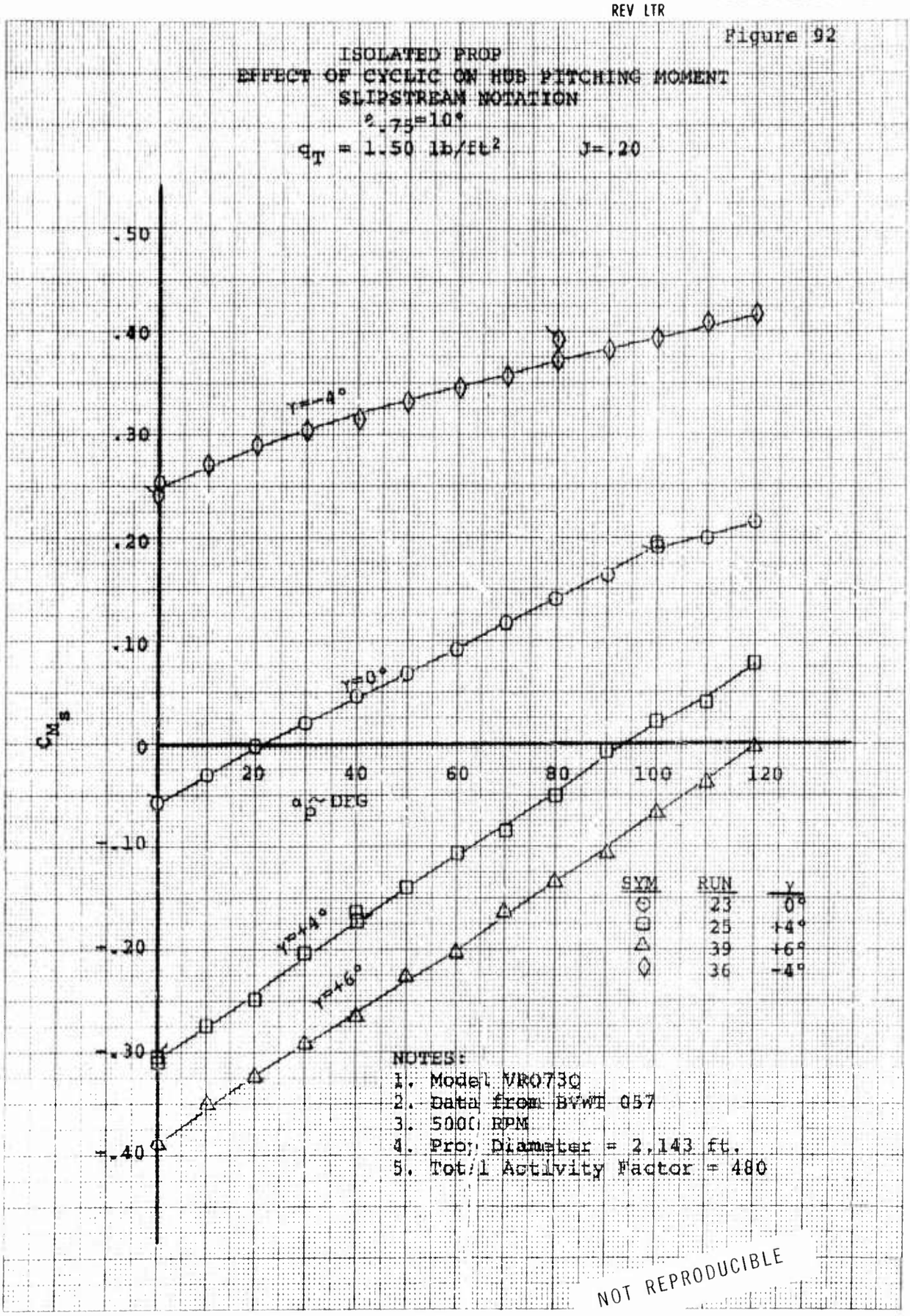

Figure 93

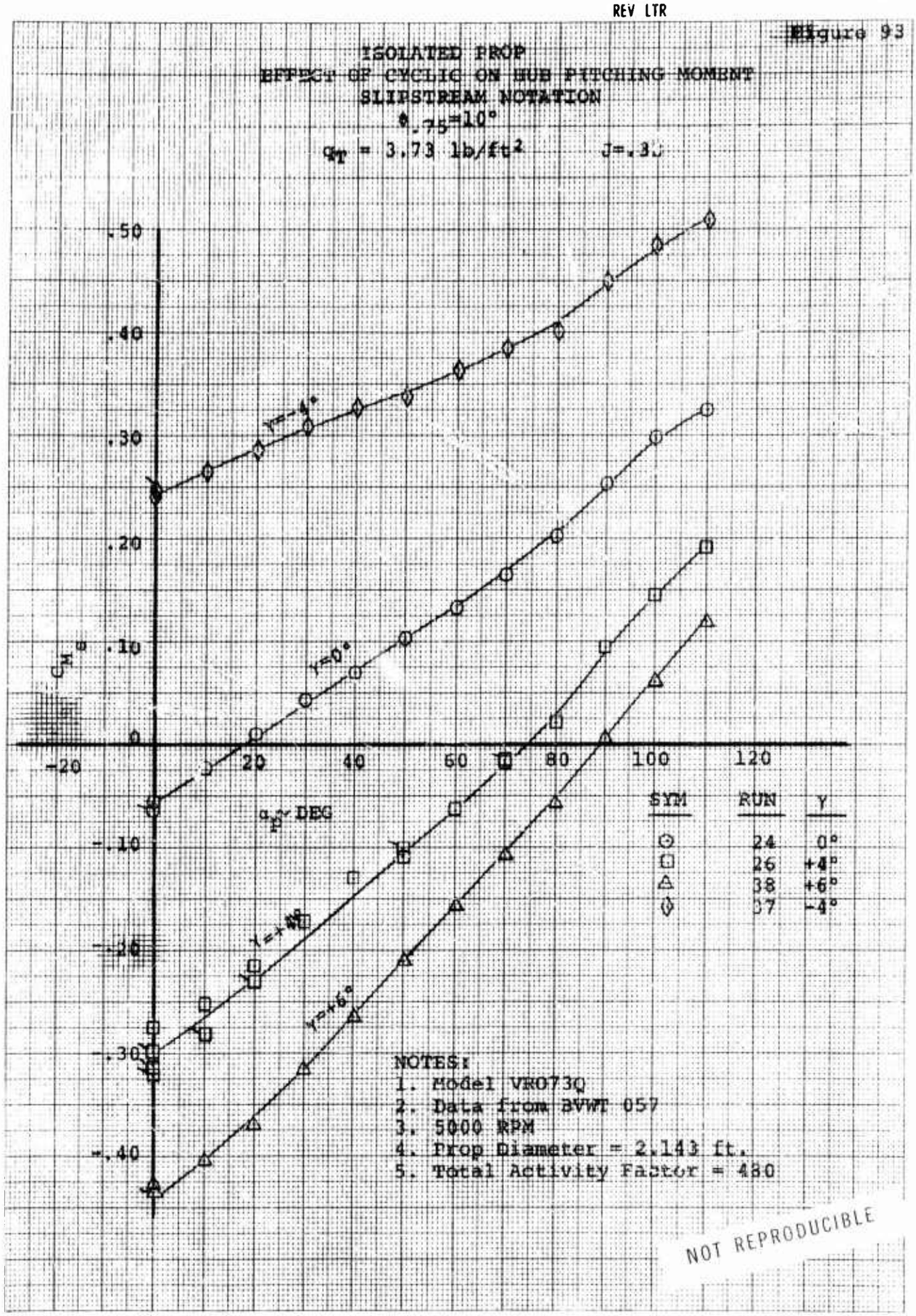

Figure 91

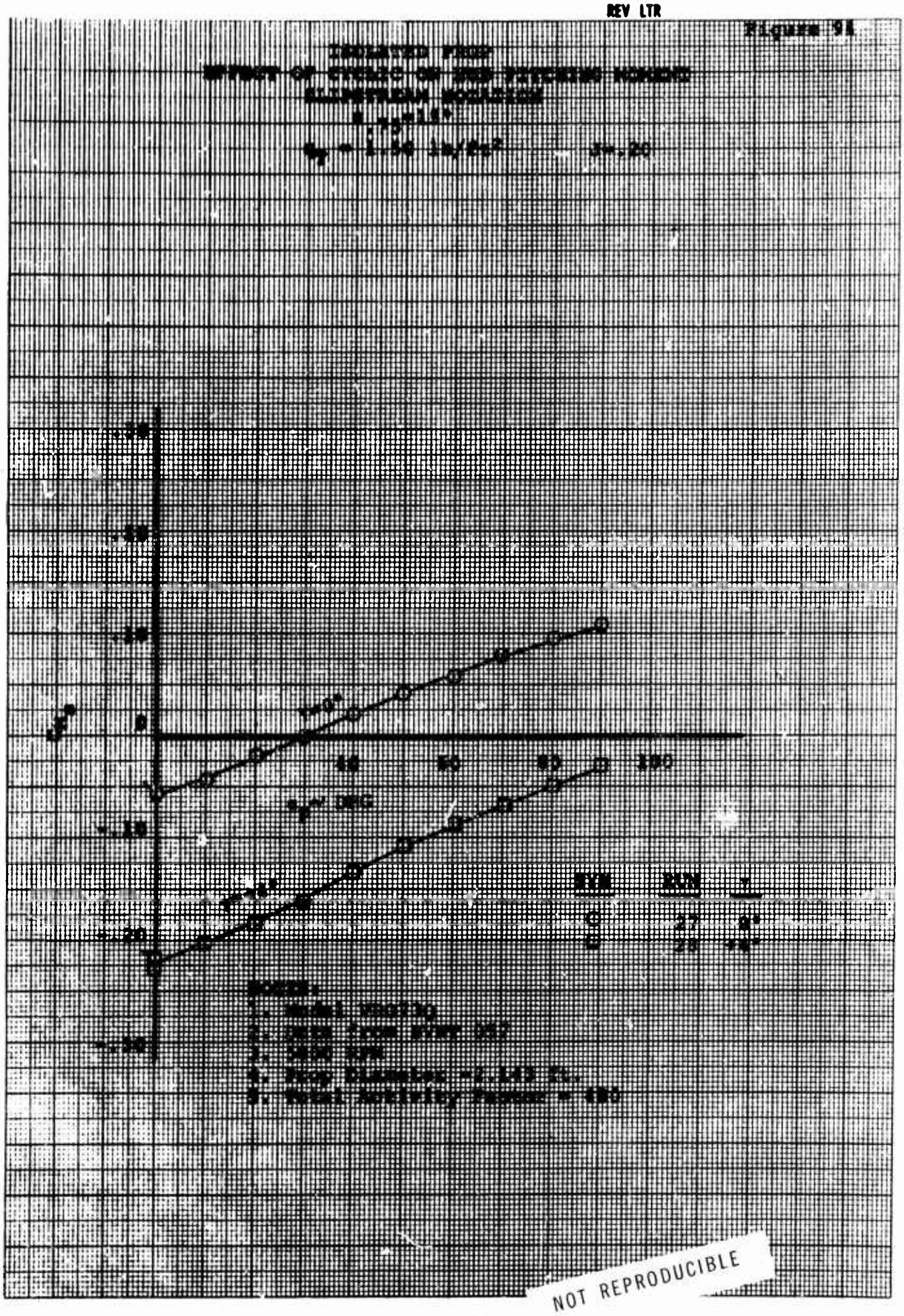

6.9 BASIC HUB PITCHING MOMENT (ZERO CYCLIC)

Figures 95 and 96 show the basic propeller hub pitching moment coefficient (zero cyclic) as a variation with shaft angle for 12° of collective in propeller and slipstream notation, respectively.

With a high shaft angle, hub pitching moment increases through the first stage of transition (up to approximately 40 kts or 0.24J) from a value of zero in hover. In the propeller notation case (Figure 95), pitching moment varies almost linearly with shaft angle at 0.2J and exhibits larger non-linear increases with shaft angle at higher J values.

In slipstream notation, the increase in q_s with shaft angles linearizes the pitching moment/shaft angle curves and the q_s variation with tunnel q results in the data acquired at J values higher than 0.2 forming a single curve.

Collective angle changes in the range tested (10° to 15°) did not significantly effect the measured hub pitching moment when expressed in propeller terms. See Figure 97. The variation of C_M with collective angle when expressed in slipstream terms as depicted in Figure 98 is due to the variation in slipstream q (q_s) with collective angle.

Figure 95

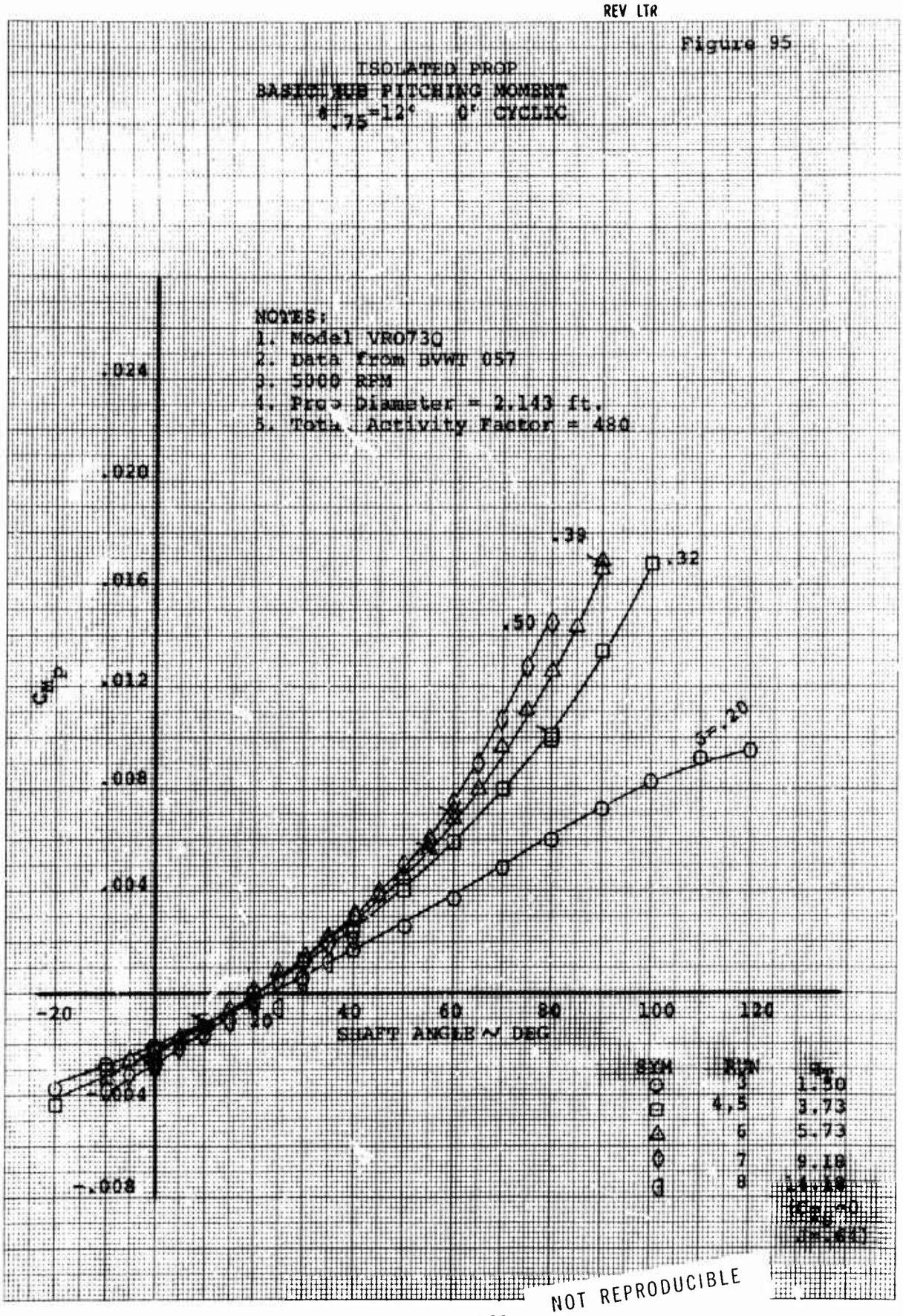

Figure 97

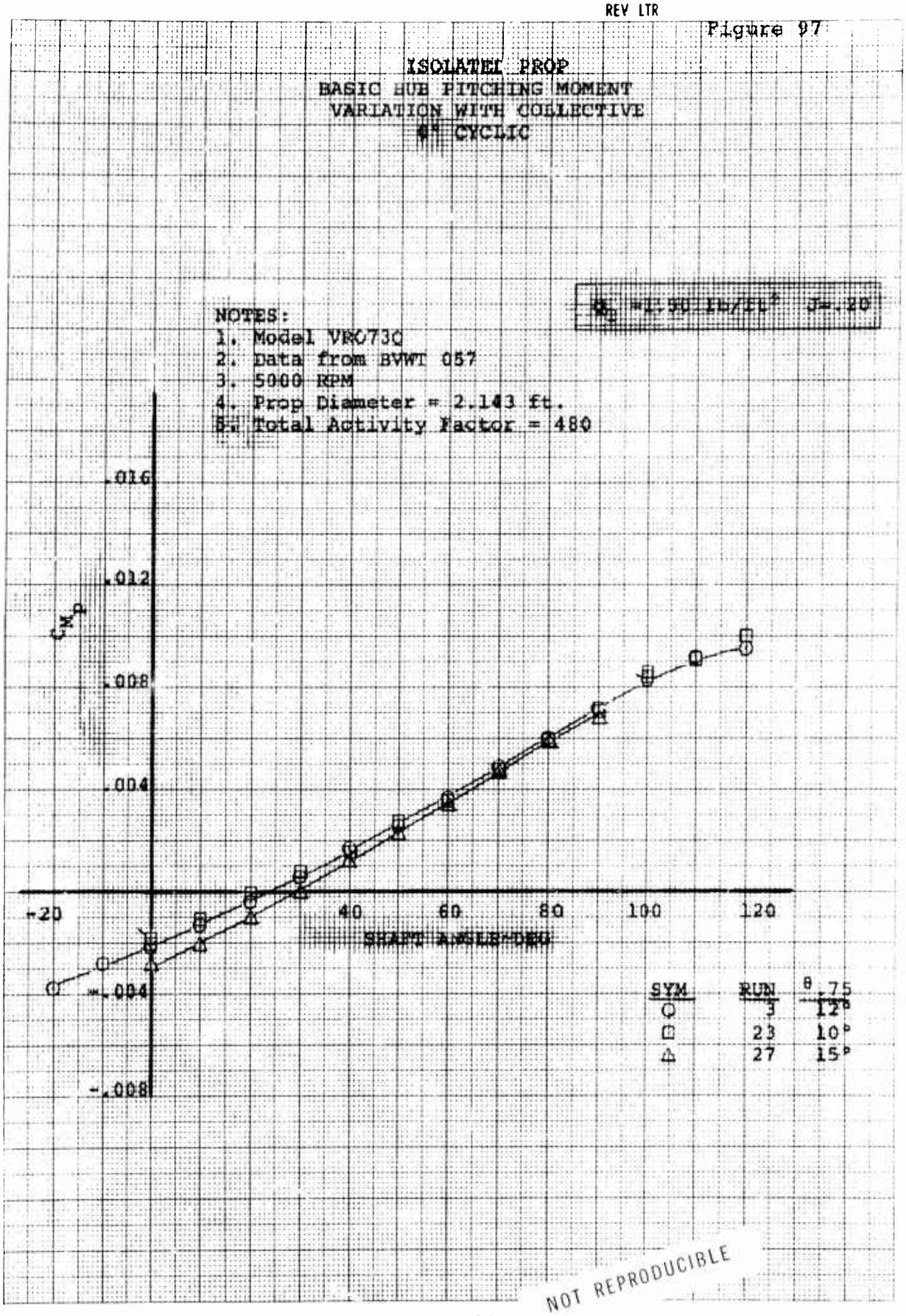

Figure 97

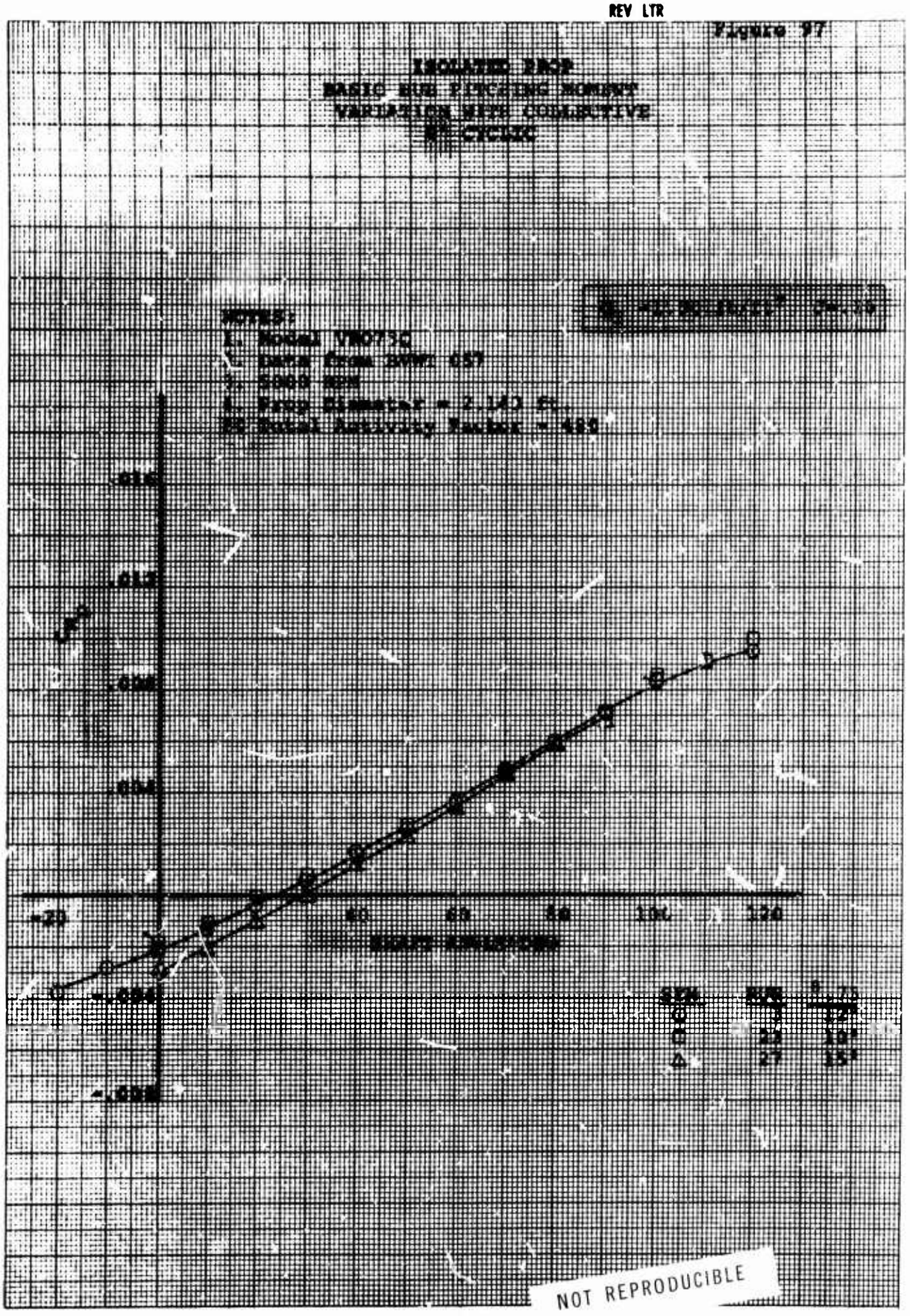

Figure 98

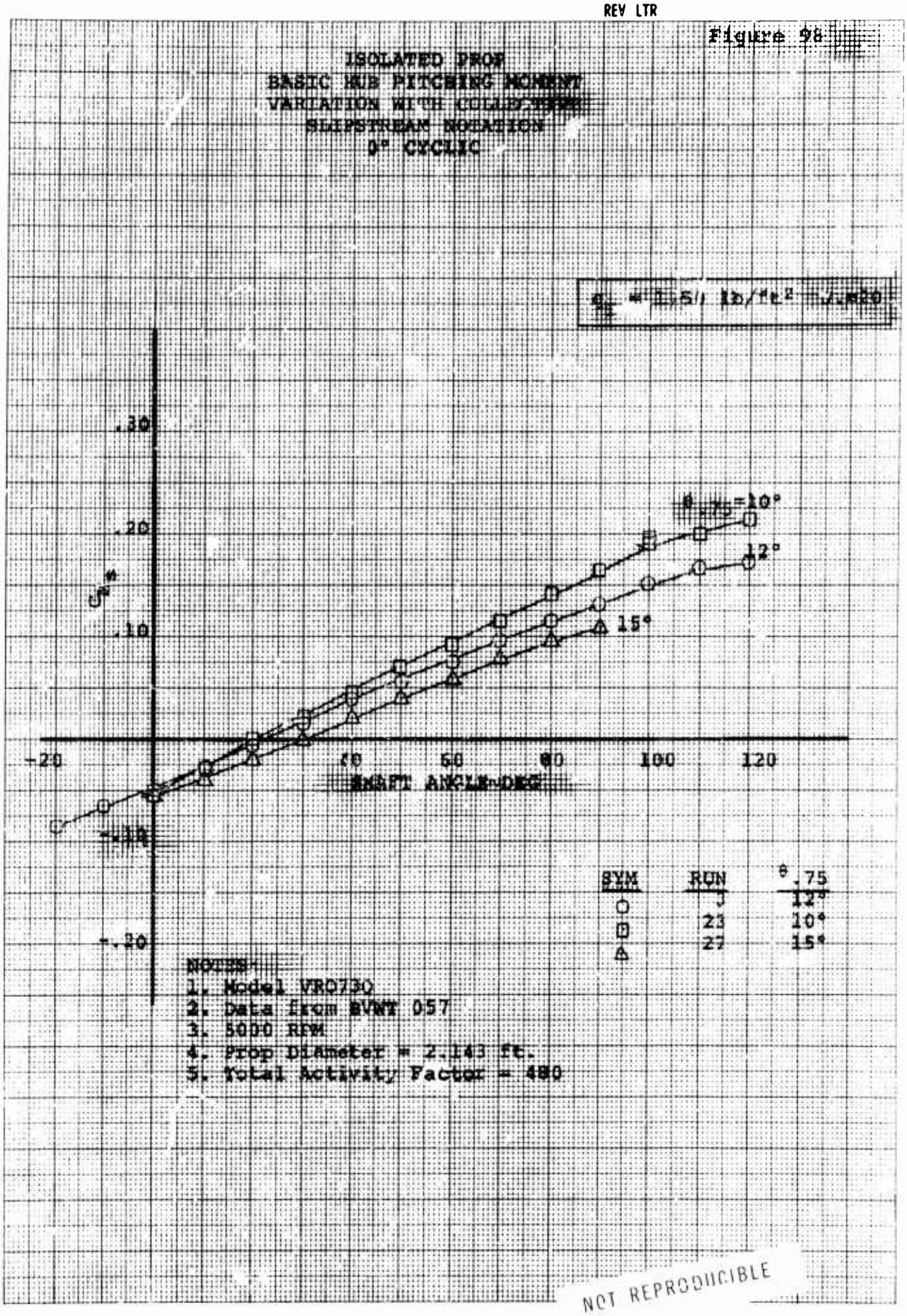

6.10 BASIC PROP NORMAL FORCE (ZERO CYCLIC)

Prop normal force increases with shaft angle up to about 90 degrees when expressed in propeller terminology. See Figure 99. The same figure shows the large change in slope of the prop normal force/shaft angle curves with tunnel q or advance ratio. Figure 99 also shows, in the lower plot, the increase in prop normal force with collective.

Transcribing prop normal force into slipstream notation produced the changes recorded in Figure 100, namely, prop normal force did not increase significantly with collective,and the curves "leveled-off" at lower shaft angle.

Figure 99

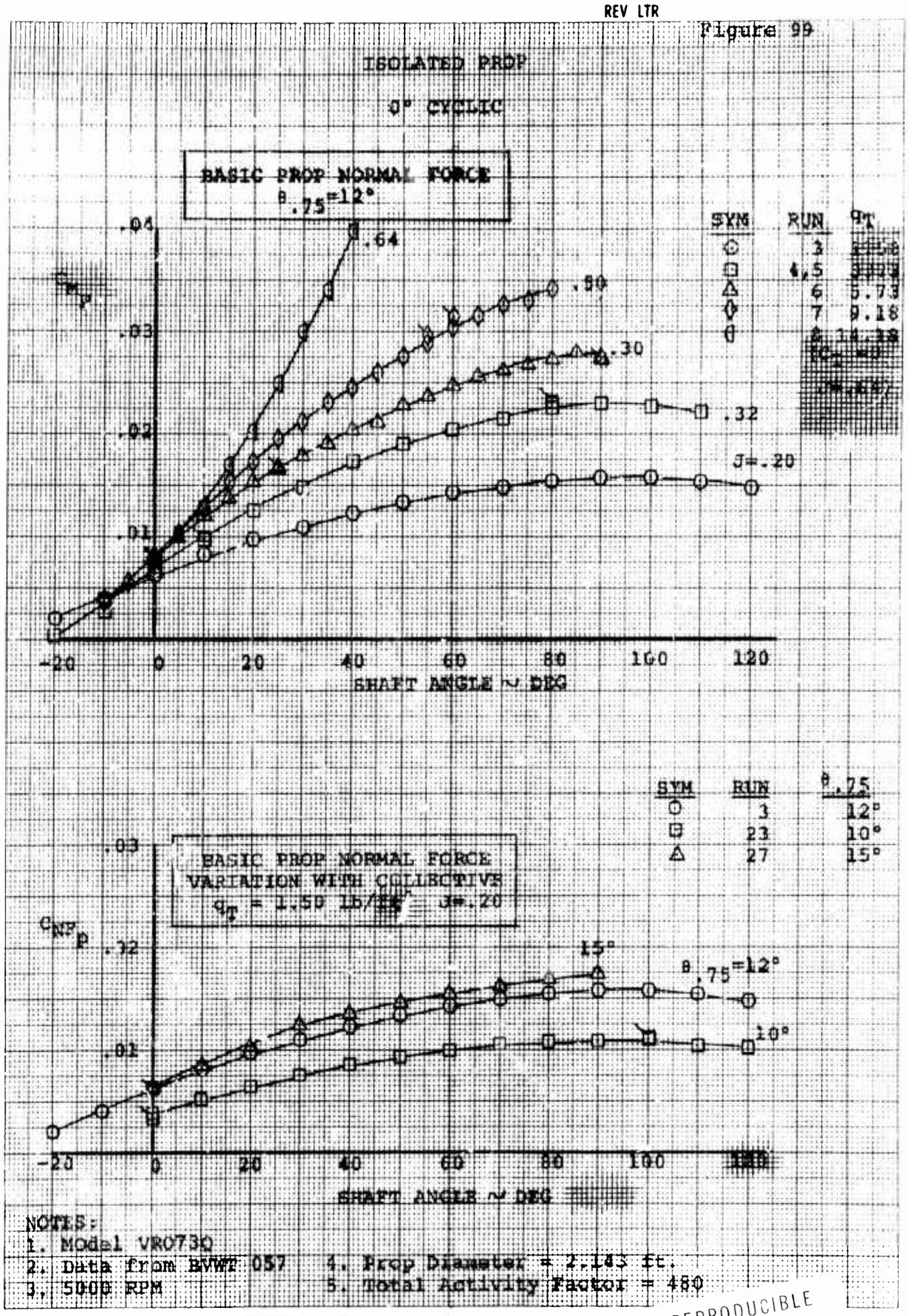

NOTES:
1. Model VR0730
2. Data from BVWT 057
3. 5000 RPM
4. Prop Diameter = 2.143 ft.
5. Total Activity Factor = 480

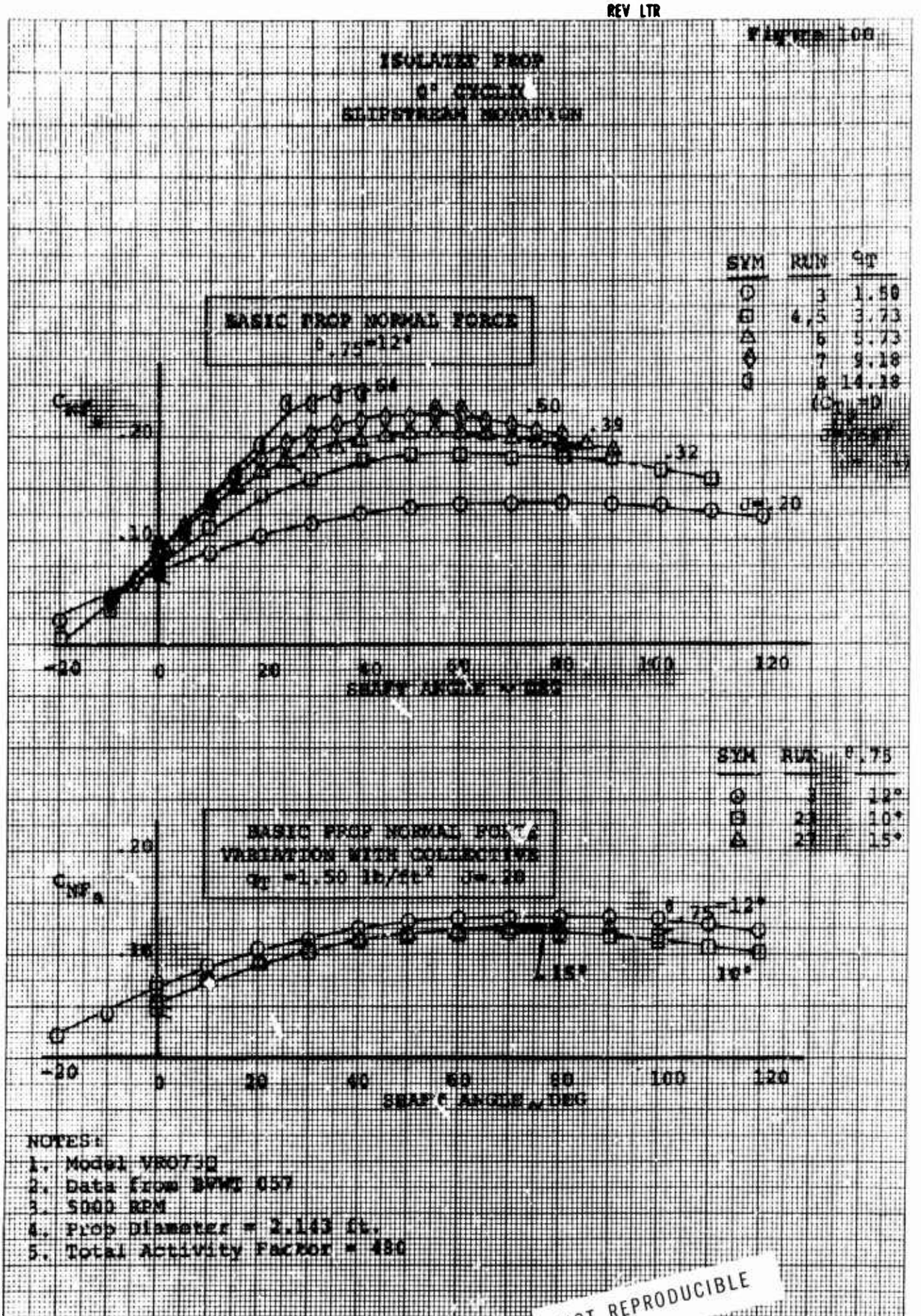

6.11 SPINNER/HUB TARES

Normal force and hub pitching moment tares were taken with a dummy spinner for the full shaft angle test range, zero to 120 degrees, for two values of tunnel dynamic pressure (3.73 and 14.2).

Both normal force and pitching moment tares are negligible at the low q. At the higher q, (corresponds to zero thrust with 12° of collective) the maximum normal force coefficient reached is 0.005 between 70 and 80 degrees shaft angle, and the maximum pitching moment coefficient reached is only about 0.0008 between 50 and 80 degrees. See Figure 101.

Figure 101

ISOLATED PROP
HUB/SPINNER TARES

NOTES:
1. Model VR0730
2. Data from BVWT 057

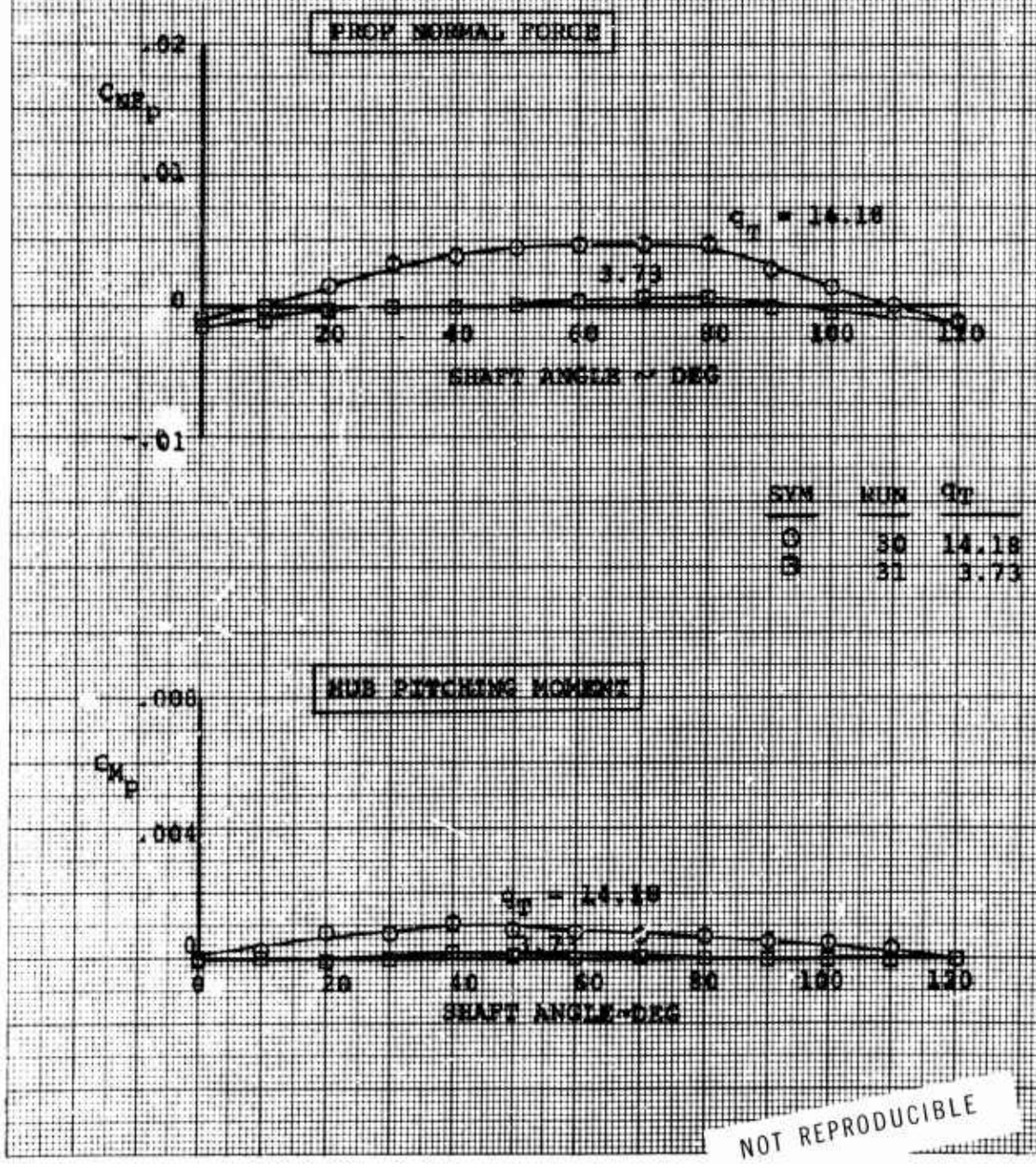

7.0 CONCLUSIONS

The primary conclusions derived from this test are listed below:

a. The hub pitching moment generated per degree of cyclic pitch was constant for the cyclic angles evaluated (-8° to +8° maximum) over a speed range from hover to 0.4 advance ratio, and was virtually independent of shaft angles up to 90°. (Figures 21 through 28).

b. Cyclic pitch effectiveness varied only to a small degree with collective setting over the range investigated, 10° to 15° $\theta_{.75}$. (Figure 21)

c. At a low forward speed, hub pitching moment reached a "peak" value at 120° of shaft angle with zero cyclic and at 110° of shaft angle with 6° of negative cyclic applied. (Figure 30).

d. The utilization of 8° of cyclic pitch in hover, increased the aerodynamic power requirement by 15%. (Figure 37).

e. The application of cyclic pitch does not have a major influence on thrust up to the highest shaft angles (120°) tested. (Figures 54 and 57, for example).

f. Positive cyclic incrementally decreased prop normal force and negative cyclic incrementally increased it. The ratio $dC_{NF_p}/d\gamma$ was essentially independent of shaft angle and advance ratio. (Figure 64 for example)

g. Virtually no lag existed between application of and full effect of the cyclic inppt.